Numerical analysis of Cauchy-type problem arising in electrical engineering

DISSERTATION

zur Erlangung des akademischen Grades

eines Doktors der Naturwissenschaften

vorgelegt von

Monika Dücker

aus Harbach

eingereicht beim Fachbereich 6 - Mathematik

der Universität Siegen

Siegen April 2010

Abstract

Inverse problems arise often in physical and technical processes. In this dissertation we consider problems of Cauchy-type based on the application of hybrid insulation. The experimental setup takes place at the NTNU Trondheim which placed at the disposal the measurements for the calculation. In this case we search Dirichlet or Neumann control for given Neumann measurements. After describing the problem of hybrid insulation and introducing the basic principals of functional analysis we analyse Nitsche's method for dealing with Dirichlet boundary conditions. The error estimates will be deduced and verified. Subsequent we give an introduction to inverse problems and their regularisation. We formulate three optimal control problems on the unit square based on the application of hybrid insulation. For given Neumann measurement we search Dirichlet or Neumann control and for given Dirichlet measurement we search Dirichlet control. For the regularisation we draw on three matrices. For all three problems we do numerical calculations with different gridrefinements, different numbers of degrees of freedom on the boundary of control and different regularisation parameters. After comparison of the results within each problem we compare the results to each other. Based on these results, at the end of this dissertation we do the numerical calculations for the application of hybrid insulation for searched Neumann control and given Neumann measurements.

Kurzfassung

Inverse Probleme sind häufig auftretende Probleme in Naturwissenschaft und Technik. In dieser Arbeit werden Probleme vom Cauchy-Typ basierend auf der elektrotechnischen Anwendung hybrider Isolierung betrachtet. Der Experimentaufbau befindet sich an der NTNU Trondheim, die die Messdaten für die Berechnungen zur Verfügung gestellt hat. In diesem Fall wird die Dirichlet- oder Neumann-Steuerung für gegebene Neumann- Messdaten gesucht. Nachdem das Problem der hybriden Isolierung beschrieben und die nötigen Grundlagen der Funktionalanalysis eingeführt wurden, wird Nitsche's Methode zur Behandlung von Dirichlet-Randdaten analysiert. Die L^2- und H^1-Fehlerabschätzungen werden hergeleitet und verifiziert. Im Anschluß wird eine Einführung zu inversen Problemen und deren Regularisierung gegeben. Es werden drei optimale Steuerungsprobleme auf dem Einheitsquadrat formuliert, basierend auf der Anwendung der hybriden Isolierung. Zu gegebenen Neumann-Messdaten werden Dirichlet- oder Neumann-Steuerung gesucht und zu gegebenen Dirichlet-Messdaten die Dirichlet-Steuerung. Zur Regularisierung werden drei Matrizen herangezogen. Für alle drei Probleme werden numerische Berechnungen für verschiedene globale Verfeinerungen, verschiedene Anzahlen an Freiheitsgraden auf dem Kontrollrand und verschiedene Regularisierungsparameter durchgeführt. Nach einem Vergleich der Ergebnisse innerhalb eines Problems werden die Ergebnisse der Probleme untereinander verglichen. Basierend auf diesen Ergebnissen werden für das Problem der hybriden Isolierung nur die numerischen Berechnungen im Fall gesuchter Neumann-Steuerung zu gegebenen Neumann-Messdaten durchgeführt.

Contents

Contents

1 Introduction

In this dissertation we study inverse problems of Cauchy type based on the application of hybrid insulation. Frank Mauseth from the NTNU Trondheim deals with this problem in his PhD thesis [26]. The description of the application in Section 2 and the measurements we need for the calculations in Section 7 are from a private correspondence with Frank Mauseth and his PhD thesis [26].

We reduce the three dimensional rotational symmetric problem to a two dimensional problem to be solved. The details can be found in Section 2. Then we have given conflicting Dirichlet and Neumann boundary data on Γ_O (see Figure 1.1) and search Dirichlet or Neumann control on Γ_C. Ivan Cherlenyak deals also with this problem in his PhD thesis [11]. He used the Laplace-equation in two dimensions for his calculation instead of reducing the three dimensional problem to a two dimensional what we will do in this dissertation.
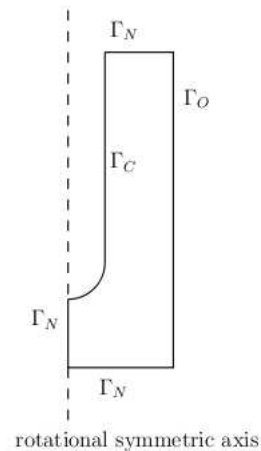

Figure 1.1: Underlying geometry of the application.

Before we treat this problem we take a look on a model problem (based on the application) with the unit square as underlying geometry (see Sections 5 and 6).

As we want to solve inverse problems we first want to introduce when to call a

problem an inverse problem. For given $A : X \to Y$ we call the calculation of Ax with $x \in X$ the direct problem. If we want to find $x \in X$ for given $y \in Y$, so that $Ax = y$, we call this an inverse problem.

Analysing inverse problems mostly leeds to the idea of ill-posed problems (see i.e. Louis [25] or Rieder [30]):

Definition 1.1. *Let $A : X \to Y$ be a mapping with the topologic spaces X, Y. The problem (A, X, Y) is called well-posed, when*

- *$\exists$ a solution to $Af = g$ for all $g \in Y$,*

- *the solution is well defined,*

- *the solution depends continuously on the data, i.e. A^{-1} is continuous.*

If one of these conditions is not satisfied the problem is called ill-posed.

Following e.g. Louis [25] or Rieder [30] a prototypical example (Cauchy problem) in classical notation reads

$$
\begin{aligned}
-\Delta u &= 0, && \text{on } \Omega = (0,1)^2, \\
\partial_n u &= 0, && \text{on } \Gamma_N = \{\, x \in \Omega \mid x_2 = 0 \text{ or } x_2 = 1 \,\}, \\
\partial_n u &= f, && \\
u &= 0, && \text{on } \Gamma_O = \{ x \in \Omega \mid x_1 = 1 \}.
\end{aligned}
\tag{1.1}
$$

The underlying solution operator cannot be continuous, because of the incompatible prescription of $\partial_n u$ and u on Γ_O. To show this, one chooses a sequence of boundary data g_k with $\|g_k\| \to 0$ for $k \to \infty$ such that for the corresponding solutions u_k there holds $|u_k| \to \infty$ for $k \to \infty$.

One possible choice for data and corresponding solution is

$$
f_k = k^{-1} \cos(k\pi y), \quad u_k = k^{-2} \cos(k\pi y) \sinh(k\pi(1-x))
\tag{1.2}
$$

In Figure 1.2 we can see data (left) and solution (right) for the case $k = 10$ (scaled for graphical output by dividing by 80.000) indicating the unstable development of u_k for small f_k.

So the inverse of the underlying solution operator cannot be continuous and the problem is ill-posed. The problems we want to solve are of the same type as this Cauchy problem.
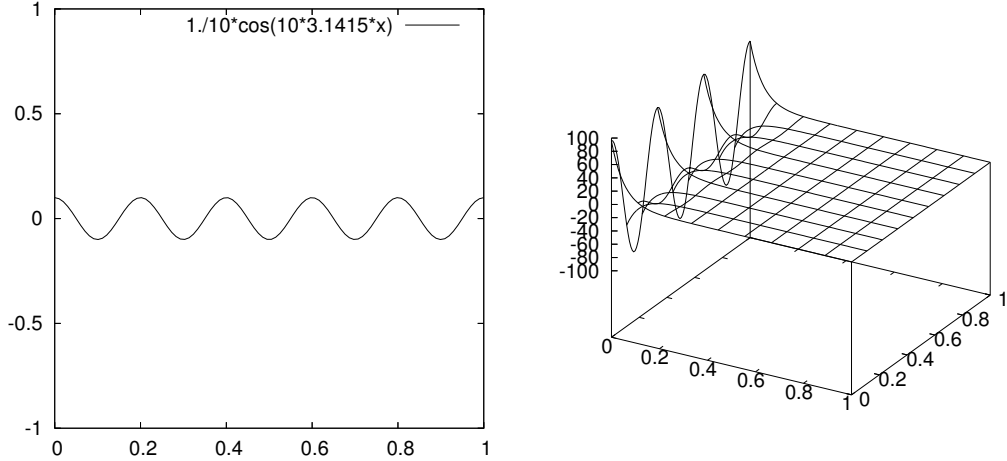

Figure 1.2: Data and solution (scaled by dividing by 80.000) for the case $k = 10$, indicating the instable development of u_k for small data f_k.

We have already mentioned that we want to solve a model problem on the unit square as underlying geometry before we solve the problem of the application. In this dissertation we want to analyse (based on the application) which type of searched control (Neumann or Dirichlet, respectively) for given Neumann measurement leads to the better results. Additionally we want to take a look on the problem where we have given Dirichlet measurement and Neumann boundary data in the underlying PDE-constraint. Now we short want to describe these optimal control problems we take care about (in detail see Sections 5 and 6).

In the following we have $\Omega = (0,1)^2$ the unit square and $\Gamma = \partial\Omega$ divided into $\Gamma_O = \{x \in \Gamma \mid x_1 = 1\}$, $\Gamma_N = \{x \in \Gamma \mid x_2 = 0 \vee x_2 = 1\}$ and $\Gamma_C = \{x \in \Gamma \mid x_1 = 0\}$. $J(w, \tau)$ defines a so-called cost functional and q denotes a control variable.

1. Find $\partial_n u = q$ on Γ_C for given measurement $\partial_n u = f$ on Γ_O

$$J(u, q) \to \min, \quad J(w, \tau) := \frac{1}{2}\|\partial_n w - f\|_{\Gamma_O}^2 \qquad (1.3)$$

5

under the PDE-constraint

$$
\begin{aligned}
-\Delta u &= g && \text{on } \Omega, \\
\partial_n u &= 0 && \text{on } \Gamma_N, \\
u &= 0 && \text{on } \Gamma_O, \\
\partial_n u &= q && \text{on } \Gamma_C.
\end{aligned}
\tag{1.4}
$$

2. Find $u = q$ on Γ_C for given measurement $\partial_n u = f$ on Γ_O

$$
J(u, q) \to \min, \quad J(w, \tau) := \frac{1}{2}\|\partial_n w - f\|_{\Gamma_O}^2
\tag{1.5}
$$

under the PDE-constraint

$$
\begin{aligned}
-\Delta u &= g && \text{on } \Omega, \\
\partial_n u &= 0 && \text{on } \Gamma_N, \\
u &= 0 && \text{on } \Gamma_O, \\
u &= q && \text{on } \Gamma_C.
\end{aligned}
\tag{1.6}
$$

3. Find $u = q$ on Γ_C for given measurement $u = 0$ on Γ_O

$$
J(u, q) \to \min, \quad J(w, \tau) := \frac{1}{2}\|w\|_{\Gamma_O}^2
\tag{1.7}
$$

under the PDE-constraint

$$
\begin{aligned}
-\Delta u &= g && \text{on } \Omega, \\
\partial_n u &= 0 && \text{on } \Gamma_N, \\
\partial_n u &= f && \text{on } \Gamma_O, \\
u &= q && \text{on } \Gamma_C.
\end{aligned}
\tag{1.8}
$$

We don't take care about the possible fourth problem where we have to find $\partial_n u = q$ on Γ_C for given measurement $u = 0$ on Γ_O such that

$$
J(u, q) \to \min, \quad J(w, \tau) := \frac{1}{2}\|w\|_{\Gamma_O}^2
\tag{1.9}
$$

under the PDE-constraint

$$
\begin{aligned}
-\Delta u &= g && \text{on } \Omega, \\
\partial_n u &= 0 && \text{on } \Gamma_N, \\
\partial_n u &= f && \text{on } \Gamma_O, \\
\partial_n u &= q && \text{on } \Gamma_C.
\end{aligned}
\tag{1.10}
$$

There the direct problem (1.10) is not uniquely solvable which makes problems in solving the inverse problem.

For analysing the problems we first introduce in Section 3 basic principals of functional analysis based on [2], [3], [14], [17] and [43] . There we introduce the spaces $H^k(\Omega)$, $H^s(\Omega)$, $H^s(\Gamma)$ with the corresponding inner products and norms.

Then we give a short introduction to the finite element method and analyse Nitsches method for solving direct problems with Dirichlet boundary data. In order to prepare an adequate mathematical formulation of the whole problem we first focus on a suitable formulation of the "forward" problem itself (see Section 3.3).

For handling Dirichlet boundary conditions we cannot use the standard weak formulation of the problem as described in the finite element theory (see e.g. Braess [8] and Johnson [22]). There the Dirichlet boundary condition q we want to calculate within the computation of the mentioned inverse problems (1.7) and (1.9) is hidden in the underlying function space of the variational formulation. Because of this we use the symmetric version of the weak formulation introduced by Nitsche [29] instead of the standard weak formulation (see also Hansbo [19], or Arnold et al. [4]).

For the given classical formulation we have to find $u \in C^2(\Omega) \cap C(\bar{\Omega})$ for given $f, q \in C(\bar{\Omega})$ such that

$$
\begin{aligned}
-\Delta u &= f \quad \text{in } \Omega \\
u &= q \quad \text{on } \Gamma = \partial\Omega.
\end{aligned}
\tag{1.11}
$$

Using Nitsche's method we have to find $u_h \in V_h \subset H^1(\Omega)$ such that

$$
a_h(u_h, v) = (f, v) + (\psi(h)q, v)_{\partial\Omega} - (q, \partial_n v)_{\partial\Omega}
\tag{1.12}
$$

with

$$
a_h(u, v) := (\nabla u, \nabla v)_\Omega - (\partial_n u, v)_{\partial\Omega} - (u, \partial_n v)_{\partial\Omega} + (\psi(h)u, v)_{\partial\Omega}.
\tag{1.13}
$$

We show that $a_h(.,.)$ is positive definite for $\psi(h) = \gamma h^{-1}$ for γ a positive constant depending on the problem to be solved. After that we derive the error estimates similar to that of the classical variational formulation:

$$\|e\|_{1,\Omega} \quad \leq \quad ch\|u\|_{2,\Omega} \tag{1.14}$$

$$\|e\|_{0,\Omega} \quad \leq \quad ch^2\|u\|_{2,\Omega}. \tag{1.15}$$

For this method we obtain an additional error estimation:

$$\|e\|_{0,\Gamma} \leq ch^{3/2}\|u\|_{2,\Omega}. \tag{1.16}$$

As we are interested in solving an inverse problem we introduce in Section 4 the basic theory of inverse problems (based on Louis [25] and Rieder [30]). There we formulate among other things that $f \in X$ minimzes the residuum $\|Af - g\|_Y$ is equivalent to $f \in X$ solves the normal equation $A^*Af = A^*g$. In our application (described in Section 2) we only have measuring data $\partial_n u|_{\Gamma_O} = f$ or $u|_{\Gamma_O} = 0$ and we have already seen that the inverse of the underlying solution operator is not continuous. This leads to errors in the calculation and we have to regularise the problem. Here we employ the Tikhonov-Phillips-regularisation.

We have formulated the problems as optimal control problems. In general we can write the three cases in the form (see Lions [24] and Tröltzsch [39]):

$$J(u,q) \quad \rightarrow \quad \min \tag{1.17}$$

$$\text{under the constraint } Au \quad = \quad Bq.$$

As A is invertible we can write

$$u = A^{-1}Bq. \tag{1.18}$$

From this there follows that we have to minimise

$$J(u,q) = J(A^{-1}Bq, q). \tag{1.19}$$

So after all we have to solve the regularised normal equation

$$(M^T M + \alpha R^T R)q = M^T f. \tag{1.20}$$

With M depending on the optimal control problem to be solved (for details see Section 5), $\alpha > 0$ the regularisation parameter and R the regularisation matrix from the Tikhonov-Phillips-regularisation.

For the implementation we use DEAL (Differential Equations Analysis Library [1], see also [36]). As solution algorithm we use the preconditioned conjugate gradient algorithm (pcg) and the multigrid method as preconditioner (see e.g. [9], [10],[31], [41]). Both algorithms are described in Section 5.2.

In Section 6 we present the numerical results for our three problems. As a test-example we use

$$-\Delta u = 12xy^2 - 12xy + 2x - 12y^2 + 12y - 2. \tag{1.21}$$

We do the calculations for the three problems with three regularisation matrices (Id and approximations of the first and second derivative) under different aspects. First we take a look on the results for the searched control on Γ_C for different grid refinements. The regularisation parameter α is choosen by trial and error. It is not part of this dissertation to formulate algorithms for the best parameter choice. As a consequence of this we do not present a detailed error analysis which is dependent of the parameter choice.

After that we reduce the number of degrees of freedom (DOF) on Γ_C as we know we can regularise the problem by reducing the dimension. Again we do this analysis for the three matrices R. At last we analyse the influence of the regularisation parameter α on the solution with reduced number of DOF on Γ_C. As a last aspect for each problem we compare the results for the three regularisation matrices with reduced number of DOF on Γ_C and the corresponding optimal regularisation parameter. After doing this analysis for each of the three problems (Section 6.1 to Section 6.3) we compare the results of the three optimal control problems (Section 6.4). Therefore we

use the approximation of the second derivative as regularisation matrix, the reduced number of DOF on Γ_C and the corresponding optimal regularisation parameter we estimated in the Sections 6.1 to 6.3.

In the following Figures we can see a few results of the calculations we will present in detail in Section 6. Figure 1.3 shows the searched Dirichlet control $q = u_h|_{\Gamma_C}$ for given Neumann measurement $\partial_n u|_{\Gamma_O}$ and the results for $\partial_n u_h|_{\Gamma_C}$ calculated with the searched control. We reach good results for the searched control but we achieve oscillations in the calculation of $\partial_n u_h|_{\Gamma_C}$ if we regularise with the identity. For the regularisation with an approximation of the first derivative we can only avoid the oscillations with an enlarged number of DOF on Γ_C (for details see Section 6.2). Figure 1.4 shows the searched Dirichlet control ($q = u|_{\Gamma_C}$) for given Dirichlet measurements and $\partial_n u_h|_{\Gamma_C}$ calculated with the searched control. There we can see the same effect as in the calculation with searched Dirichlet control and given Neumann measurements. In the case of searched Neumann control and given Neumann measurements we haven't this effect. There we reach good approximations of all boundary data for all regularisations without the need to enlarge the number of DOF on Γ_C. This can be seen in detail in Section 6.1.
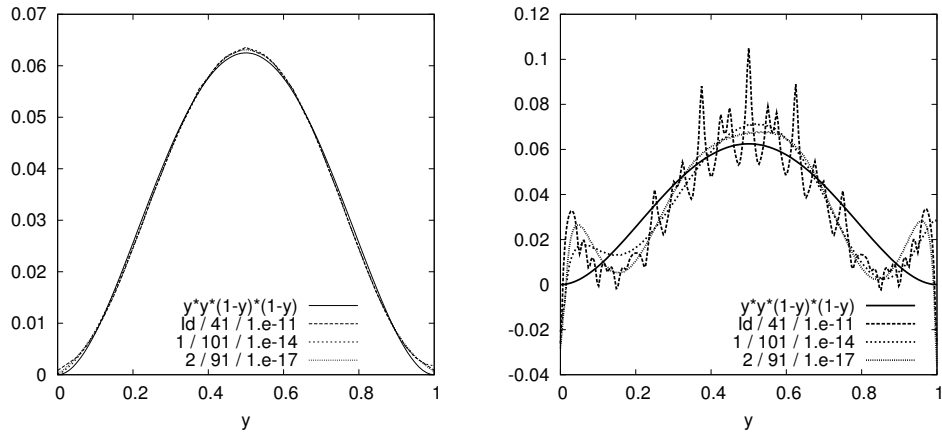

Figure 1.3: Results for searched Dirichlet control and given Neumann measurements: $u|_{\Gamma_C} = y^2(1-y)^2$ and $u_h|_{\Gamma_C}$ (left), $\partial_n u|_{\Gamma_C} = y^2(1-y)^2$ and $\partial_n u_h|_{\Gamma_C}$ (right) for the three regularisations with reduced number of DOF on Γ_C and optimal regularisation parameter.

Figure 1.4: Results for searched Dirichlet control and given Dirichlet measurements: $u|_{\Gamma_C} = y^2(1-y)^2$ and $u_h|_{\Gamma_C}$ (left), $\partial_n u|_{\Gamma_C}$ and $\partial_n u_h|_{\Gamma_C}$ (right) for the three regularisations with reduced number of DOF on Γ_C and optimal regularisation parameter.
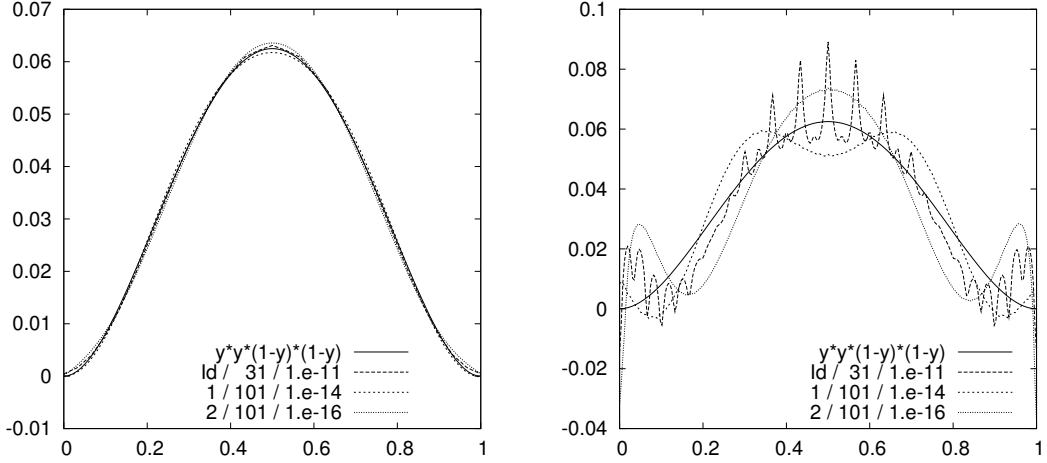
For the model problem these results show that the case of searched Neumann control and given Neumann measurements delivers the best results. As a conclusion we can say, the more Dirichlet data (as searched control or/and given measurement) we have the worse results.

At the end of this dissertation we present the numerical results for the application of hybrid insulation based on the knowledge from the model problem, i.e. we only present the results for searched Neumann control and given Neumann measurements which delivered the best results for the model problem. Caused by the reduction from three to two dimensions and the underlying geometry (see Figure 1.1) we have to modify our calculations (for details see Section 7). Figure 1.5 shows the calculated control $q = \partial_n u_h|_{\Gamma_C}$, the given measurements and their approximation ($\partial_n u_h|_{\Gamma_O}$), calculated with the computed control. In Figure 1.6 we can see a video image (from F. Mauseth, NTNU Trondheim) and the calculated u_h on the simplified geometry. Both Figures show that we achieve good approximations of the given measurements $\partial_n u|_{\Gamma_O}$ and also of u on the simplified geometry. More numerical results will be
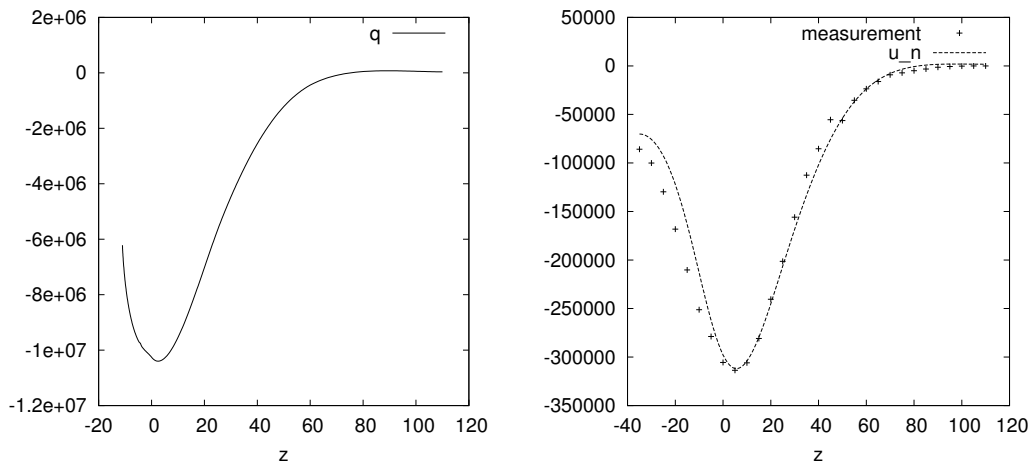
presented in Section 7 and appendix B.

Figure 1.5: The calculated control $q = \partial_n u_h|_{\Gamma_C}$ (left), the given measurements and the calculated normal derivative $\partial_n u_h|_{\Gamma_O}$ (right).
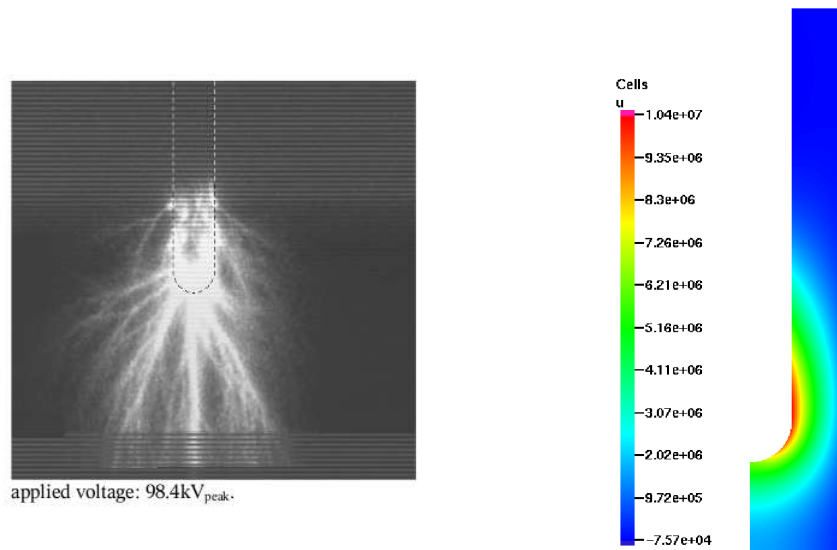

Figure 1.6: Video image (left, from F. Mauseth NTNU Trondheim) and calculated u_h on Ω for the given measurements $\partial_n u|_{\Gamma_O}$ (illustrated in Figure 1.5 right).

2 Description of the application: Hybrid insulation

Now we want to describe the application of hybrid insulation which we deal with the NTNU Trondheim, where they do the measurements. The description is from Frank Mauseth from the NTNU Trondheim who deals with the problem of hybrid insulation in his PhD thesis ([26]). We only present the fundamental idea and the resulting differential equation to be solved when we reduce the problem to a two dimensional one.

The breakdown voltage of an air gap between two electrodes can be improved considerably if one or both of the electrodes are covered with a thick (several millimeters) dielectric coating. If free charges are available in the gap or in the air volume surrounding the structure, charges accumulate in the dielectric surfaces due to electrostatic attraction. As long as there is a driving field this accumulation process continues.

The electrical field in the hybrid insulation system can be calculated as the vector sum of the charge induced field and the applied field.

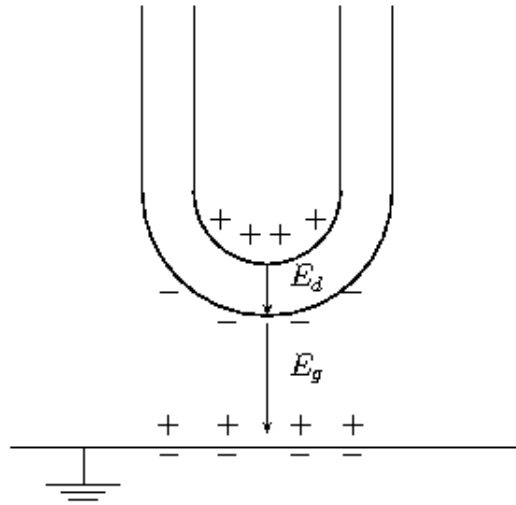$$E_{total} = E_{capacitive} + E_{charge\ induced}$$

Figure 2.1: The fundamental idea of hybrid insulation: A cutout of the experimental
        setup.

The charge formation on the insulation surface builds up an electric field that reduces
the field E_g in the air gap and increases the field E_d in the solid insulation. The net
result is an overall increased insulation performance. This technique may be used in
design a construction of compact high voltage equipment in the future. The physics
of this phenomena is not yet fully understood.

In order to increase the knowledge of the phenomena, insight in the surface charge
distribution is vital. The surface charge densities, and thus the surface potential,
associated with this kind of insulation system is quite high necessitating a large dis-
tance between surface and measuring probe. Due to the large measurement distance
(about 20 mm) a direct reading of the surface charge density is not possible since
surrounding areas also will influence and give a contribution to the read out.

To get a better insight of the surface charge distribution on the insulating surface,
the electrical field along a cylinder around the rod was measured. After applying a
lightning impulse and grounding the rod, the cylinder with a field mill mounted on
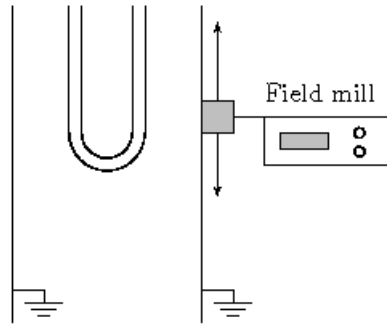it as shown in the following Figure was placed around the rod.

Figure 2.2: Cylinder with field mill.

This leads to a rotational symmetric geometry as shown in Figure 2.3 (left).
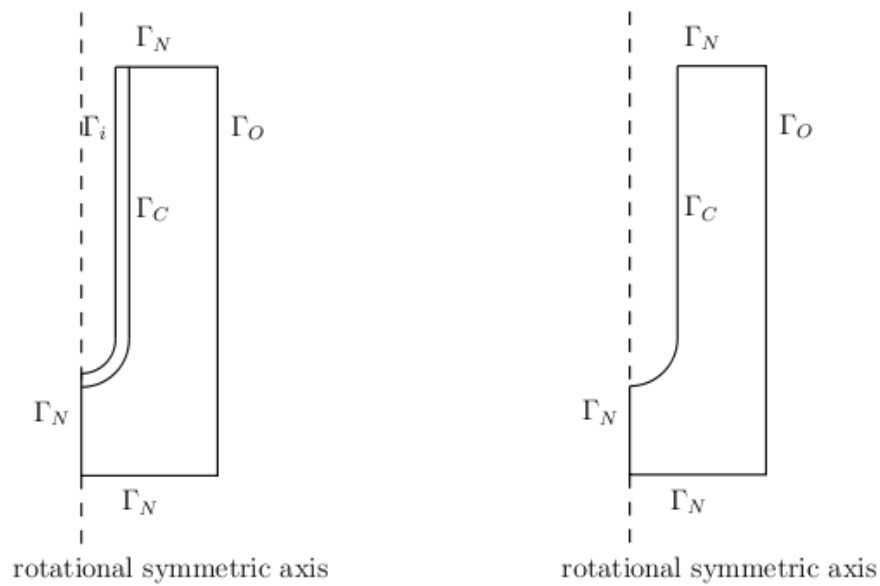

Figure 2.3: Rotational symmetric geometry of the application (left) and the simplified rotational symmetric geometry (right).

The surface charge distribution can be indirectly found as the solution of an inverse problem. By finding the electrical field $\left(\dfrac{du}{dn}\right)$ on the surface (Γ_C), the surface charge

distribution can be found by the capacitive distribution between the surface and the electrodes.

Therefore we can simplify the problem. I.e. we solve the Laplace-equation on the simplified geometry (without the boundary Γ_i) shown in Figure 2.3 (right).

Using a cylinder simplifies the electrical field calculations with FEM-software since the problem is rotational symmetric. Introducing cylinder coordinates

$$
\begin{aligned}
x &= r\cos\varphi \\
y &= r\sin\varphi \\
z &= z
\end{aligned}
\tag{2.1}
$$

leads to:

$$
\begin{aligned}
\frac{\partial^2 u(x,y,z)}{\partial x^2} &= \frac{\partial^2 u(r,\varphi,z)}{\partial r^2}\cos^2\varphi - 2\frac{\partial^2 u(r,\varphi,z)}{\partial r\partial\varphi}\frac{\sin\varphi\cos\varphi}{r} \\
&\quad +2\frac{\partial u(r,\varphi,z)}{\partial\varphi}\frac{\sin\varphi\cos\varphi}{r^2} + \frac{\partial u(r,\varphi,z)}{\partial r}\frac{\sin^2\varphi}{r} \\
&\quad +\frac{\partial^2 u(r,\varphi,z)}{\partial\varphi^2}\frac{\sin^2\varphi}{r^2},
\end{aligned}
\tag{2.2}
$$

$$
\begin{aligned}
\frac{\partial^2 u(x,y,z)}{\partial y^2} &= \frac{\partial^2 u(r,\varphi,z)}{\partial r^2}\sin^2\varphi + 2\frac{\partial^2 u(r,\varphi,z)}{\partial r\partial\varphi}\frac{\sin\varphi\cos\varphi}{r} \\
&\quad -2\frac{\partial u(r,\varphi,z)}{\partial\varphi}\frac{\sin\varphi\cos\varphi}{r^2} + \frac{\partial u(r,\varphi,z)}{\partial r}\frac{\cos^2\varphi}{r} \\
&\quad +\frac{\partial^2 u(r,\varphi,z)}{\partial\varphi^2}\frac{\cos^2\varphi}{r^2},
\end{aligned}
\tag{2.3}
$$

$$
\frac{\partial^2 u(x,y,z)}{\partial z^2} = \frac{\partial^2 u(r,\varphi,z)}{\partial z^2}.
\tag{2.4}
$$

After summation and eliminating one dimension we have to solve the Laplace equation in cylinder coordinates reduced to a two-dimensional problem:

$$
-\frac{1}{r}\frac{\partial u}{\partial r} - \frac{\partial^2 u}{\partial r^2} - \frac{\partial^2 u}{\partial z^2} = 0
\tag{2.5}
$$

with the boundary conditions

$$
\begin{aligned}
\partial_n u &= 0 \quad \text{on } \Gamma_N, \\
u &= 0 \quad \text{on } \Gamma_O
\end{aligned}
\tag{2.6}
$$

given measurements $\partial_n u|_{\Gamma_O} = f$ and the searched control q on Γ_C on the simplified geometry (Figure 2.3 right).

With equation (2.5) and equation (2.6) we have given the underlying PDE constraint we need to solve the optimal control problem described later on (see Section 7).

Based on this application there are two possible cases we can solve within the inverse problem (see Section 5 and Section 7): On the one hand we can calculate the control $q = u|_{\Gamma_C}$ and on the other hand we can calculate the control $q = \partial_n u|_{\Gamma_C}$. First we will do this for a model problem: The Laplace equation on the unit square. Before we can do this we introduce in the next Section the basic principals of functional analysis and Nitsche's method for handling Dirichlet boundary conditions.

3 A model problem

Before we treat the inverse problems mentioned in the introduction we want to take a look on the direct problem. Therefore we need some principals of functional analysis. In Section 3.1 we define the spaces $H^k(\Omega)$ ($k \in \mathbb{N}$), $H^s(\Omega)$ and $H^s(\Gamma)$ ($s \in \mathbb{R}^+$) which we need for the analysis of our problem. We also introduce the trace and embedding theorem.

After that in Section 3.2 we take a short look on the abstract problem and the finite element method.

In Section 3.3 we study the variational formulation of the forward problem with Dirichlet boundary data. In the standard weak formulation $q = u|_\Gamma$ is hidden in the underlying function space, but in view that we have to determine q within the inverse problem we prefer q to appear more directly. Therefore we use a symmetric variant of Nitsche´s method (see Nitsche [29], Hansbo [19]).

3.1 Basic principals of functional analysis

First we introduce some spaces we need for the variational formulation of our problem. This basic principals and their proofs can be found in the literature about functional analysis (e.g. Hackbusch [17] and Dobrowolski [14]).

Let Ω be a bounded subset of $\mathbb{R}^d$. Then $L^2(\Omega)$ is defined as the space of functions where the integral over the square is finite:

Definition 3.1.

$$L^2(\Omega) := \left\{ v \mid v \text{ defined on } \Omega, \int_\Omega v^2 \, dx < \infty \right\} \tag{3.1}$$

$L^2(\Omega)$ is a Hilbert space with the (L^2-) inner product

$$(v, w)_0 := (v, w)_{L^2(\Omega)} = \int_\Omega vw \, dx \tag{3.2}$$

and the corresponding norm

$$\|v\|_{L^2(\Omega)} = \left(\int_\Omega v^2 \, dx \right)^{\frac{1}{2}} = (v, v)^{\frac{1}{2}}. \tag{3.3}$$

For the following weak derivative we need a multiindex $\alpha = (\alpha_1, \ldots, \alpha_n)^T$ with $\alpha_i \in \mathbb{N}_0, \ i = 1, \ldots, n$ for which we have:

$$|\alpha| = \sum_{i=1}^n \alpha_i, \quad x^\alpha = x_1^{\alpha_1} \ldots x_n^{\alpha_n}, \quad D^\alpha u = \frac{\partial^{|\alpha|}}{\partial_{x_1}^{\alpha_1} \ldots \partial_{x_n}^{\alpha_n}} u. \tag{3.4}$$

Definition 3.2. *For $u \in L^2(\Omega)$ exists a weak derivative $v := D^\alpha u \ \in L^2(\Omega)$ if for $v \in L^2(\Omega)$ holds:*

$$(w, v)_0 = (-1)^{|\alpha|}(D^\alpha w, u)_0 \ \ \forall \ w \in C_0^\infty(\Omega). \tag{3.5}$$

Now we define the Sobolev-spaces $H^k(\Omega)$ which we need for our variational formulation of the problem.

Definition 3.3. *Let $k \in \mathbb{N} \cup \{0\}$.*

$$H^k(\Omega) := \{ u \in L^2(\Omega) \mid \exists \ D^\alpha u \in L^2(\Omega) \text{ for } |\alpha| \leq k \}. \tag{3.6}$$

$H^k(\Omega)$ is a Hilbert space with the inner product

$$(u, v)_k := (u, v)_{H^k(\Omega)} := \sum_{|\alpha| \leq k} (D^\alpha u, D^\alpha v)_0 \tag{3.7}$$

and the (Sobolev-) norm

$$\|u\|_k := \|u\|_{H^k(\Omega)} := \sqrt{\sum_{|\alpha| \leq k} \|D^\alpha u\|_0^2}. \tag{3.8}$$

$$|u|_k := \sqrt{\sum_{\alpha=k} \|D^\alpha u\|_0^2} \tag{3.9}$$

is called semi norm of H^k.

We can also define $H^k(\Omega)$ as completion of $X_0 := \{u \in C^\infty(\Omega) \mid \|u\|_k < \infty\}$ in $L^2(\Omega)$ with respect to $\|.\|_{H^k}$. $H_0^k(\Omega)$ is the completion of $C_0^\infty(\Omega)$ in $L^2(\Omega)$ corresponding to (3.8).

Now we define the inner product $(.,.)_s$ with $s \in \mathbb{R}_0^+$ and the so called Sobolev-Slobodeckij-norm $\|.\|_{H^s(\Omega)}$. With the Sobolev-Slobodeckij-norm we can define $H^s(\Omega)$, $s \in \mathbb{R}_0^+$ in the same way as $H^k(\Omega)$ for $k \in \mathbb{N}_0$ as completion of X_0 with respect to $\|.\|_{H^s}$.

Definition 3.4. *Let $\Omega \subset \mathbb{R}^n$, $s \geq 0$ with $s = k + \lambda$, $k \in \mathbb{N} \cup \{0\}$ and $0 < \lambda < 1$. Then $(u,v)_s$ is defined as*

$$(u,v)_s := (u,v)_k + \sum_{|\alpha|=k} (D^\alpha u, D^\alpha v)_\lambda \tag{3.10}$$

with the known $(u,v)_k$ from (3.7) and

$$(D^\alpha u, D^\alpha v)_\lambda = \int_\Omega \int_\Omega \frac{(D^\alpha u(x) - D^\alpha u(y))(D^\alpha v(x) - D^\alpha v(y))}{|x-y|^{n+2\lambda}}. \tag{3.11}$$

With this inner product we get the Sobolev-Slobodeckij-norm

$$\|u\|_s := \|u\|_{H^s(\Omega)} := \sqrt{(u,u)_s}. \tag{3.12}$$

With the Sobolev-Slobodeckij-norm $H^s(\Omega)$ is a Banach space. With the inner product $(.,.)_s$ $H^s(\Omega)$ is a Hilbert space.

For $s \in \mathbb{N}$ we have $H^s = H^k$ from definition 3.3. $H_0^s(\Omega)$ is the completion of $C_0^\infty(\Omega)$ in $L^2(\Omega)$ with respect to $\|.\|_{H^s(\Omega)}$. For these Sobolev-spaces we have the following features (see Hackbusch [17]):

Theorem 3.1.

1. C_0^∞ *is dense in* $H_0^s(\Omega)$.

2. $\{u \in C^\infty(\Omega) \mid \mathrm{Tr}(u) \text{ compact}, \ \|u\|_s < \infty\}$ *is dense in* $H^s(\Omega)$.

3. $H^s(\Omega) \subset H^t(\Omega)$, $H_0^s(\Omega) \subset H_0^t(\Omega)$ *for* $s \geq t$.

4. $aD^\alpha(bu) \in H^{s-|\alpha|}$, *for* $|\alpha| < s$, $u \in H^s(\Omega)$, $a \in C^{t-|\alpha|}(\overline{\Omega})$, $b \in C^t(\overline{\Omega})$ *with* $t = s \in \mathbb{N} \cup \{0\}$ *or* $t > s$.

We also need the space $H^s(\Gamma)$, trace- and embedding operators because of the given boundary values. Following Hackbusch [17] we first take a look on this function space and operators with respect to $\Omega = \mathbb{R}_+^n := \{(x_1, \ldots, x_n) \in \mathbb{R}^n \mid x_n > 0\}$ with $\Gamma = \partial \Omega = \mathbb{R}^{n-1} \times \{0\}$.

Theorem 3.2. *Let* $s \geq 0$. *It exists an embedding operator* $\phi_s \in L(H^s(\mathbb{R}_+^n), H^s(\mathbb{R}^n))$ *so that the embedding* $\bar{u} = \phi_s u$ *and* u *are equal on* $\mathbb{R}_+^n$ *for all* $u \in H^s(\mathbb{R}_+^n)$.

Now we have the embedding operator. The trace operator γ is first defined on $C_0^\infty(\mathbb{R}^n)$:

$$\gamma : C_0^\infty(\mathbb{R}^n) \to C_0^\infty(\Gamma) \subset L^2(\mathbb{R}^{n-1}), \quad \gamma u(x) := u(x) \ \forall x \in \Gamma = \mathbb{R}^{n-1} \times \{0\}. \quad (3.13)$$

Then we have the following theorem:

Theorem 3.3. *Let* $s > 1/2$. γ *from equation (3.13) can be extended to* $\gamma \in L(H^s(\mathbb{R}^n), H^{s-1/2}(\mathbb{R}^{n-1}))$. *Specially :* $|\gamma u|_{s-1/2} \leq C_s |u|_s$, $u \in H^s(\mathbb{R}^n)$.

Corollary 3.1. *Let* $s > 1/2$. *For* $\gamma u := u(., 0)$ *we have* $\gamma \in L(H^s(\mathbb{R}_+^n), H^{s-1/2}(\mathbb{R}^{n-1}))$.

With the restriction $x_n = 0$ we loose a half order of differentiability. On the other side with the continuation of $w \in H^{s-1/2}(\mathbb{R}^{n-1})$ on $\mathbb{R}^n$ we gain a half order of differentiability:

Theorem 3.4. *Let* $s > 1/2$, $w \in H^{s-1/2}(\mathbb{R}^{n-1})$. *There exists* $u \in H^s(\mathbb{R}^n)$ *with* $|u|_s \leq C_s |w|_{s-1/2}$ *and* $\gamma u = w$, *i.e.* $w = u(., 0)$.

Until now we only took a look on $H^s(\mathbb{R}^n_+)$ and $H^s(\mathbb{R}^{n-1})$, but we need $H^s(\Gamma)$, $\Gamma = \partial\Omega$ and $\Omega \subset \mathbb{R}^n$ a general domain. Therefore we need the following definition:

Definition 3.5. *Let $0 < t \in \mathbb{R} \cup \{\infty\}$. We call $\Omega \in C^t$ if for all $x \in \Gamma := \partial\Omega$ there exists a surrounding area $U \subset \mathbb{R}^n$, where we can define a bijective mapping $\phi : U \to K_1(0) = \{\xi \in \mathbb{R}^n \mid |\xi| < 1\}$ with*

$$\phi \in C^t(\bar{U}), \ \phi^{-1} \in C^t(\overline{K_1(0)}), \tag{3.14}$$

$$\phi(U \cap \Gamma) = \{\xi \in K_1(0) \mid \xi_n = 0\}, \tag{3.15}$$

$$\phi(U \cap \Omega) = \{\xi \in K_1(0) \mid \xi_n > 0\}, \tag{3.16}$$

$$\phi(U \cap (\mathbb{R}^n \backslash \Omega)) = \{\xi \in K_1(0) \mid \xi_n < 0\}. \tag{3.17}$$

Lemma 3.1. *Let $\Omega \in C^t$ be a bounded domain. There exists $N \in \mathbb{N}$, U^i $(0 \le i \le N)$, U_i, α_i $(1 \le i \le N)$ with*

$$U^i \text{ open, bounded } (0 \le i \le N), \ \ \bar{\Omega} \subset \bigcup_{i=0}^{N} U^i, \ U^0 \subset\subset \Omega, \tag{3.18}$$

$$U_i := U^i \cap \Gamma \ (1 \le i \le N), \ \ \bigcup_{i=1}^{N} U_i = \Gamma, \tag{3.19}$$

$$\alpha_i : U_i \to \alpha_i(U_i) \subset \mathbb{R}^{n-1} \text{ bijective for } i = 1, \dots, N, \tag{3.20}$$

$$\alpha_i \circ \alpha_j^{-1} \in C^t(\overline{\alpha_j(U_i \cap U_j)}). \tag{3.21}$$

On U^i $(1 \le i \le N)$ the mappings ϕ_i with the features (3.14)-(3.17) are defined.

Lemma 3.2. *(Partition of unity)*

$\{U^i \mid 0 \le i \le N\}$ satisfy (3.18). There exist functions $\sigma_i \in C_0^\infty(\mathbb{R}^n)$, $0 \le i \le N$ with

$$\text{Tr}(\sigma_i) \subset U^i, \ \ \sum_{i=0}^{N} \sigma_i^2(x) = 1 \ \ \forall x \in \bar{\Omega}. \tag{3.22}$$

With α_i and σ_i we are now able to define $H^s(\Gamma)$.

Definition 3.6. *Let $\Omega \in C^t$. (U_i, α_i) and σ_i satisfy (3.17)-(3.20). Let $s \le t \in \mathbb{N}$ or $s < t \in \mathbb{N}$, $t > 1$. The Sobolev-space $H^s(\Gamma)$ is the set of all functions $u : \Gamma \to \mathbb{R}$ with $(\sigma_i u) \circ \alpha_i^{-1} \in H_0^s(\mathbb{R}^{n-1})$ $(1 \le i \le N)$.*

We can now formulate the trace and embedding theorems (3.2, 3.3) on a general domain Ω:

Theorem 3.5. *Let $\Omega \in C^t$ with $1/2 < s \leq t \in \mathbb{N}$ or $1/2 < s < t$.*

1. *The trace γu of $u \in H^s(\Omega)$ is element of $H^{s-1/2}(\Gamma) : \gamma \in L(H^s(\Omega), H^{s-1/2}(\Gamma))$.*

2. *For every $w \in H^{s-1/2}(\Gamma)$ there exist an $u \in H^s(\Omega)$ with $w = \gamma u$, $\|u\|_s \leq C_s\|w\|_{s-1/2}$.*

3. *For every $w \in H^s(\Omega)$ exists an extension $E \in L(H^s(\Omega), H^s(\mathbb{R}^n))$ with $Ew \in H^s(\mathbb{R}^n)$.*

The dual space of $H_0^s(\Omega)$ is called $H^{-s}(\Omega)$ or $H_0^{-s}(\Omega)$. The norm is then defined as

$$\|u\|_{-s} := \sup\left\{ \frac{\|(u,v)\|_{L^2(\Omega)}}{\|v\|_s} \mid 0 \neq v \in H_0^s(\Omega) \right\}. \tag{3.23}$$

These are the basics we need for this work. Now we take a look on the abstract formulation of the problem with the finite element method.

3.2 The Finite Element Method (FEM)

As typical for numerical methods we want to solve the problem approximately. Here we use the finite element method. Therefore we search the solution u_h of the problem in a finite dimensional subspace. But first we want to introduce the abstract problem analog to Johnson [22] and Braess [8].

Let V a linear space, $a : V \times V \to \mathbb{R}$ a symmetric, positive definite bilinear form and $l : V \to \mathbb{R}$ a linear functional. Then we want to solve:

$$a(u,v) = (l,v) \quad \forall\, v \in V. \tag{3.24}$$

As mentioned before, we don't search the solution in V but in a finite dimensional subspace $V_h \subset V$. I.e. we search the discrete solution $u_h \in V_h$ such that:

$$a(u_h,v) = (l,v) \quad \forall\, v \in V_h. \tag{3.25}$$

Now let $\{\varphi_1, \ldots, \varphi_n\}$ be basis of V_h. Hence we can illustrate u_h and v as linear combination of φ_i, $i = 1, \ldots, n$. This leads us to the following system of equations, if $u_h = \sum_{k=1}^{n} x_k \varphi_k$:

$$\sum_{k=1}^{n} a(\varphi_k, \varphi_i) x_k = (l, \varphi_i), \quad i = 1, \ldots, n \tag{3.26}$$

or in matrix-vector-form:

$$Ax = b \tag{3.27}$$

with $A_{ik} = a(\varphi_k, \varphi_i)$ and $b_i = (l, \varphi_i)$.

In practice we divide the domain Ω in (finite) subdomains and take a look on functions which are polynoms on every subdomain. These subdomains are called elements. In this work we use bilinear elements on quadrilaterals.

Let Ω be a polygonal domain which can be divided in triangles or quadrilaterals. We call the partition $\mathcal{T} = \{T_1, T_2, \ldots T_N\}$ of Ω in triangles or quadrilaterals allowed if the following properties are fulfilled:

- $\overline{\Omega} = \cup_{i=1}^{N} T_i$.

- Is $T_i \cap T_j$ one point, then this point is vertex of T_i and T_j.

- Is $T_i \cap T_j$, $i \neq j$ more than one point, then $T_i \cap T_j$ is edge of T_i and T_j.

If this is not fulfilled we have hanging nodes.

3.3 Variational formulation

Here we consider the variational formulation of the direct problem. As mentioned before the Dirichlet boundary in the standard variational formulation is hidden in the function space. In Section 5 (the inverse problem for a model problem) we want to calculate the control $u|_{\Gamma_C} = q$, where Γ_C is a part of the boundary Γ. Therefore we want to appear q in the variational formulation instead of being hidden in the function space. For this we use a symmetric variant of Nitsche's method.

Nitsche's Method

For simplicity we introduce Nitsche's method for Dirichlet boundary data on the whole boundary instead of only on parts of it. We show consistency, stability and reach the error estimates for $\|e\|_{0,\Gamma}$, $\|e\|_{0,\Omega}$ and $\|e\|_{1,\Omega}$.

For generality we want to solve the potential equation on the unit square with Dirichlet boundary data, i.e. we search $u \in C^2(\Omega) \cap C(\bar{\Omega})$ such that

$$
\begin{aligned}
-\Delta u &= g &&\text{on}\quad \Omega = (0,1)^2 \\
u &= q &&\text{on}\quad \Gamma = \partial\Omega.
\end{aligned}
\tag{3.28}
$$

In the standard variational formulation we have to find $u \in V := \{\varphi \in H^1(\Omega) \mid \varphi = q \text{ on } \Gamma\}$ such that

$$
(\nabla u, \nabla \varphi) = (g, \varphi) \quad \forall\, \varphi \in V.
\tag{3.29}
$$

If we use this variational formulation the Dirichlet boundary data is hidden in the function space V. In Section 5 we have the case that we want to calculate the control $q = u|_{\Gamma_C}$. So we want to appear q more directly.

This leads us to Nitsche´s method (see e.g. [29], [19]). Here we use a symmetric form of it.

Nitsche's method for (3.28) determines a solution $u_h \in V_h \subset H^1(\Omega)$ such that

$$
a_h(u_h, \varphi) = (g, \varphi)_{0,\Omega} + (\psi(h)q, \varphi)_{0,\Gamma} - (q, \partial_n\varphi)_{0,\Gamma} \quad \forall \varphi \in V_h
\tag{3.30}
$$

with

$$
a_h(u, \varphi) := (\nabla u, \nabla\varphi)_{0,\Omega} - (\partial_n u, \varphi)_{0,\Gamma} - (u, \partial_n\varphi)_{0,\Gamma} + (\psi(h)u, \varphi)_{0,\Gamma}.
\tag{3.31}
$$

The second term of the bilinear form arises from Green's formula, the third term is for symmetry and ensures consistency and the penalize last term guarantees stability which is shown later. Instead of $-(u, \partial_n\varphi)_\Gamma$ as third term we can also use $+(u, \partial_n\varphi)_\Gamma$. Then the bilinearform is positive definite for each choice of $\psi(h)$ but we have an unsymmetric problem to be solved (see [4]).

Now we want to analyse the symmetric version of Nitsche's method used here ((3.30) and (3.31)). Later we will show that $\|e\|_{1,\Omega} \in O(h)$ and $\|e\|_{0,\Omega} \in O(h^2)$ as for the classical variational formulation of problem (3.28). By (3.28) and using Green's formula we have consistency with the original problem:

$$
\begin{aligned}
a_h(u,\varphi) \quad &- \quad (g,\varphi)_{0,\Omega} - (\psi(h)q,\varphi)_{0,\Gamma} + (q,\partial_n\varphi)_{0,\Gamma} \qquad\qquad (3.32)\\
&= \quad (\nabla u, \nabla\varphi)_{0,\Omega} - (\partial_n u, \varphi)_{0,\Gamma} - (g,\varphi)_{0,\Omega} \equiv 0.
\end{aligned}
$$

Next we want to show, that the resulting bilinear form $a_h(.,.)$ is positive definite. The ideas are based on the results of Nitsche ([29]). Hansbo ([19]) uses a mesh dependent norm for the convergence analysis caused by the continuity of $a_h(.,.)$ in this norm. In the following estimates c is a positive constant changing in every estimation.

$$
\begin{aligned}
a_h(u_h,u_h) \quad &= \quad \|\nabla u_h\|_{0,\Omega}^2 - (\partial_n u_h, u_h)_{0,\Gamma} - (u_h, \partial_n u_h)_{0,\Gamma} + \psi(h)\|u_h\|_{0,\Gamma}^2 \\
&\geq \quad |u_h|_{1,\Omega}^2 - 2\|\partial_n u_h\|_{0,\Gamma}\|u_h\|_{0,\Gamma} + \psi(h)\|u_h\|_{0,\Gamma}^2. \qquad (3.33)
\end{aligned}
$$

Using the standard inverse estimate as in Hansbo ([19]) (proof: see Thomee [38]).

$$
\|\partial_n v\|_{0,\Gamma}^2 \leq c_1^2 h^{-1}|v|_{1,\Omega}^2 \quad \forall v \in V_h \qquad\qquad (3.34)
$$

we have:

$$
a_h(u_h,u_h) \geq |u_h|_{1,\Omega}^2 - 2c_1 h^{-1/2}|u_h|_{1,\Omega}\|u_h\|_{0,\Gamma} + \psi(h)\|u_h\|_{0,\Gamma}^2. \qquad (3.35)
$$

Now we want to estimate the product of norms $(|u_h|_{1,\Omega}\|u_h\|_{0,\Gamma})$ with a sum of these norms. Therefore we use for real numbers $a, b, \sqrt{\varepsilon} \neq 0$

$$
ab \leq \frac{\varepsilon}{2}a^2 + \frac{1}{2\varepsilon}b^2 \quad \Leftrightarrow \quad \left(\frac{b}{\sqrt{\varepsilon}} - a\sqrt{\varepsilon}\right)^2 \geq 0. \qquad (3.36)
$$

With $\varepsilon = 2$ we have in our case

$$
c_1 h^{-1/2}|u_h|_{1,\Omega}\|u_h\|_{0,\Gamma} \leq \frac{1}{4}|u_h|_{1,\Omega}^2 + c_1^2 h^{-1}\|u_h\|_{0,\Gamma}^2. \qquad (3.37)
$$

By this we can show that $a_h(.,.)$ is positive definite depending on $\psi(h)$:

$$
\begin{aligned}
a_h(u_h,u_h) \quad &\geq \quad |u_h|_{1,\Omega}^2 - \frac{1}{2}|u_h|_{1,\Omega}^2 - 2c_1^2 h^{-1}\|u_h\|_{0,\Gamma}^2 + \psi(h)\|u_h\|_{0,\Gamma}^2 \qquad (3.38)\\
&= \quad \frac{1}{2}|u_h|_{1,\Omega}^2 + (\psi(h) - 2c_1^2 h^{-1})\|u_h\|_{0,\Gamma}^2 \\
&\geq \quad 0 \quad \text{for } \psi(h) \geq 2c_1^2 h^{-1}.
\end{aligned}
$$

So we have stability in the sense that $a_h(.,.)$ is a positive definite bilinear form if $\psi(h) \geq 2c_1^2 h^{-1}$. With (3.38) we can now choose $\psi(h) = \gamma h^{-1}$. With $\gamma \geq 2c_1^2$ we still have a positive definite bilinear form $a_h(.,.)$.

Now we have to solve: Find $u_h \in V_h \subset H^1(\Omega)$, so that:

$$a_h(u_h, \varphi) = (g, \varphi)_{0,\Omega} + (\gamma h^{-1} q, \varphi)_{0,\Gamma} - (q, \partial_n \varphi)_{0,\Gamma} \tag{3.39}$$

with

$$a_h(u, \varphi) := (\nabla u, \nabla \varphi)_{0,\Omega} - (\partial_n u, \varphi)_{0,\Gamma} - (u, \partial_n \varphi)_{0,\Gamma} + (\gamma h^{-1} u, \varphi)_{0,\Gamma}. \tag{3.40}$$

Next we want to do the error analysis. We will show, that

$$\|e\|_{0,\Gamma} \leq ch^{3/2} \|u\|_{2,\Omega} \quad \text{and} \tag{3.41}$$
$$\|e\|_{1,\Omega} \leq ch \|u\|_{2,\Omega}.$$

And later on we proove

$$\|e\|_{0,\Omega} \leq ch^2 \|u\|_{2,\Omega}. \tag{3.42}$$

First we take a look on (3.41). Therefore we need the linear interpolant $I_h u$ of u and the appropriate estimates for the differences $u - I_h u$ on Ω and the boundary Γ:

$$\|u - I_h u\|_{k,\Omega} \leq ch^{2-k} \|u\|_{2,\Omega} \quad (k = 0, 1), \tag{3.43}$$

$$\|u - I_h u\|_{k,\Gamma} \leq ch^{3/2-k} \|u\|_{2,\Omega} \quad (k = 0, 1). \tag{3.44}$$

Now we take a look on $a(e, e)$. We can write this as:

$$\begin{aligned} a(e, e) &= (\nabla e, \nabla e)_{0,\Omega} - (\partial_n e, e)_{0,\Gamma} - (e, \partial_n e)_{0,\Gamma} + (\gamma h^{-1} e, e)_{0,\Gamma} \tag{3.45} \\ &= \|\nabla e\|_{0,\Omega}^2 - (\partial_n e, e)_{0,\Gamma} - (e, \partial_n e)_{0,\Gamma} + \gamma h^{-1} \|e\|_{0,\Gamma}^2. \end{aligned}$$

We estimate $a(e, e)$ in both directions and can than evaluate $|e|_{1,\Omega}$ and $\|e\|_{0,\Gamma}$. We start with the lower bound. For this we have to estimate $(\partial_n e, e)_{0,\Gamma}$. In the following we write e_n instead of $\partial_n e$.

By addition of $I_h u - I_h u$ we can write $\int_\Gamma ee_n \, d\Gamma$ in the following sense:

$$
\begin{aligned}
\int_\Gamma ee_n \, d\Gamma &= \int_\Gamma e(u - u_h)_n \, d\Gamma \\
&= \int_\Gamma e(u - I_h u + I_h u - u_h)_n \, d\Gamma \\
&= \int_\Gamma \left(e(u - I_h u)_n + e(I_h u - u_h)_n \right) d\Gamma.
\end{aligned}
\tag{3.46}
$$

We are now able to estimate $|\int ee_n \, d\Gamma|$ by using equation (3.34) and (3.43):

$$
\begin{aligned}
\left| \int_\Gamma ee_n \, d\Gamma \right| &\leq \|e\|_{0,\Gamma} \left(\|(u - I_h u)_n\|_{0,\Gamma} + \|(I_h u - u_h)_n\|_{0,\Gamma} \right) \\
&\overset{(3.34)}{\leq} c\|e\|_{0,\Gamma} \left(h^{-1/2}|u - I_h u|_{1,\Omega} + h^{-1/2}|I_h u - u_h|_{1,\Omega} \right) \\
&\leq c\|e\|_{0,\Gamma} \left(h^{-1/2}\|u - I_h u\|_{1,\Omega} + h^{-1/2}|I_h u - u_h|_{1,\Omega} \right) \\
&\overset{(3.43)}{\leq} c\|e\|_{0,\Gamma} \left(h^{-1/2}ch\|u\|_{2,\Omega} + h^{-1/2}|I_h u - u_h|_{1,\Omega} \right) \\
&\leq c\|e\|_{0,\Gamma} \left(ch^{1/2}\|u\|_{2,\Omega} + h^{-1/2}|I_h u - u_h|_{1,\Omega} \right).
\end{aligned}
\tag{3.47}
$$

Using again (3.43) for the estimation of $|I_h u - u_h|_{1,\Omega}$ leads to:

$$
\begin{aligned}
|I_h u - u_h|_{1,\Omega} &= |I_h u - u + u - u_h|_{1,\Omega} \\
&\leq |I_h u - u|_{1,\Omega} + |u - u_h|_{1,\Omega} \\
&\leq \|I_h u - u\|_{1,\Omega} + |e|_{1,\Omega} \\
&\overset{(3.43)}{\leq} ch\|u\|_{2,\Omega} + |e|_{1,\Omega}.
\end{aligned}
\tag{3.48}
$$

By (3.48) we then have for $\int_\Gamma ee_n d\Gamma$:

$$
\begin{aligned}
\left| \int_\Gamma ee_n \, d\Gamma \right| &\overset{(3.48)}{\leq} c\|e\|_{0,\Gamma} \left(h^{1/2}\|u\|_{2,\Omega} + h^{-1/2}\left(ch\|u\|_{2,\Omega} + |e|_{1,\Omega} \right) \right) \\
&\leq c\|e\|_{0,\Gamma} \left((1+c)h^{1/2}\|u\|_{2,\Omega} + h^{-1/2}|e|_{1,\Omega} \right) \\
&\leq ch^{1/2}\|e\|_{0,\Gamma}\|u\|_{2,\Omega} + ch^{-1/2}\|e\|_{0,\Gamma}|e|_{1,\Omega} \\
&\leq ch^{-1/2}\|e\|_{0,\Gamma} \, h \, \|u\|_{2,\Omega} + ch^{-1/2}\|e\|_{0,\Gamma}|e|_{1,\Omega}.
\end{aligned}
\tag{3.49}
$$

Using (3.36) with $\varepsilon = 2$ this results in:

$$\left| \int_{\Gamma} e e_n \, d\Gamma \right| \quad \leq \quad \frac{1}{4} h^{-1} \|e\|_{0,\Gamma}^2 + c^2 h^2 \|u\|_{2,\Omega}^2 + ch^{-1}\|e\|_{0,\Gamma}^2 + \frac{1}{4}|e|_{1,\Omega}^2 \qquad (3.50)$$

$$\leq \quad \frac{1}{4}|e|_{1,\Omega}^2 + ch^{-1}\|e\|_{0,\Gamma}^2 + ch^2\|u\|_{2,\Omega}^2.$$

Afterall we have for $a(e,e)$:

$$\begin{aligned}
a(e,e) \quad &= \quad \|\nabla e\|_{0,\Omega}^2 - 2(e_n, e)_{0,\Gamma} + \gamma h^{-1}\|e\|_{0,\Gamma}^2 \qquad (3.51) \\[4pt]
&\overset{(3.50)}{\geq} \quad |e|_{1,\Omega}^2 - 2\Big(\frac{1}{4}|e|_{1,\Omega}^2 + ch^{-1}\|e\|_{0,\Gamma}^2 + ch^2\|u\|_{2,\Omega}^2\Big) + \gamma h^{-1}\|e\|_{0,\Gamma}^2 \\[4pt]
&\geq \quad \frac{1}{2}|e|_{1,\Omega}^2 + (\gamma - 2c)h^{-1}\|e\|_{0,\Gamma}^2 - 2ch^2\|u\|_{2,\Omega}^2.
\end{aligned}$$

So we have found a lower bound for $a(e,e)$. Now we want to estimate $a(e,e)$ in the other direction. By addition of zero and Galerkin orthogonality we achieve:

$$\begin{aligned}
a(e,e) \quad &= \quad a(u - u_h, u - u_h) \qquad (3.52) \\[4pt]
&= \quad a(u - u_h, u - I_h u + I_h u - u_h) \\[4pt]
&= \quad a(u - u_h, u - I_h u) + \underbrace{a(u - u_h, I_h u - u_h)}_{=0} \\[4pt]
&= \quad a(u - u_h, u - I_h u) \\[4pt]
&= \quad (\nabla e, \nabla(u - I_h u))_{0,\Omega} - (\partial_n e, u - I_h u)_{0,\Gamma} - (\partial_n(u - I_h u), e)_{0,\Gamma} + \\[4pt]
&\quad\quad + (\gamma h^{-1} e, u - I_h u)_{0,\Gamma} \\[4pt]
&\leq \quad |e|_{1,\Omega}|u - I_h u|_{1,\Omega} + \|e_n\|_{0,\Gamma}\|u - I_h u\|_{0,\Gamma} + \\[4pt]
&\quad\quad + \|(u - I_h u)_n\|_{0,\Gamma}\|e\|_{0,\Gamma} + \gamma h^{-1}\|e\|_{0,\Gamma}\|u - I_h u\|_{0,\Gamma}.
\end{aligned}$$

We estimate every summand on its own. For this we will need (3.36), (3.43) and (3.44).

- $|e|_{1,\Omega}|u - I_h u|_{1,\Omega}$: Using (3.43) and (3.36) leads to:

$$\begin{aligned}
|e|_{1,\Omega}|u - I_h u|_{1,\Omega} \quad &\leq \quad |e|_{1,\Omega}\|u - I_h u\|_{1,\Omega} \\[4pt]
&\overset{(3.43)}{\leq} \quad |e|_{1,\Omega}\, ch\|u\|_{2,\Omega} \\[4pt]
&\overset{(3.36)}{\leq} \quad \frac{1}{2\varepsilon}|e|_{1,\Omega}^2 + \frac{\varepsilon}{2}ch^2\|u\|_{2,\Omega}^2 \\[4pt]
&= \quad c|e|_{1,\Omega}^2 + ch^2\|u\|_{2,\Omega}^2. \qquad (3.53)
\end{aligned}$$

- $\|e_n\|_{0,\Gamma}\|u - I_h u\|_{0,\Gamma}$: By (3.34) and (3.44) we have:

$$
\begin{aligned}
\|e_n\|_{0,\Gamma}\|u - I_h u\|_{0,\Gamma} \quad &= \quad \|(u - u_h)_n\|_{0,\Gamma}\|u - I_h u\|_{0,\Gamma} &(3.54)\\[4pt]
&= \quad \|(u - I_h u + I_h u - u_h)_n\|_{0,\Gamma}\|u - I_h u\|_{0,\Gamma}\\[4pt]
&\leq \quad \big(\|(u - I_h u)_n\|_{0,\Gamma} + \|(I_h u - u_h)_n\|_{0,\Gamma}\big)\|u - I_h u\|_{0,\Gamma}\\[4pt]
&= \quad \|(u - I_h u)_n\|_{0,\Gamma}\|u - I_h u\|_{0,\Gamma} +\\[4pt]
&\quad\quad + \|(I_h u - u_h)_n\|_{0,\Gamma}\|u - I_h u\|_{0,\Gamma}\\[4pt]
&\overset{(3.34)}{\leq} \quad ch^{-1/2}|u - I_h u|_{1,\Omega}\|u - I_h u\|_{0,\Gamma} +\\[4pt]
&\quad\quad + ch^{-1/2}|I_h u - u_h|_{1,\Omega}\|u - I_h u\|_{0,\Gamma}\\[4pt]
&\leq \quad ch^{-1/2}\|u - I_h u\|_{1,\Omega}\|u - I_h u\|_{0,\Gamma} +\\[4pt]
&\quad\quad + ch^{-1/2}|I_h u - u_h|_{1,\Omega}\|u - I_h u\|_{0,\Gamma}\\[4pt]
&\overset{(3.44)}{\leq} \quad ch^{1/2}\|u\|_{2,\Omega}\; ch^{3/2}\|u\|_{2,\Omega} +\\[4pt]
&\quad\quad + h^{-1/2}|I_h u - u_h|_{1,\Omega}\; ch^{3/2}\|u\|_{2,\Omega}\\[4pt]
&\leq \quad ch^2\|u\|_{2,\Omega}^2 + ch|I_h u - u_h|_{1,\Omega}\|u\|_{2,\Omega}.
\end{aligned}
$$

Using (3.48) and (3.36) leads to:

$$
\begin{aligned}
\|e_n\|_{0,\Gamma}\|u - I_h u\|_{0,\Gamma} \quad &\overset{(3.48)}{\leq} \quad ch^2\|u\|_{2,\Omega}^2 + ch^2\|u\|_{2,\Omega}^2 + ch\|u\|_{2,\Omega}|e|_{1,\Omega}\\[4pt]
&\overset{(3.36)}{\leq} \quad ch^2\|u\|_{2,\Omega}^2 + \frac{\varepsilon}{2}ch^2\|u\|_{2,\Omega}^2 + \frac{1}{2\varepsilon}|e|_{1,\Omega}^2\\[4pt]
&\leq \quad ch^2\|u\|_{2,\Omega}^2 + c|e|_{1,\Omega}^2. &(3.55)
\end{aligned}
$$

- $\|(u - I_h u)_n\|_{0,\Gamma}\|e\|_{0,\Gamma}$: For this estimation we use (3.34),(3.44) and (3.36).

$$
\begin{aligned}
\|(u - I_h u)_n\|_{0,\Gamma}\|e\|_{0,\Gamma} \quad &\overset{(3.34)}{\leq} \quad ch^{-1/2}|u - I_h u|_{1,\Omega}\|e\|_{0,\Gamma} &(3.56)\\[4pt]
&\overset{(3.44)}{\leq} \quad ch^{1/2}\|u\|_{2,\Omega}\|e\|_{0,\Gamma}\\[4pt]
&= \quad ch\|u\|_{2,\Omega}\; h^{-1/2}\|e\|_{0,\Gamma}\\[4pt]
&\overset{(3.36)}{\leq} \quad \frac{1}{2\varepsilon}h^{-1}\|e\|_{0,\Gamma}^2 + \frac{\varepsilon}{2}ch^2\|u\|_{2,\Omega}^2\\[4pt]
&= \quad ch^{-1}\|e\|_{0,\Gamma}^2 + ch^2\|u\|_{2,\Omega}^2.
\end{aligned}
$$

- $\gamma h^{-1}\|e\|_{0,\Gamma}\|u - I_h u\|_{0,\Gamma}$: Here we use again (3.44) and (3.36).

$$\gamma h^{-1}\|e\|_{0,\Gamma}\|u - I_h u\|_{0,\Gamma} \overset{(3.44)}{\leq} \gamma h^{-1}\|e\|_{0,\Gamma}\, ch^{3/2}\|u\|_{2,\Omega} \tag{3.57}$$

$$\leq \gamma h^{-1/2}\|e\|_{0,\Gamma}\, ch\|u\|_{2,\Omega}$$

$$\overset{(3.36)}{\leq} \frac{1}{2\varepsilon}\gamma h^{-1}\|e\|_{0,\Gamma}^2 + \frac{\varepsilon}{2}ch^2\|u\|_{2,\Omega}^2$$

$$\leq c\gamma h^{-1}\|e\|_{0,\Gamma}^2 + ch^2\|u\|_{2,\Omega}^2.$$

By these four inequalities (3.53), (3.55)- (3.57) we are now able to estimate $a(e,e)$:

$$a(e,e) \overset{(3.52)}{\leq} |e|_{1,\Omega}|u - I_h u|_{1,\Omega} + \|e_n\|_{0,\Gamma}\|u - I_h u\|_{0,\Gamma} \tag{3.58}$$

$$+\|(u - I_h u)_n\|_{0,\Gamma}\|e\|_{0,\Gamma} + \gamma h^{-1}\|e\|_{0,\Gamma}\|u - I_h u\|_{0,\Gamma}$$

$$\leq c|e|_{1,\Omega}^2 + ch^2\|u\|_{2,\Omega}^2 + ch^2\|u\|_{2,\Omega}^2 + c|e|_{1,\Omega}^2 + ch^{-1}\|e\|_{0,\Gamma}^2$$

$$+ch^2\|u\|_{2,\Omega}^2 + c\gamma h^{-1}\|e\|_{0,\Gamma}^2 + ch^2\|u\|_{2,\Omega}^2$$

$$\leq c|e|_{1,\Omega}^2 + ch^2\|u\|_{2,\Omega}^2 + c\gamma h^{-1}\|e\|_{0,\Gamma}^2.$$

The upper bound from (3.58) together with the lower bound from (3.51) results in

$$c|e|_{1,\Omega}^2 + ch^2\|u\|_{2,\Omega}^2 + c\gamma h^{-1}\|e\|_{0,\Gamma}^2 \geq a(e,e) \tag{3.59}$$

$$\geq \frac{1}{2}|e|_{1,\Omega}^2 + (\gamma - 2\tilde{c})h^{-1}\|e\|_{0,\Gamma}^2 - 2\tilde{c}h^2\|u\|_{2,\Omega}^2.$$

By (3.59) we can now estimate the sum of the error e in the H^1-seminorm over Ω and e in the L^2-norm over Γ with u in the H^2-norm over Ω:

$$ch^2\|u\|_{2,\Omega}^2 \geq c_2|e|_{1,\Omega}^2 + c_3(\gamma)h^{-1}\|e\|_{0,\Gamma}^2. \tag{3.60}$$

For $c_2 > 0$ and $c_3 > 0$, we achieve the following inequalities:

$$|e|_{1,\Omega}^2 \leq ch^2\|u\|_{2,\Omega}^2, \tag{3.61}$$

$$\|e\|_{0,\Gamma}^2 \leq ch^3\|u\|_{2,\Omega}^2 \tag{3.62}$$

and so

$$\|e\|_{0,\Gamma} \leq ch^{3/2}\|u\|_{2,\Omega}. \tag{3.63}$$

In (3.61) we only have the error in the H^1-seminorm but we want to have it in the H^1-norm. For this we have by the inequalities for $|e|_{1,\Omega}^2$ and $\|e\|_{0,\Gamma}^2$ ($h \leq 1$):

$$
\begin{aligned}
\|e\|_{1,\Omega}^2 \quad &= \quad |e|_{1,\Omega}^2 + \|e\|_{0,\Omega}^2 \\
&\leq \quad |e|_{1,\Omega}^2 + c\Big(|e|_{1,\Omega} + \|e\|_{0,\Gamma}\Big)^2 \\
&\leq \quad |e|_{1,\Omega}^2 + c|e|_{1,\Omega}^2 + c|e|_{1,\Omega}\|e\|_{0,\Gamma} + c\|e\|_{0,\Gamma}^2 \\
&\overset{(3.61)-(3.63)}{\leq} \quad ch^2\|u\|_{2,\Omega}^2 + ch\|u\|_{2,\Omega}\ ch^{3/2}\|u\|_{2,\Omega} + ch^3\|u\|_{2,\Omega}^2 \\
&\leq \quad ch^2\|u\|_{2,\Omega}^2.
\end{aligned}
\tag{3.64}
$$

This results in:

$$
\|e\|_{1,\Omega} \leq ch\|u\|_{2,\Omega}. \tag{3.65}
$$

I.e. we have for Nitsche's method the same order of convergence for the error with respect to the H^1-norm as for the classical variational formulation. For the L^2-error we expect a better result than for the H^1- error. Now we want to prove this. Therefore we take a look at the dual problem to (3.39).

For $v \in V_h$ we have:

$$
(\nabla e, \nabla v)_{0,\Omega} - (\partial_n e, v)_{0,\Gamma} - (e, \partial_n v)_{0,\Gamma} + \gamma h^{-1}(e, v)_{0,\Gamma} = 0. \tag{3.66}
$$

We choose $v = I_h w$ with w from:

$$
\begin{aligned}
-\Delta w &= e \quad \text{on } \Omega, \tag{3.67} \\
w &= 0 \quad \text{on } \Gamma. \tag{3.68}
\end{aligned}
$$

Because of $w \in H^2(\Omega)$ we have: $\|w\|_{2,\Omega} \leq c\|e\|_{0,\Omega}$. Using equation (3.67) and Green's formula we are able to estimate $\|e\|_{0,\Omega}$.

$$\|e\|_{0,\Omega}^2 = -(e, \Delta w)_{0,\Omega} \tag{3.69}$$

$$= (\nabla e, \nabla w)_{0,\Omega} - (e, \partial_n w)_{0,\Gamma}$$

$$\overset{-(3.66)}{=} (\nabla e, \nabla w)_{0,\Omega} - (e, \partial_n w)_{0,\Gamma} - (\nabla e, \nabla I_h w)_{0,\Omega} + (e, \partial_n I_h w)_{0,\Gamma}$$

$$+ (\partial_n e, I_h w)_{0,\Gamma} - \gamma h^{-1}(e, I_h w)_{0,\Gamma}$$

$$= (\nabla e, \nabla(w - I_h w))_{0,\Omega} - (e, \partial_n(w - I_h w))_{0,\Gamma} + (\partial_n e, I_h w)_{0,\Gamma}$$

$$- \gamma h^{-1}(e, I_h w)_{0,\Gamma}$$

$$\overset{w=0 \text{ on } \Gamma}{=} (\nabla e, \nabla(w - I_h w))_{0,\Omega} - (e, \partial_n(w - I_h w))_{0,\Gamma} - (\partial_n e, w - I_h w)_{0,\Gamma}$$

$$+ \gamma h^{-1}(e, w - I_h w)_{0,\Gamma}.$$

By equations (3.63), (3.65) and equations (3.43), (3.44) we can estimate every term on its own:

- $(\nabla e, \nabla(w - I_h w))_{0,\Omega}$

$$(\nabla e, \nabla(w - I_h w))_{0,\Omega} \leq \|e\|_{1,\Omega}\|w - I_h w\|_{1,\Omega} \tag{3.70}$$

$$\overset{(3.65),(3.43)}{\leq} ch\|u\|_{2,\Omega} \; ch\|w\|_{2,\Omega}$$

$$\leq ch^2\|u\|_{2,\Omega}\|e\|_{0,\Omega}$$

- $(e, \partial_n(w - I_h w))_{0,\Gamma}$

$$(e, \partial_n(w - I_h w))_{0,\Gamma} \leq \|e\|_{0,\Gamma}\|(w - I_h w)_n\|_{0,\Gamma} \tag{3.71}$$

$$\overset{(3.34)}{\leq} \|e\|_{0,\Gamma} \; ch^{-1/2}|w - I_h w|_{1,\Omega}$$

$$\overset{(3.63),(3.43)}{\leq} ch^{3/2}\|u\|_{2,\Omega} \; ch^{1/2}\|w\|_{2,\Omega}$$

$$\leq ch^2\|u\|_{2,\Omega}\|e\|_{0,\Omega}$$

- $\gamma h^{-1}(e, w - I_h w)_{0,\Gamma}$

$$\gamma h^{-1}(e, w - I_h w)_{0,\Gamma} \leq \gamma h^{-1}\|e\|_{0,\Gamma}\|w - I_h w\|_{0,\Gamma} \tag{3.72}$$

$$\overset{(3.63),(3.43)}{\leq} \gamma h^{-1}ch^{3/2}\|u\|_{2,\Omega} \; ch^{3/2}\|w\|_{2,\Omega}$$

$$\leq ch^2\|u\|_{2,\Omega}\|e\|_{0,\Omega}$$

- $(\partial_n e, w - I_h w)_{0,\Gamma}$

  $(\partial_n e, w - I_h w)_{0,\Gamma} \leq \|e_n\|_{0,\Gamma} \|w - I_h w\|_{0,\Gamma}.$

  First we write e as $e = u - I_h u + I_h u - u_h$ and estimate $\|e\|_{0,\Gamma}$:

$$
\begin{aligned}
\|e_n\|_{0,\Gamma} &\leq \quad \|(u - I_h u)_n\|_{0,\Gamma} + \|(I_h u - u_h)_n\|_{0,\Gamma} \qquad (3.73)\\
&\overset{(3.34)}{\leq} \quad ch^{-1/2}|u - I_h u|_{1,\Omega} + ch^{-1/2}|I_h u - u_h|_{1,\Omega}\\
&\overset{(3.43)}{\leq} \quad ch^{-1/2}ch\|u\|_{2,\Omega} + ch^{-1/2}|I_h u - u_h|_{1,\Omega}\\
&\overset{(3.48)}{\leq} \quad ch^{1/2}\|u\|_{2,\Omega} + ch^{-1/2}(ch\|u\|_{2,\Omega} + |e|_{1,\Omega})\\
&\leq \quad ch^{1/2}\|u\|_{2,\Omega} + ch^{-1/2}ch\|u\|_{2,\Omega} + ch^{-1/2}\|e\|_{1,\Omega}\\
&\leq \quad ch^{1/2}\|u\|_{2,\Omega} + ch^{-1/2}\|e\|_{1,\Omega}\\
&\overset{(3.65)}{\leq} \quad ch^{1/2}\|u\|_{2,\Omega} + ch^{-1/2}h\|u\|_{2,\Omega}\\
&\leq \quad ch^{1/2}\|u\|_{2,\Omega}.
\end{aligned}
$$

So, afterall we have:

$$
\begin{aligned}
(\partial_n e, w - I_h w)_{0,\Gamma} &\leq \quad \|e_n\|_{0,\Gamma}\|w - I_h w\|_{0,\Gamma} \qquad (3.74)\\
&\overset{(3.73),(3.43)}{\leq} \quad ch^{1/2}\|u\|_{2,\Omega}\ ch^{3/2}\|w\|_{2,\Omega}\\
&\leq \quad ch^2\|u\|_{2,\Omega}\|e\|_{0,\Omega}
\end{aligned}
$$

and for $\|e\|_{0,\Omega}^2$ we reach by the equations (3.70), (3.71),(3.72) and (3.74):

$$
\begin{aligned}
\|e\|_{0,\Omega}^2 &\leq \|e\|_{1,\Omega}\|\|w - I_h w\|_{1,\Omega} + \|e\|_{0,\Gamma}\|(w - I_h w)_n\|_{0,\Gamma} \qquad (3.75)\\
&\quad + \gamma h^{-1}\|e\|_{0,\Gamma}\|w - I_h w\|_{0,\Gamma} + \|e_n\|_{0,\Gamma}\|w - I_h w\|_{0,\Gamma}\\
&\leq ch^2\|u\|_{2,\Omega}\|e\|_{0,\Omega}.
\end{aligned}
$$

After division by $\|e\|_{0,\Omega}$ we reach the expected result:

$$
\|e\|_{0,\Omega} \leq ch^2\|u\|_{2,\Omega}. \qquad (3.76)
$$

Compared to the classical variational formulation we have the same order of convergence for the L^2-error. We have another function space because the Dirichlet

boundary condition isn't hidden in the function space but the more complex problem to be solved. Also we have used a constant γ which we haven't determined yet.

From inequality (3.34)

$$\|\partial_n u\|_{0,\Gamma}^2 \le c_1^2 h^{-1} |u|_{1,\Omega}^2$$

and (3.38) (stability) we know, that $\gamma \ge 2c_1^2$ must be fulfilled. Therefore we have to determine the constant c_1^2. Following Hansbo [19] we have to calculate c_1^2 as the largest eigenvalue in the problem of finding $u_h \in V_h$ and $\lambda \in \mathbb{R}$ such that

$$(h^{1/2}\partial_n u_h, \partial_n \varphi)_{0,E} = \lambda(\nabla u_h, \nabla \varphi)_{0,T} \quad \forall \varphi \in V_h. \tag{3.77}$$

Where T is an element of the triangulation and $E = \partial T \cap \Gamma$. We can see that c_1^2 depends on the geometry of the element and the degree of the polynomials we choose for the approximation. If we choose linear elements, we know that $\nabla \varphi$ is constant on each element. If we call $meas(F)$ the length, area or volume of the set F we have according to Hansbo [19]:

$$\|h^{1/2}\partial_n \varphi\|_{0,E}^2 \le \frac{h \; meas(E)}{meas(T)} \|\nabla \varphi\|_{0,T}^2. \tag{3.78}$$

If we define h we can determine c_1^2. If we choose triangles T and h as the distance from the interior node to the boundary E we have

$$meas(T) = \frac{h \; meas(E)}{2} \tag{3.79}$$

and by equation (3.78) follows:

$$\|h^{1/2}\partial_n \varphi\|_{0,E}^2 \le \frac{h \; meas(E)}{\dfrac{h \; meas(E)}{2}} \|\nabla \varphi\|_{0,T}^2 = 2\|\nabla \varphi\|_{0,T}^2 \tag{3.80}$$

By equation (3.34) we have $c_1^2 = 2$. Because we need $\gamma \ge 2c_1^2$ we have $\gamma \ge 4$.

3.3.1 Numerical Results

Now we want to verify the theoretical results. We do the calculations for a test example and choose $\gamma = 1$ and $\gamma = 10$. For the two cases of γ we take a look on

$\|e\|_{0,\Omega}$ and $\|e\|_{1,\Omega}$. We will see that $\gamma = 1$ is too small, the H^1-error increases. But for $\gamma = 10$ we ratify the theoretical results. If we choose γ too big, the penalty term $\gamma h^{-1}(u_h, \varphi)_\Gamma$ has too much importance.

As a test example we choose

$$\begin{aligned} -\Delta u \;\; &= x - x^2 + y - y^2 \qquad \text{on } \Omega = (0,1)^2 \\ u \;\; &= 0 \qquad\qquad\qquad\quad\; \text{on } \Gamma. \end{aligned} \qquad (3.81)$$

For this problem we know the analytical solution:

$$u(x,y) = \frac{1}{2}\, x\, y\, (1-x)\, (1-y).$$

From the theory we know that $\|e\|_{1,\Omega} \in O(h)$ and $\|e\|_{0,\Omega} \in O(h^2)$ if we choose the constant γ adequate. We want to verify this by the example.

For the discretisation we choose quadrilaterals. For the parameter γ we analyse two cases. First in table 3.1 we present the results for the L^2- and H^1- error calculated with $\gamma = 10$. There we see that the decrease of the L^2- error is quadratic and that of the H^1-error is linear which verifies the theoretical results.

In the second case we do the calculation with $\gamma = 1$. The results in table 3.2 show, that this parameter is too small. The L^2- error decreases, but is not in $O(h^2)$ and the H^1-error increases while getting smaller with h.

These results are graphically presented in the Figures 3.1 and 3.2. In Figure 3.1 we see the L^2-error depending on h for $\gamma = 1$ and $\gamma = 10$. For $\gamma = 10$ we see the quadratic decreasing and for $\gamma = 1$ that the error decrease, but not quadratic. Figure 3.2 shows the linear decreasing of the H^1-error for $\gamma = 10$ and the increasing for $\gamma = 1$ depending on h.

h	$\|e\|_{0,\Omega}$	ratio	$\|e\|_{1,\Omega}$	ratio
1/2	$3.744433 * 10^{-3}$		$3.942599 * 10^{-2}$	
1/4	$1.04092 * 10^{-3}$	0.2779	$1.899091 * 10^{-2}$	0.4816
1/8	$2.752370 * 10^{-4}$	0.2644	$9.378373 * 10^{-3}$	0.4938
1/16	$7.117707 * 10^{-5}$	0.2586	$4.671045 * 10^{-3}$	0.498
1/32	$1.813167 * 10^{-5}$	0.2547	$2.332117 * 10^{-3}$	0.4993
1/64	$4.578049 * 10^{-6}$	0.2525	$1.165313 * 10^{-3}$	0.4997
1/128	$1.150350 * 10^{-6}$	0.2513	$5.824802 * 10^{-4}$	0.4998
1/256	$2.8833 * 10^{-7}$	0.2506	$2.911971 * 10^{-4}$	0.4999
1/512	$7.217610 * 10^{-8}$	0.2503	$1.455879 * 10^{-4}$	0.4999

Table 3.1: L^2- and H^1-error for the test example using Nitsche's method with $\gamma = 10$.

h	$\|e\|_{0,\Omega}$	ratio	$\|e\|_{1,\Omega}$	ratio
1/2	$5.370479 * 10^{-2}$		$1.925762 * 10^{-1}$	
1/4	$3.923868 * 10^{-2}$	0.73	$3.709428 * 10^{-1}$	1.9262
1/8	$2.227989 * 10^{-2}$	0.5678	$2.202936 * 10^{-1}$	0.5939
1/16	$1.576394 * 10^{-2}$	0.7075	$4.483295 * 10^{-1}$	2.0351
1/32	$1.119507 * 10^{-2}$	0.7102	$6.247318 * 10^{-1}$	1.3935
1/64	$7.951525 * 10^{-3}$	0.7103	$8.829628 * 10^{-1}$	1.4133
1/128	$5.639546 * 10^{-3}$	0.7092	1.250846	1.4166
1/256	$3.994662 * 10^{-3}$	0.7083	1.771445	1.4162
1/512	$2.8277263 * 10^{-3}$	0.7079	2.507313	1.4154

Table 3.2: L^2- and H^1-error for the test example using Nitsche's method with $\gamma = 1$.
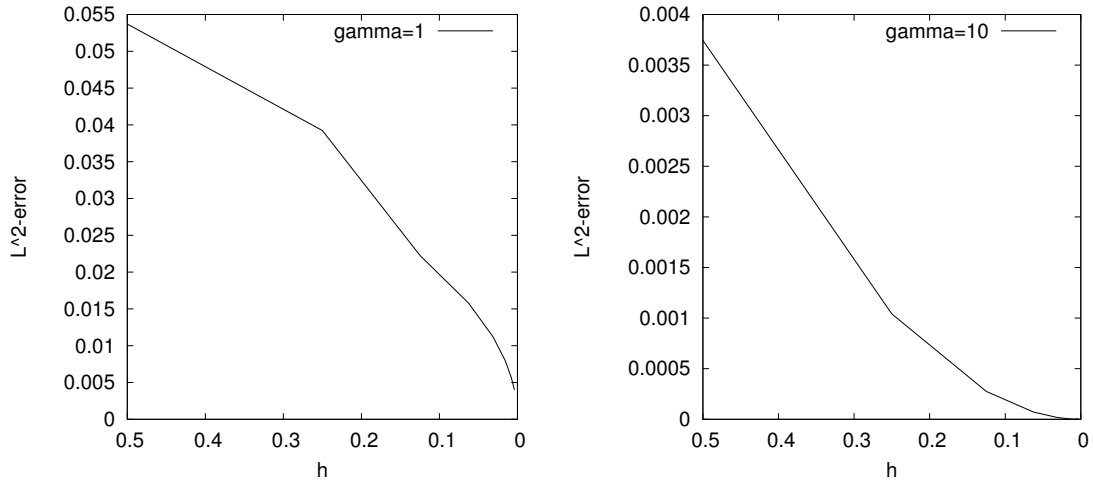
Figure 3.1: L^2-error for the test example with $\gamma = 1$ (left) and $\gamma = 10$ (right).
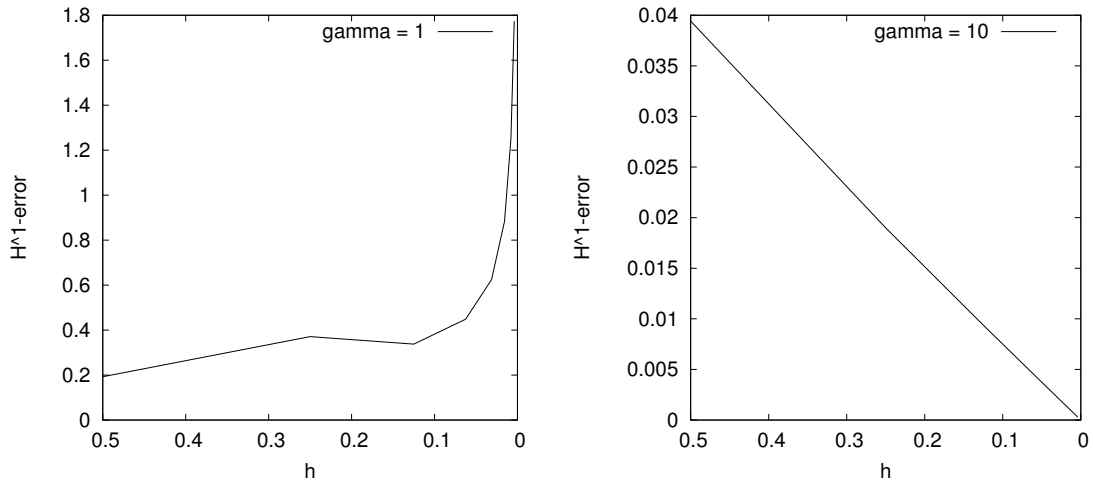
Figure 3.2: H^1-error for the test example with $\gamma = 1$ (left) and $\gamma = 10$ (right).

In this Section we have introduced a symmetric variant of Nitsches method to handle Dirichlet boundary data in variational formulation without hide them in the function space. We have shown that the error estimates are of the same order as in the classical variational formulation if we choose γ large enough. For this formulation we have in contrast to the classical variational formulation another underlying function space but we have the comnplexer problem to solve and we have to estimate the constant γ which is important for the convergence of the method.

4 Inverse Problems

As described in the introduction we want to solve inverse problems. Before we do this in Section 5 we need some theoretical results about solving inverse problems. Here we only want to present the basics. For proofs and more information see the literature, e.g. Louis [25] and Rieder [30] on which this Section is based.

4.1 The theory of inverse problems

In this Section we define what is an inverse problem and when to call it ill-posed. We reduce solving the inverse problem to solving the normal equation $A^*Af = A^*g$, introduce the Moore-Penrose inverse A^+ and the singular system which we need in the next Section for the regularisation methods.

At first we want to recapitulate from the introduction what is an inverse problem and when we call a problem ill-posed.

> For given $A : X \to Y$ we call the calculation of Ax with $x \in X$ the direct problem. If we want to find $x \in X$ for given $y \in Y$, so that $Ax = y$, we call this an inverse problem.

Definition 4.1. *Let $A : X \to Y$ be a mapping between the topologic spaces X, Y. The problem (A, X, Y) is called well-posed, if*

- *$\forall\ g \in Y\ \ \exists\ a\ solution\ to\ Af = g$.*

- *The solution is well defined.*

- *The solution depends continuously on the data, i.e. A^{-1} is continuous.*

If one of these conditions is not satisfied the problem is called ill-posed.

If $g \notin R(A)$ there doesn't exist a solution to $Af = g$. So we have to define a new solution idea. In the following X and Y are Hilbert spaces. We call $f \in X$ solution to $Af = g$ with $g \notin R(A)$ if f minimizes the residual

$$\|Af - g\|_Y \leq \|A\phi - g\|_Y \quad \forall \phi \in X. \tag{4.1}$$

For $g \in R(A)$ this definition is also valid and results in the solution f.

In theorem 4.1 we formulate equivalent results for reaching this f. Therefore we need the adjoint operator to $A \in \mathcal{L}(X, Y)$ $A^* \in \mathcal{L}(Y, X)$ which is characterised by

$$\forall\, x \in X : \ (Ax, y)_Y = (x, A^*y)_X \tag{4.2}$$

and the orthogonal projector $P_M \in \mathcal{L}(Z)$ from the Hilbert space Z onto a subset $M \subset Z$. By the following theorem we are able to find $f \in X$ which minimizes the residual by solving the normal equation.

Theorem 4.1. *Let $g \in Y$ and $A \in \mathcal{L}(X, Y)$. Then the following declarations are equivalent*

a) *$f \in X$ satisfies $Af = P_{\overline{R(A)}}g$.*

b) *$f \in X$ minimizes the residual:*

$$\|Af - g\|_Y \leq \|A\phi - g\|_Y \quad \forall \phi \in X. \tag{4.3}$$

c) *$f \in X$ solves the normal equation*

$$A^*Af = A^*g. \tag{4.4}$$

If we call $\mathbb{L}(g) := \{\varphi \in X \mid A^*A\varphi = A^*g\}$ the set of solutions of the normal equation, we can formulate the following properties of the set $\mathbb{L}(g)$:

Lemma 4.1. *Let $g \in Y$. Then*

- $\mathbb{L}(g) \neq \emptyset \quad \Leftrightarrow \quad g \in R(A) \oplus R(A)^{\perp}$.

- $\mathbb{L}(g)$ *is closed and convex.*

As we are interested in only one solution of the normal equation, we need a distinguished solution in the set $\mathbb{L}(g)$. We choose the element with minimal norm.

Lemma 4.2. *For $g \in R(A) \oplus R(A)^{\perp}$ $\mathbb{L}(g)$ contains a well defined f^{+} with minimal norm:*

$$\|f^{+}\|_X < \|\phi\|_X \quad \forall \phi \in \mathbb{L}(g) \backslash \{f^{+}\}. \tag{4.5}$$

By this lemma we have the existence of a unique solution of the normal equation if $g \in R(A) \oplus R(A)^{\perp}$.

Definition 4.2. *The mapping $A^{+} : D(A^{+}) \subset Y \rightarrow X$ with $D(A^{+}) = R(A) \oplus R(A)^{\perp}$ which assign every $g \in D(A^{+})$ the well defined element $f^{+} \in \mathbb{L}(g)$ with minimal norm, is called Moore-Penrose-Inverse of $A \in \mathcal{L}(X,Y)$.*

The element $f^{+} = A^{+}g$ is called minimum-norm-solution of $Af = g$.

It can be shown, that $f^{+} = A^{+}g$ is the unique solution of the normal equation in $N(A)^{\perp}$ if $g \in D(A^{+})$. The properties of A^{+} are listed in the following theorem.

Theorem 4.2. *The Moore-Penrose-Inverse A^{+} for $A \in \mathcal{L}(X,Y)$ has the following qualities:*

- A^{+} *is defined on the whole space Y iff $R(A)$ is closed.*

- $R(A^{+}) = N(A)^{\perp}$.

- A^{+} *is linear.*

- A^{+} *is continuous iff $R(A) = \overline{R(A)}$.*

A^+ is uniquely characterised by the four Moore-Penrose-Axioms:

$$
\begin{aligned}
AA^+A &= A, & A^+AA^+ &= A^+, \\
A^+A &= P_{\overline{R(A^*)}}, & AA^+ &= P_{\overline{R(A)}}.
\end{aligned}
\tag{4.6}
$$

By A^+ and f^+ we have a well defined solution to our problem. So the ill-posedness of the problem is caused by A^{-1} which is not continuous. This leads us to a new definition of ill-posedness in the sense of Nashed.

Definition 4.3. *We call a problem (A, X, Y) ill-posed in the sense of Nashed when $R(A)$ is not closed in Y. Otherwise the problem is called well-posed in the sense of Nashed.*

A typical example for ill-posed problems are problems with compact operators which have infinite dimensional range. For analytical results we need the singular value decomposition. Let $A \in \mathcal{L}(X)$ with X a normed space. A is called self-adjoint if $A^* = A$. $\sigma(A) = \{\lambda \in \mathbb{C} \mid \lambda I - A \text{ is not invertible}\}$ is called spectrum of A. $\lambda \in \mathbb{C}$ is eigenvalue of A, if there exist $x \neq 0$ with $Ax = \lambda x$.

Theorem 4.3. *Let X be a Hilbert space and $A \in \mathcal{K}(X)$ a self-adjoint compact operator with eigenvalues $\lambda_n \in \mathbb{R}$ and orthonormal eigenvectors $v_n \in X$. For every $x \in X$ we have:*

$$
Ax = \sum_{n=1}^{\infty} \lambda_n \langle x, v_n \rangle v_n.
\tag{4.7}
$$

Now, let $A \in \mathcal{K}(X, Y)$ with X, Y Hilbert spaces. Then $T = A^*A \in \mathcal{K}(X)$ is self-adjoint. The corresponding eigenvalues λ_n of T have been arranged according to size:

$$
\lambda_1 \geq \lambda_2 \geq \ldots > 0.
$$

With $\sigma_n := +\sqrt{\lambda_n}$ and $u_n := \sigma_n^{-1} A v_n$, $n \in \mathbb{N}$ we have

$$
Av_n = \sigma_n u_n, \quad A^* u_n = \sigma_n v_n
\tag{4.8}
$$

where $\{u_n\}$ is an orthonormal system for $\overline{R(A)} = N(A^*)^{\perp}$ because

$$
\langle u_j, u_k \rangle_Y = \frac{1}{\sigma_j \sigma_k} \langle Av_j, Av_k \rangle_Y = \frac{1}{\sigma_j \sigma_k} \langle A^*Av_j, v_k \rangle_X = \frac{\sigma_j}{\sigma_k} \langle v_j, v_k \rangle_X = \delta_{j,k}
\tag{4.9}
$$

and $\{v_n\}$ for $\overline{R(A^*)} = N(A)^\perp$. With these we are able to define the singular system of A.

Definition 4.4. $\{v_n, u_n; \sigma_n\}_{n \geq 0} \subset X \times Y \times (0, \infty)$ *is called singular system of A.*

$$Af = \sum_{n=1}^{\infty} \sigma_n \langle f, v_n \rangle_X u_n. \tag{4.10}$$

is called singular value decomposition.

We can also describe A^*g and A^+g as a series with coefficients of the singular system of A.

If $A \in \mathcal{K}(X, Y)$ with singular system $\{v_n, u_n; \sigma_n\}$ then

$$A^*g = \sum_{n=1}^{\infty} \sigma_n \langle g, u_n \rangle_Y v_n \tag{4.11}$$

$$A^+g = \sum_{n=1}^{\infty} \sigma_n^{-1} \langle g, u_n \rangle_Y v_n \quad \text{for } g \in D(A^+). \tag{4.12}$$

If $R(A)$ is finite dimensional, A^+ is continuous.

Now, let $A \in \mathcal{K}(X, Y)$ with singular system $\{v_n, u_n; \sigma_n\}$ and $\phi : [0, \infty) \to \mathbb{R}$ a piecewise continuous function with jump discontinuity. Therefore we define:

$$\phi(A^*A)x := \sum_{n=1}^{\infty} \phi(\sigma_n^2) \langle x, v_n \rangle_X v_n + \phi(0) P_{\mathcal{N}(A)} x. \tag{4.13}$$

For $\phi(t) = +\sqrt{t}$ we call $\phi(A^*A)$ absolute value of A:

$$|A|x := (A^*A)^{1/2} x = \sum_{n=1}^{\infty} \sigma_n \langle x, v_n \rangle_X v_n. \tag{4.14}$$

For $|A^*|$ we get:

$$|A^*|y = (AA^*)^{1/2} y = \sum_{n=1}^{\infty} \sigma_n \langle y, u_n \rangle_Y u_n. \tag{4.15}$$

By this we can represent the range of A^* as the range of $|A|$ and the range of A as the range of $|A^*|$:

Theorem 4.4. *Let $A \in \mathcal{L}(X, Y)$ with X, Y Hilbert spaces. Then:*

$$
\begin{aligned}
R(A^*) &= R(|A|) &= R((AA^*)^{1/2}). \\
R(A) &= R(|A^*|) &= R((A^*A)^{1/2}).
\end{aligned}
\tag{4.16}
$$

For later use we generalise equation (4.14):

$$
|A|^{2\nu} x := (A^*A)^\nu x = \sum_{n=1}^\infty \sigma_n^{2\nu} \langle x, v_n \rangle_X v_n.
\tag{4.17}
$$

We need this for the following theory of regularisation.

4.2 Regularisation

In this Section we define a regularisation method, introduce the worst case error and how to reach a regularisation method by using the singular system. As a special regularisation which we use for the calculation in the next Section, we introduce the Tikhonov-Phillips-regularisation.

If $R(A)$ is not closed, the generalized inverse A^+ is not continuous. For this problem we need the regularisation of inverse problems, i.e. an approximation of A^+ with a family of continuous operators $\{R_t\}_{t>0}$ defined on Y. With a suitable choice of t this leads us to

Definition 4.5. *Let $A \in \mathcal{L}(X, Y)$ and $\{R_t\}_{t>0}$ a family of continuous (maybe not linear) operators from Y to X with $R_t 0 = 0$. If there exists a mapping $\gamma : (0, \infty) \times Y \to (0, \infty)$ so that for all $g \in R(A)$*

$$
\sup \left\{ \|A^+ g - R_{\gamma(\epsilon, g^\epsilon)} g^\epsilon\|_X \;\middle|\; g^\epsilon \in Y, \; \|g - g^\epsilon\|_Y \le \epsilon \right\} \to 0 \quad (\epsilon \to 0)
\tag{4.18}
$$

is satisfied, the pair $(\{R_t\}_{t>0}, \gamma)$ is called regularisation or regularisation method for A^+. If all R_t are linear, the regularisation is linear. The mapping γ is a parameter choice with

$$
\lim_{\epsilon \to 0} \sup \{ \gamma(\epsilon, g^\epsilon) \mid g^\epsilon \in Y, \; \|g - g^\epsilon\|_Y \le \epsilon \} = 0.
\tag{4.19}
$$

The value $\gamma(\epsilon, g^\epsilon)$ is the regularisation parameter. If it depends only on ϵ it is called a-priori, else a-posteriori parameter choice.

From equation (4.18) we have the convergence:

$$\lim_{\epsilon \to 0} \| R_{\gamma(\epsilon,g)} g - A^+ g \|_X = 0 \quad \forall \, g \in R(A). \tag{4.20}$$

The reconstruction error $\| A^+ g - R_\gamma g^\epsilon \|_X$ for a linear regularisation is bounded by the sum of approximation error and data error:

$$\| A^+ g - R_\gamma g^\epsilon \|_X \leq \underbrace{\| A^+ g - R_\gamma g \|_X}_{\text{approximation error}} + \underbrace{\| R_\gamma (g - g^\epsilon) \|_X}_{\text{data error}} \tag{4.21}$$

For information about the convergence rate of regularisation methods we need additional assumptions to the general solution. Therefore we need the spaces $X_\nu \subset X$ with

$$X_\nu := R(|A|^\nu) = \{ |A|^\nu z \mid z \in \mathcal{N}(A)^\perp \}, \quad \nu \geq 0. \tag{4.22}$$

For these we have $X_\nu \subset X_\mu$ for $\nu \geq \mu$ and $X_0 = \mathcal{N}(A)^\perp$. Due to this definition we can illustrate $x \in X_\nu$ as sum with coefficients of the singular system. For $x \in X_\nu$ exists $z \in \mathcal{N}(A)^\perp$ with $x = |A|^\nu z = \sum_{k=1}^{\infty} \sigma_k^\nu \langle z, v_k \rangle_X v_k$. Now we can define a norm $\|.\|_\nu$:

$$\| x \|_\nu^2 := \| z \|_X^2 = \sum_{k=1}^{\infty} \sigma_k^{-2\nu} |\langle x, v_k \rangle_X|^2, \tag{4.23}$$

by which we can give an alternative characterisation of the space X_ν:

$$X_\nu = \{ x \in \mathcal{N}(A)^\perp \mid \| x \|_\nu < \infty \}. \tag{4.24}$$

We call a continuous mapping $T : Y \to X$ with $T0 = 0$ reconstruction method for solving the operator equation with operator $A \in \mathcal{L}(X, Y)$. The question is now, what is the worst reconstruction error for a smooth solution with noisy data. The answer is delivered by the following supremum under the assumption $f \in X_\nu$ with $\| f \|_\nu \leq \rho$:

$$
\begin{aligned}
E_\nu(\epsilon, \rho, T) \; := \; & \sup \{ \| T g^\epsilon - A^+ g \|_X \mid g \in \mathcal{R}(A), \; g^\epsilon \in Y, \\
& \| g - g^\epsilon \|_Y \leq \epsilon, \; \| A^+ g \|_\nu \leq \rho \} \tag{4.25} \\
= \; & \sup \{ \| T g^\epsilon - x \|_X \mid x \in X_\nu, \; g^\epsilon \in Y, \; \| A x - g^\epsilon \|_Y \leq \epsilon, \; \| x \|_\nu \leq \rho \}.
\end{aligned}
$$

The adequate reconstruction method is the method with smallest error $E_\nu(\epsilon, \rho, T)$. So we are interested in the error

$$E_\nu(\epsilon, \rho) := \inf\{E_\nu(\epsilon, \rho, T) \mid T : Y \to X \text{ continuous, } T0 = 0\}. \tag{4.26}$$

For $A \in \mathcal{L}(X, Y)$ has been shown (see e.g. Louis [25])

$$E_\nu(\epsilon, \rho) = e_\nu(\epsilon, \rho) := \sup\{\|x\|_X \mid x \in X_\nu, \ \|Ax\|_Y \leq \epsilon, \ \|x\|_\nu \leq \rho\}. \tag{4.27}$$

By $e_\nu(\epsilon, \rho)$ we are able to declare the worst case error of the best reconstruction-method without knowing the reconstruction method if we know the noise level ϵ, $f \in X_\nu$ and $\|f\|_\nu$ is bounded by ρ.

Theorem 4.5. *Let $A \in \mathcal{L}(X, Y)$ and $\nu > 0$. Then*

$$e_\nu(\epsilon, \rho) \leq \rho^{1/(\nu+1)} \epsilon^{\nu/(\nu+1)}. \tag{4.28}$$

Moreover there exists $\{\epsilon_k\}_{k \in \mathbb{N}}$ with $\epsilon_k \to 0$ for $k \to \infty$, for which we have

$$e_\nu(\epsilon_k, \rho) = \rho^{1/(\nu+1)} \epsilon_k^{\nu/(\nu+1)}. \tag{4.29}$$

For a proof see Rieder [30].

By equation (4.28) we are able to establish the new notations optimal and of optimal order.

Definition 4.6. *Let $A \in \mathcal{L}(X, Y)$ with an open range. The family of reconstruction methods $\{T_\epsilon\}_{\epsilon>0}$ is called of optimal order concerning X_ν if there exists a constant $C_\nu > 1$ so that for all $\epsilon > 0$ sufficiently small and $\rho \geq 0$:*

$$E_\nu(\epsilon, \rho, T_\epsilon) \leq C_\nu \rho^{1/(\nu+1)} \epsilon^{\nu/(\nu+1)}. \tag{4.30}$$

If this estimation is fulfilled with $C_\nu = 1$, the reconstruction method is called optimal.

Regularisation methods are reconstruction methods. Due to this the above definition is also valid for regularisation methods.

Theorem 4.6. *Let $A \in \mathcal{L}(X, Y)$ with open range. There exists a family of continuous operators $\{R_t\}_{t \geq 0}$, $R_t : Y \to X$, $R_t 0 = 0$ and a mapping $\gamma : (0, \infty) \times Y \to (0, \infty)$, so that $\{R_{\gamma(\epsilon, .)}.\}_{\epsilon > 0}$ is of optimal order concerning X_ν. For $b > 1$ γ_b is defined as $\gamma_b(\epsilon, .) := \gamma(b\epsilon, .)$. Then $(\{R_t\}_{t > 0}, \gamma_b)$ is a regularisation method for A^+ which is of optimal order concerning X_μ for all $\mu \in (0, \nu]$.*

Till now we only define regularisation. Now we want to construct some. The following notations and definitions are based on Rieder [30] where $A^+ = (A^*A)^{-1}A^*$ and the series description of A^* is used to construct regularisation methods. In Louis [25] the series description of A^+ is used for the construction. The resulting methods are equal because of choosing different filter functions.

For injective $A \in \mathcal{K}(X, Y)$ we can illustrate A^+ as $A^+ = (A^*A)^{-1}A^*$. For stabilising $(A^*A)^{-1}$ (which is not continuous) we use a family of piecewise continuous functions $F_\gamma : [0, \|A\|^2] \to \mathbb{R}$ with jump discontinuity. These functions satisfy

$$\lim_{\gamma \to 0} F_\gamma(\lambda) = \frac{1}{\lambda} \quad \forall \, \lambda \in (0, \|A\|^2]. \tag{4.31}$$

By this we have a continuous operator $F_\gamma(A^*A)$ which converges pointwise to $(A^*A)^{-1}$ for $\gamma \to 0$. We call $\{F_\gamma\}_{\gamma > 0}$ filter and define:

$$R_\gamma g := F_\gamma(A^*A)A^*g. \tag{4.32}$$

By the singular system $\{v_n, u_n; \sigma_n\}$ of A and using equation (4.13) we have

$$F_\gamma(A^*A)A^*g = \sum_{n=1}^{\infty} F_\gamma(\sigma_n^2)\sigma_n\langle g, u_n\rangle_Y v_n + F_\gamma(0) \underbrace{P_{\mathcal{N}(A)}A^*g}_{=0 \, (\overline{R(A^*)}=N(A)^\perp)}. \tag{4.33}$$

In the following we need another description of $A^+g - R_\gamma g$. Therefore we use, that A^+g solves the normal equation $A^*Af = A^*g$:

$$\begin{aligned}
A^+g - R_\gamma g &= A^+g - F_\gamma(A^*A)A^*g \tag{4.34} \\
&= A^+g - F_\gamma(A^*A)A^*AA^+g \\
&= p_\gamma(A^*A)A^+g
\end{aligned}$$

with

$$p_\gamma(t) := 1 - tF_\gamma(t). \tag{4.35}$$

Theorem 4.7. *Let $A \in \mathcal{K}(X, Y)$. The filter $\{F_\gamma\}_{\gamma>0}$ satisfies (4.31) and*

$$\lambda |F_\gamma(\lambda)| \le C_F \quad \forall \; \lambda \in [0, \|A\|^2], \; \gamma > 0. \tag{4.36}$$

Then

$$\lim_{\gamma \to 0} F_\gamma(A^*A)A^*g = \begin{cases} A^+g & g \in D(A^+) \\ \infty & g \notin D(A^+). \end{cases} \tag{4.37}$$

Theorem 4.8. *The filter $\{F_\gamma\}_{\gamma>0}$ satisfies in equation (4.36). Set $f_\gamma := R_\gamma g = F_\gamma(A^*A)A^*g$ and $f_\gamma^\epsilon := R_\gamma g^\epsilon$ with $g, g^\epsilon \in Y$ and $\|g - g^\epsilon\| \le \epsilon$. Then:*

$$\|Af_\gamma - Af_\gamma^\epsilon\|_Y \le C_F \, \epsilon \tag{4.38}$$

and

$$\|f_\gamma - f_\gamma^\epsilon\|_X \le \epsilon \sqrt{C_F M(\gamma)} \tag{4.39}$$

with

$$M(\gamma) := \sup\{F_\gamma(\lambda) \mid \lambda \in [0, \|A\|^2]\}. \tag{4.40}$$

As mentioned in equation (4.21) we can split the total error in approximation error and data error. By theorem 4.8 we are able to estimate the data error:

$$\|A^+g - R_\gamma g^\epsilon\|_X \quad \le \quad \|A^+g - R_\gamma g\|_X + \|R_\gamma(g - g^\epsilon)\|_X \tag{4.41}$$

$$\le \quad \|A^+g - R_\gamma g\|_X + \epsilon\sqrt{C_F M(\gamma)}. \tag{4.42}$$

By theorem 4.7 we have $\lim_{\gamma \to 0} \|A^+g - R_\gamma g\|_X = 0$ but by equation (4.31) we have divergence for $M(\gamma)$. As a consequence the total error grows for $\gamma \to 0$. If we connect γ and ϵ we can enforce convergence.

Corollary 4.1. *The filter $\{F_\gamma\}_{\gamma>0}$ satisfies equation (4.31) and in equation (4.36). If we choose $\gamma : (0, \infty) \to (0, \infty)$ such, that*

$$\gamma(\epsilon) \to 0 \quad and \quad \epsilon\sqrt{M(\gamma(\epsilon))} \to 0, \quad for \; \epsilon \to 0 \tag{4.43}$$

then $(\{R_t\}_{t>0}, \gamma)$ is a regularisation method for A^+.

This leads us to the definition of a regularising filter:

Definition 4.7. *For $A \in \mathcal{L}(X, Y)$ we call a family $\{F_\gamma\}_{\gamma > 0}$ of piecewise continuous functions with jump discontinuity regularising filter if (4.31) and (4.36) are satisfied.*

Lemma 4.3. *Let the filter $\{F_t\}_{t>0}$ be regularising for $A \in \mathcal{L}(X, Y)$. For $p_t(\lambda) = 1 - \lambda F_t(\lambda)$ and $\mu > 0$ exist $t_0 > 0$ and $\omega_\mu : (0, t_0] \to \mathbb{R}$ such that*

$$\sup_{0 \leq \lambda \leq \|A\|^2} \lambda^{\mu/2} |p_t(\lambda)| \leq \omega_\mu(t) \quad \forall \, t \in (0, t_0]. \tag{4.44}$$

Let $g \in R(A)$ and $f^+ = A^+ g \in X_\mu$ with $\|f^+\|_\mu \leq \rho$. For $f_t = R_t g$ and $0 < t \leq t_0$ we then have:

$$\|f^+ - f_t\|_X \leq \omega_\mu(t)\rho \tag{4.45}$$

and

$$\|Af^+ - Af_t\|_Y \leq \omega_{\mu+1}(t)\rho. \tag{4.46}$$

This leads us to an a-priori parameter choice which results in an regularisation method of optimal order.

Theorem 4.9. *Let $\{F_t\}_{t>0}$ a regularising filter for $A \in \mathcal{L}(X, Y)$. For $p_t(\lambda)$ and $\mu > 0$ exist $t_0 > 0$ and $\omega_\mu : (0, t_0] \to \mathbb{R}$ such that*

$$\sup_{0 \leq \lambda \leq \|A\|^2} \lambda^{\mu/2} |p_t(\lambda)| \leq \omega_\mu(t) \quad \forall \, t \in (0, t_0].$$

Farther we have

$$\omega_\mu(t) \leq C_p t^{\mu/2} \quad for \ t \to 0 \tag{4.47}$$

and

$$M(t) \leq C_M t^{-1} \quad for \ t \to 0 \tag{4.48}$$

with C_p , $C_M = const > 0$. The a-priori parameter choice $\gamma : (0, \infty) \to (0, \infty)$ satisfies

$$C_\gamma \left(\frac{\epsilon}{\rho}\right)^{\frac{2}{\mu+1}} \leq \gamma(\epsilon) \leq C_\Gamma \left(\frac{\epsilon}{\rho}\right)^{\frac{2}{\mu+1}} \quad for \ \epsilon \to 0 \tag{4.49}$$

with C_γ, $C_\Gamma = const > 0$.

Then $(\{R_t\}_{t>0}, \gamma)$ is a regularisation method of optimal order for A^+ corresponding X_μ.

We want to define the qualification of a filter before we want to present the idea of the Tikhonov-Phillips-regularisation.

Definition 4.8. *Let $\{F_t\}_{t>0}$ a regularising filter for $A \in \mathcal{L}(X,Y)$ with $M(t) \leq C_M t^{-1}$, $t \to 0$. The maximal μ_0 so that there exists a constant $C_p = C_p(\mu)$ for every $\mu \in (0, \mu_0]$ with*

$$\sup_{0 \leq \lambda \leq \|A\|^2} \lambda^{\mu/2} |p_t(\lambda)| \leq C_p t^{\mu/2}, \quad t \to 0 \tag{4.50}$$

is called qualification of the filter.

Now we want to present the idea of the Tikhonov-Phillips-regularisation, starting with the classical method. There the filter

$$F_\gamma(\lambda) = \frac{1}{\lambda + \gamma}, \quad \gamma > 0 \tag{4.51}$$

is used. By this filter the regularisation is

$$R_\gamma y = F_\gamma(A^*A)A^*y, \quad y \in Y \tag{4.52}$$

and $R_\gamma y$ is the unique solution of the regularised normal equation

$$(A^*A + \gamma I)R_\gamma y = A^*y. \tag{4.53}$$

It can be shown that the classical Tikhonov-Phillips-regularisation has the qualification $\mu_0 = 2$ and is of optimal order corresponding to X_μ with $0 < \mu \leq 2$ and the a-priori parameter choice (4.49). By $\gamma(\epsilon) = \mu^{-1}(\epsilon/\rho)^{2/(\mu+1)}$ the Tikhonov-Phillips-regularisation is optimal for $0 < \mu \leq 2$. (see Rieder [30]).

Instead of the classical we want to use the general method of Tikhonov-Phillips where we replace the identity I by a general operator B.

Let $A \in \mathcal{L}(X,Y)$ and $B : X \to Z$ a linear, continuous operator where Z is a banach space. Additionally exists $\beta > 0$ with

$$\beta \|f\|_X \leq \|Bf\|_Z \quad \forall f \in X. \tag{4.54}$$

Under these constraints exists a unique solution $f_\gamma \in X$ to

$$(A^*A + \gamma B^*B)f = A^*y \tag{4.55}$$

where f_γ depends continuously on $y \in Y$ for $\gamma > 0$.

We can characterise the solution f_γ of equation (4.55) as minimising argument of the Tikhonov-Phillips-functional

$$J_{\gamma,y}x := \|Ax - y\|_Y^2 + \gamma\|Bx\|_Z^2, \tag{4.56}$$

where $\|Bx\|_Z^2$ is called penalty term. So, if f_γ is the unique solution to equation (4.55), f_γ is the unique minimum of $J_{\gamma,y}$ and contrary. By this we can define $\{R_\gamma\}_{\gamma > 0}$ as:

$$R_\gamma y := f_\gamma = (A^*A + \gamma B^*B)^{-1}A^*y = argmin\{J_{\gamma,y}(f) \mid f \in Y\}. \tag{4.57}$$

5 The inverse model problem

In this Section we want to describe the problems to be solved. As underlying PDE-constraint we have the potential equation on the unit square with different boundary conditions. After introducing the resulting variational equations to be solved, we shortly describe the preconditioned cg-method (pcg) and the multigrid method, which we use for the computation of the solutions.

5.1 Description of the problems

For generality we regard the differential equation $-\Delta u = g$ on $\Omega = (0,1)^2$ instead of $-\Delta u = 0$, which is the underlying differential equation for the application. Also we take a look on different boundary conditions and given measurements on Γ_O.

This leads us to the following problems with $\Omega = (0,1)^2$, $\Gamma = \partial\Omega$ and Γ divided into $\Gamma_O = \{x \in \partial\Omega \mid x_1 = 1\}, \Gamma_N = \{x \in \partial\Omega \mid x_2 = 0 \vee x_2 = 1\}$, $\Gamma_C = \{x \in \partial\Omega \mid x_1 = 0\}$.
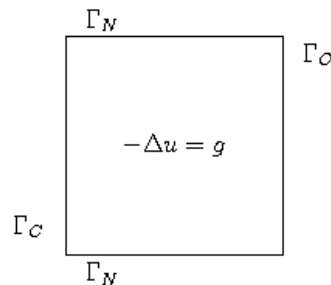
Figure 5.1: The unit square as underlying geometry for the poisson equation with the boundaries Γ_O, Γ_C and Γ_N.

We have four possible problems to solve on this geometry. We can search Neumann or Dirichlet control on Γ_C for given Neumann measurement or Dirichlet measurement on Γ_O. In the following we will introduce the four cases which we formulate as optimal control problems, i.e. we search the control q on Γ_C to minimise the difference between the calculated solution and the given measurements on Γ_O.

1. Find $\partial_n u = q$ on Γ_C, for given measurement $\partial_n u = f$ on Γ_O such that

$$J(u,q) \rightarrow \min, \quad J(w,\tau) := \frac{1}{2}\|\partial_n w - f\|_{\Gamma_O}^2 \tag{5.1}$$

under the PDE-constraint

$$
\begin{aligned}
-\Delta u &= g && \text{on} \quad \Omega, \\
\partial_n u &= 0 && \text{on} \quad \Gamma_N, \\
u &= 0 && \text{on} \quad \Gamma_O, \\
\partial_n u &= q && \text{on} \quad \Gamma_C.
\end{aligned}
\tag{5.2}
$$

Where $J(w,\tau)$ defines a so-called cost functional and q denotes a control variable.

2. Find $u = q$ on Γ_C for given measurement $\partial_n u = f$ on Γ_O such that

$$J(u,q) \rightarrow \min, \quad J(w,\tau) := \frac{1}{2}\|\partial_n w - f\|_{\Gamma_O}^2 \tag{5.3}$$

under the PDE-constraint

$$
\begin{aligned}
-\Delta u &= g && \text{on} \quad \Omega, \\
\partial_n u &= 0 && \text{on} \quad \Gamma_N, \\
u &= 0 && \text{on} \quad \Gamma_O, \\
u &= q && \text{on} \quad \Gamma_C.
\end{aligned}
\tag{5.4}
$$

These are the two problems based on the application where we have given Neumann measurements on Γ_O. As another two cases we want to formulate the problems where we search the control q on Γ_C ($q = u|_{\Gamma_C}$ or $q = \partial_n u|_{\Gamma_C}$) for given Dirichlet measurements $u|_{\Gamma_O} = 0$:

3. Find $u = q$ on Γ_C for given measurement $u = 0$ on Γ_O such that

$$J(u, q) \rightarrow \min, \quad J(w, \tau) := \frac{1}{2}\|w\|_{\Gamma_O}^2 \tag{5.5}$$

under the PDE-constraint

$$
\begin{aligned}
-\Delta u &= g & \text{on} \quad \Omega\,, \\
\partial_n u &= 0 & \text{on} \quad \Gamma_N\,, \\
\partial_n u &= f & \text{on} \quad \Gamma_O\,, \\
u &= q & \text{on} \quad \Gamma_C\,.
\end{aligned}
\tag{5.6}
$$

Following Lions [24] these problems are uniquely solvable.

4. Find $\partial_n u = q$ on Γ_C for given measurement $u = 0$ on Γ_O such that

$$J(u, q) \rightarrow \min, \quad J(w, \tau) := \frac{1}{2}\|w\|_{\Gamma_O}^2 \tag{5.7}$$

under the PDE-constraint

$$
\begin{aligned}
-\Delta u &= g & \text{on} \quad \Omega\,, \\
\partial_n u &= 0 & \text{on} \quad \Gamma_N\,, \\
\partial_n u &= f & \text{on} \quad \Gamma_O\,, \\
\partial_n u &= q & \text{on} \quad \Gamma_C\,.
\end{aligned}
\tag{5.8}
$$

In the fourth case we have the problem that the direct problem (5.8) with Neumann boundary conditions is not uniquely solvable. If exist a solution u of the problem we know that $u + \text{const}$ is also a solution. Because of this we only take care of the problems 1. to 3.. For the moment we want to take a look on a general problem.

After discretisation and using Nitsche's method we can write all three problems as (see e.g. [24] or [39])

$$
\begin{aligned}
J(u_h, q) &\rightarrow & min \tag{5.9} \\
A u_h &= & g + Bq. \tag{5.10}
\end{aligned}
$$

A, B, g and q depending on the problem to be solved with u_h and q are unknown. If A is regular we can write:

$$u_h = A^{-1}g + A^{-1}Bq. \tag{5.11}$$

We want to solve minimisation problems. From Section 4.1 we know that solving the minimisation problem is equivalent in solving the normal equation. Following Louis [25] we can introduce a positive definite matrix C so that we can write

$$\|Du - f\|_1^2 = (Du - f)^* C (Du - f). \tag{5.12}$$

In our case D is the identity. Using equations (5.11), (5.12) and the fact we want to solve a minimisation problem we have:

$$B^T A^{-T} C A^{-1} B q + B^T A^{-T} C A^{-1} g - B^T A^{-T} C f = 0 \tag{5.13}$$

By the Tikhonov-Phillips regularisation we have to solve in matrix vector notation

$$\left(B^T A^{-T} C A^{-1} B + \alpha \ \mathrm{Reg} \right) q = B^T A^{-T} (C f - C A^{-1} g). \tag{5.14}$$

with α the regularisation parameter and Reg the regularisation matrix from the Tikhonov-Philips regularisation.

For the determination of A, B and g we take again a look on the direct problems we have to solve, using Nitsche's method. If we call n the number of vertices in Ω and Nq the number of degrees of freedom (DOF) on Γ_C we have:

1. In the first case, where we search $\partial_n u|_{\Gamma_C} = q$ for given $\partial_n u|_{\Gamma_O} = f$, we have to solve for the direct problem in variational formulation $\forall \ \varphi \in V_h$:

$$
\begin{aligned}
(\nabla u_h, \nabla \varphi)_{0,\Omega} - (\partial_n u_h, \varphi)_{0,\Gamma} \ &- \ (u_h, \partial_n \varphi)_{0,\Gamma_O} + \gamma h^{-1} (u_h, \varphi)_{0,\Gamma_O} \\
&= \ (g_h, \varphi)_{0,\Omega} + \gamma h^{-1} (0, \varphi)_{0,\Gamma_O} - (0, \partial_n \varphi)_{0,\Gamma_O}
\end{aligned} \tag{5.15}
$$

In the matrix-vector-notation $A u_h = g + B q$ we have here:

A is a $(n \times n)$-matrix corresponding to ($\psi \in V_h$):

$$(\nabla \psi, \nabla \varphi)_{0,\Omega} - (\partial_n \psi, \varphi)_{0,\Gamma_O} - (\psi, \partial_n \varphi)_{0,\Gamma_O} + \gamma h^{-1} (\psi, \varphi)_{0,\Gamma_O}$$

g is a vector with n rows corresponding to:

$$(g_h, \varphi)_{0,\Omega}$$

and B is a $(n \times Nq)$-matrix with entries from:

$$(\psi, \varphi)_{0, \Gamma_C}$$

The terms $(\partial_n u_h, \varphi)_{0, \Gamma_N}$ and $\gamma h^{-1}(0, \varphi)_{0, \Gamma_O} - (0, \partial_n \varphi)_{0, \Gamma_O}$ are zero so they are ignored in the formulation.

In the calculation of the inverse problem we have in the regularised normal equation (5.14) resulting from the minimisation problem:

Cf is a vector with n rows and entries from

$$(\partial_n \psi, \partial_n \varphi)_{0, \Gamma_O}$$

and for the $(n \times n)$-matrix C we have the entries from:

$$(\partial_n \psi, \partial_n \varphi)_{0, \Gamma_O}.$$

2. In the second case, where we search $u|_{\Gamma_C} = q$ for given $\partial_n u|_{\Gamma_O} = f$, we have to solve in the direct problem using Nitsche's method:

$$
\begin{aligned}
(\nabla u_h, \nabla \varphi)_{0, \Omega} \quad &- \quad (\partial_n u_h, \varphi)_{0, \Gamma} - (u_h, \partial_n \varphi)_{0, \Gamma_O \cup \Gamma_C} + \gamma h^{-1}(u_h, \varphi)_{0, \Gamma_O \cup \Gamma_C} \\
&= \quad (g_h, \varphi)_{0, \Omega} - (0, \partial_n \varphi)_{\Gamma_O} + \gamma h^{-1}(0, \varphi)_{\Gamma_O} \qquad (5.16) \\
&\quad + (q, \partial_n u \varphi)_{\Gamma_C} + \gamma h^{-1}(q, \varphi)_{\Gamma_C}
\end{aligned}
$$

In the matrix-vector-notation we have here:

A the $(n \times n)$-matrix corresponding to $(\psi \in V_h)$:

$$(\nabla \psi, \nabla \varphi)_{0, \Omega} - (\partial_n \psi, \varphi)_{0, \Gamma} - (\psi, \partial_n \varphi)_{0, \Gamma_O \cup \Gamma_C} + \gamma h^{-1}(\psi, \varphi)_{0, \Gamma_O \cup \Gamma_C}$$

g the vector with n rows corresponding to:

$$(g_h, \varphi)_{0, \Omega}$$

and B the $(n \times Nq)$-matrix with entries from:

$$\gamma h^{-1}(\psi, \varphi)_{0, \Gamma_C} - (\psi, \partial_n \varphi)_{0, \Gamma_C}.$$

Again we have caused by the boundary conditions $(\partial_n u_h, \varphi)_{0,\Gamma_N} = 0$ which is ignored in the formulation.

In the calculation of the inverse problem we have

Cf the vector with n rows and entries from

$$(\partial_n \psi, \partial_n \varphi)_{0,\Gamma_O}$$

and for the $(n \times n)$-matrix C we use again the entries:

$$(\partial_n \psi, \partial_n \varphi)_{0,\Gamma_O}.$$

3. In the third case where we search $u|_{\Gamma_C} = q$ for given $u|_{\Gamma_O} = 0$ we have to solve in the direct problem in variational formulation:

$$
\begin{aligned}
(\nabla u_h, \nabla \varphi)_{0,\Omega} - (\partial_n u_h, \varphi)_{0,\Gamma} \quad &- \quad (u_h, \partial_n \varphi)_{0,\Gamma_C} + \gamma h^{-1}(u_h, \varphi)_{0,\Gamma_C} \qquad (5.17) \\
&= \quad (g_h, \varphi)_{0,\Omega} - (q_h, \partial_n \varphi)_{0,\Gamma_C} + \gamma h^{-1}(q_h, \varphi)_{0,\Gamma_C}
\end{aligned}
$$

A is the $(n \times n)$-matrix corresponding to $(\psi \in V_h)$:

$$(\nabla \psi, \nabla \varphi)_{0,\Omega} - (\partial_n \psi, \varphi)_{0,\Gamma_C} - (\psi, \partial_n \varphi)_{0,\Gamma_C} + \gamma h^{-1}(\psi, \varphi)_{0,\Gamma_C}$$

g is the vector with n rows corresponding to:

$$(g_h, \varphi)_{0,\Omega} + (\partial_n \psi, \varphi)_{0,\Gamma_O}$$

and B the $(n \times Nq)$-matrix with the entries:

$$\gamma h^{-1}(\psi, \varphi)_{0,\Gamma_C} - (\psi, \partial_n \varphi)_{0,\Gamma_C}$$

As in the previous cases we have zero Neumann conditions on Γ_N and this term doesn't appear in the formulation.

In the calculation of the inverse problem we have here

Cf the n-vector with the entries

$$(\partial_n \psi, \varphi)_{0,\Gamma_O}$$

and for the $(n \times n)$-matrix C we have here the entries from:

$$(\psi, \varphi)_{0,\Gamma_O}$$

We have introduced A, B, C, f and g depending on the problem to be solved. In the following we describe how to solve the regularised normal equation

$$(B^T A^{-T} C A^{-1} B + \alpha \ Reg) \ q = B^T A^{-T} (Cf - CA^{-1}g)$$

with general given A, B, C, f and g for searched control q.

After initializing and assembling the matrices and vectors we have to do the following steps:

1. Calculate $G := A^{-1}B$ by using the pcg-method.

2. Compute $M := G^T C G = B^T A^{-T} C A^{-1} B$.

3. Calculate $A^{-1}g$ by using the pcg-method.

4. Estimate $MtF := G^T (Cf_h - CA^{-1}g)$.

5. Use the Gauß-Jordan algorithm for $(M + \alpha \cdot Reg)$ and

6. compute with this q from $(M + \alpha \cdot Reg) \ q = MtF$.

7. At last compute $u_h = A^{-1}(g + Bq)$ with the calculated q by using the pcg-method.

The calculation of A^{-1} occures by the pcg-method where the multigrid method (see Section 5.2) is used as preconditioner. We want to describe briefly the pcg method and the multigrid method in the next Section.

5.2 Numerical methods

In this Section we want to present the pcg algorithm and the basics of the multigrid method the twogrid method respectively. We use the multigrid method as preconditioner in the pcg-method for solving the inverse problem. For more information see the literature (e.g. [8], [9], [18], [10], [31], [41]).

We start the description of the numerical methods with the preconditioned cg-method (pcg) (see Braess [8]).

Let us assume we know a positive definite matrix C which is an approximation of A from the equation $Ax = b$ to be solved. For $x_0 \in \mathbb{R}^n$ we consider

$$x_1 = x_0 - \alpha C^{-1} g_0 \tag{5.18}$$

with $g_0 = Ax_0 - b$. If we have $C = A$ we have solved the problem in the first step.

This leads us to the pcg-algorithm.

Algorithm 5.1. *(PCG)*

   i) Let $x_0 \in \mathbb{R}^n$. Set $g_0 = Ax_0 - b$, $d_0 = -h_0 = -C^{-1} g_0$

   ii) Calculate for $k \geq 0$:

- $\alpha_k = \dfrac{g_k^T h_k}{d_k^T A d_k}$

- $x_{k+1} = x_k + \alpha_k d_k$

- $g_{k+1} = g_k + \alpha_k A d_k$

- $h_{k+1} = C^{-1} g_{k+1}$

- $\beta_k = \dfrac{g_{k+1}^T h_{k+1}}{g_k^T h_k}$

- $d_{k+1} = -h_{k+1} + \beta_k d_k$

The matrix C is the preconditioner, i.e. the approximation of A calculated in our case by the multigrid method. With C positive definite we have the following properties:

If we have $g_{k-1} \neq 0$ holds:

- $d_{k-1} \neq 0$

- $V_k := span[g_0, \; AC^{-1}g_0, \ldots, (AC^{-1})^{k-1}g_0] = span[g_0, \; g_1, \ldots, \; g_{k-1}]$ and

  $span[d_0, \; d_1, \ldots, d_{k-1}] = C^{-1} span[g_0, \; g_1, \ldots, g_{k-1}]$

- The vectors $d_0, \; d_1, \ldots, d_{k-1}$ are conjugate.

- $f(x_k) = \min\limits_{z \in V_k} f(x_0 + C^{-1}z)$.

Now we want to present the basics of the multigrid method. For more details see the literature (e.g. [9], [10], [41]) We start the description with the twogrid method where the multigrid method is based on. We want to solve the problem

$$Ax = b. \tag{5.19}$$

As an example we use here the Laplace equation with Dirichlet boundary.

We discretise equidistant so that we have $h = \dfrac{1}{N+1}$ where N is the number of inner points of the discretisation. We call l the level of discretisation for which we have

$$h_0 > h_1 > \ldots > h_l > \ldots, \qquad \lim_{l \to \infty} h_l = 0. \tag{5.20}$$

For each level l we have to solve the system

$$A_l x_l = b_l. \tag{5.21}$$

The idea of the twogrid method is to combine two levels for solving the system. Therefore we do some smoothing steps S_l for the calculation of x_l on level l and evaluate the defect $d_l = A_l x_l - b_l$. S_l damps the oscillatory part of the error and we obtain a smooth function which we can approximate well by a function on the coarse grid (level $l-1$). I.e. we restrict the defect d_l to level $l-1$ and calculate there the error e_{l-1}. Now we have e_{l-1} as approximation of e_l on level $l-1$. We need a map (called prolongation) which displays e_{l-1} to e_l on level l. By the error e_l we are able to calculate x_l. The following diagram illustrates this idea again. There we use for simplicity only a presmoothing procedure.

initial value	x_l^0			
	$\downarrow$			
level l	$x_l^\nu = S_l^\nu x_l^0$	$\rightarrow$	$d_l = b_l - A_l x_l^\nu$	$x_l = x_l^\nu - e_l$
			$\downarrow$	$\uparrow$
restriction/ prolongation			$d_{l-1} = R d_l$	$e_l = P e_{l-1}$
			$\downarrow \quad \nearrow$	
level $l-1$			$A_{l-1} e_{l-1} = d_{l-1}$	
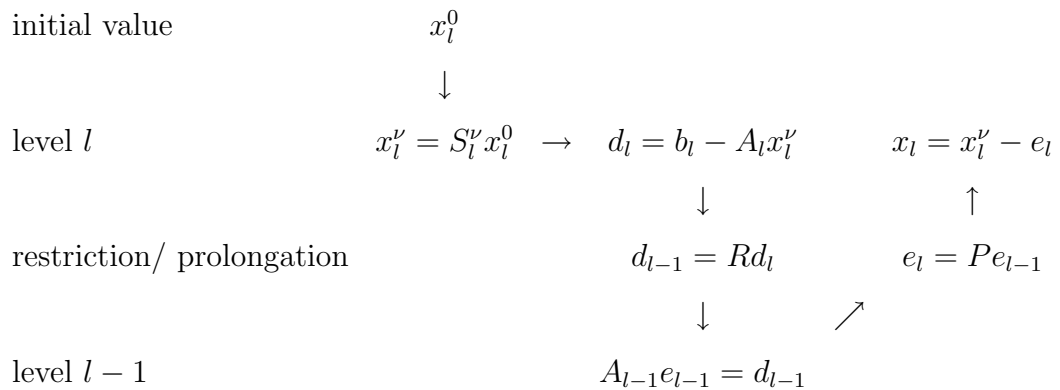
Now we want to take a short look on the different steps.

The smoothing procedure S_l is an iterative solver for the problem (5.21) e.g. as in Hackbusch [18] the Richardson method.

The problem is now, that e_l and e_{l-1} are elements of different spaces X_l and X_{l-1}. Because of this we need the prolongation and restriction operators. The prolongation $P : X_{l-1} \rightarrow X_l$ is a linear, injective mapping from the coarse grid to the fine grid. As a simple prolongation the linear interpolant can be chosen.

The restriction $R : X_l \rightarrow X_{l-1}$ is a linear, surjective mapping from the fine grid to the coarse grid. The simplest restriction is the trivial restriction where we omit the needless gridpoints but the literature gives the advise not to use this simple restriction. One alternative is, to choose the restriction as the adjungate of the prolongation.

By smoothing procedure S_l, prolongation P and restriction R we are able to describe the two grid algorithm. In the general version we use ν_1 presmoothing operations S_l and ν_2 postsmoothing operations $\tilde{S}_l$. It's not essential that the presmoothing and postsmoothing operations are identical.

Algorithm 5.2. *(Two grid-algorithm)*

0) Choose $x_l^{0,0}$ as initial value

i) for $k = 0, 1, 2, \ldots$

        for $i = 0, \ldots, \nu_1 - 1$

$$x_l^{k,i+1} := S_l x_l^{k,i}$$

        end

$$e_{l-1} := A_{l-1}^{-1} R (b_l - A_l x_l^{k,\nu_1})$$

$$x_l^{k+1,0} := x_l^{k,\nu-1} - P e_{l-1}$$

        for $i = 0, \ldots, \nu_2 - 1$

$$x_l^{k+1,i+1} := \tilde{S}_l x_l^{k+1,i}$$

end

$$x_l^{k+1,0} := x_l^{k+1,\nu_2}$$

end

In the two grid algorithm we have now to solve on level $l-1$

$$A_{l-1}e_{l-1} = R(b_l - A_l x_l^{k,\nu-1}) \tag{5.22}$$

which has the same structure as the original problem $A_l x_l = b_l$ on level l. We want to solve equation (5.22) iterative, by solving it again with the two grid algorithm. This method is called multigrid method.

We call the multigrid method Φ_M with wich we can formulate the multigrid algorithm:

Algorithm 5.3. *(Multigrid-algorithm $\Phi^M(x_l, b_l)$)*

0) if $l = 0$:

$$x_0 = A_0^{-1} b_0$$

else

i) for $k = 0, 1, 2, \ldots$

for $i = 0, \ldots, \nu_1 - 1$

$$x_l^{k,i+1} := S_l x_l^{k,i}$$

end

$$d_{l-1} := R(b_l - A_l(x_l^{k,\nu_1}))$$

$$e_{l-1}^{(0)} := 0$$

for $i = 1, \ldots, \gamma$

$$e_{l-1}^{(i)} := \Phi_{l-1}^M(e_{l-1}^{(i-1)}, d_{l-1})$$

end

$$x_l^{k+1,0} := x_l^{k,\nu_1} - P e_{l-1}^{(\gamma)}$$

$$for \ i = 0, \ldots, \nu_2 - 1$$

$$x_l^{k+1,i+1} = S_l x_l^{k+1,i}$$

end

$$x_l^{k+1,0} := x_l^{k+1,\nu_2}$$

end

In step i) we have a loop over $i = 1, \ldots, \gamma$ which is unknown till now. Following the literature γ is choosen as 1 or 2. Then we speak of a V-cycle ($\gamma = 1$) or a W-cycle ($\gamma = 2$), respectively.

These are the basics of the numerical methods we use for solving the model problems on the unit square. For convergence analysis and more details see the literature already cited. In the next Section we want to present the numerical results for the model problems using a test example.

6 Numerical results for the model problem

In this Section we present the numerical results for the calculation of the model problem. We set $\gamma = 10$ in the terms resulting from Nitsche's method (Section 3.3). The special focus lies on the calculation of the searched control q on Γ_C. With this calculated control we compute u on Ω and so we can also analyse how good is the approximation of the given boundary values u and $\partial_n u$ on Γ_O and of $u|_{\Gamma_C}$ and $\partial_n u|_{\Gamma_C}$ respectively (which we know from our analytic solution).

As underlying model problem we have

$$-\Delta u = g. \tag{6.1}$$

with $g = 12xy^2 - 12xy + 2x - 12y^2 + 12y - 2$. We know the corresponding analytic solution of this problem is

$$u(x, y) = y^2(1 - y)^2(1 - x). \tag{6.2}$$

with the outward pointing normals

$$\partial_n u|_{\Gamma_C} = y^2(1 - y)^2, \quad \partial_n u|_{\Gamma_O} = -y^2(1 - y)^2. \tag{6.3}$$

We use bilinear elements on quadrilaterals. If we say, we refine three times, we divide the unit square into $(2^3)^2 = 64$ cells, i.e we have $2^3 + 1$ vertices on each boundary. We present the results of calculation for different global grid refinements,

different degrees of freedom on Γ_C and different regularisation parameters. For the calculation we use the three regularisation matrices:

$$
R := Id, \; R_1 := \frac{1}{h} \begin{pmatrix} -1 & 1 & & & \\ & -1 & 1 & & \\ & & \ddots & \ddots & \\ & & & \ddots & 1 \\ & & & & -1 \end{pmatrix}, R_2 := \frac{1}{h^2} \begin{pmatrix} 2 & -1 & & & \\ -1 & 2 & -1 & & \\ & \ddots & \ddots & \ddots & \\ & & \ddots & \ddots & -1 \\ & & & -1 & 2 \end{pmatrix}
$$

We start the analysis of the results for given Neumann measurement on Γ_O and searched Neumann control on Γ_C.

6.1 Neumann measurements on Γ_O and Neumann control on Γ_C

In this Section we want to find the Neumann control $q = \partial_n u|_{\Gamma_C}$ for given Neumann measurements $f = \partial_n u|_{\Gamma_O}$ such that

$$
J(u, q) \to \min, \quad J(w, \tau) = \frac{1}{2} \|\partial_n w - f\|_{\Gamma_O}^2 \tag{6.4}
$$

under the PDE-constraint

$$
\begin{aligned}
-\Delta u &= g && \text{on} \;\; \Omega, \\
\partial_n u &= 0 && \text{on} \;\; \Gamma_N, \\
u &= 0 && \text{on} \;\; \Gamma_O, \\
\partial_n u &= q && \text{on} \;\; \Gamma_C.
\end{aligned} \tag{6.5}
$$

First we analyse the results for the searched control $\partial_n u|_{\Gamma_C} = q$ for different grid refinements and the different regularisation matrices. As regularisation parameter we choose $\alpha = 1.e - 13$ and discretise Ω up to eight times (65536 cells). On every boundary, especially on Γ_C we have $2^i + 1$ degrees of freedom (DOF), if we discretise i times. From the analytic solution (equation (6.2)) we know $\partial_n u|_{\Gamma_C} = y^2(1 - y)^2$.

In Figure 6.1 we have illustrated the analytic $\partial_n u|_{\Gamma_C} = y^2(1-y)^2$ and the computed $\partial_n u_h|_{\Gamma_C}$ for different grid refinements and different regularisation matrices. Caused by the scale we don't present the results for small grid refinements in all Figures.
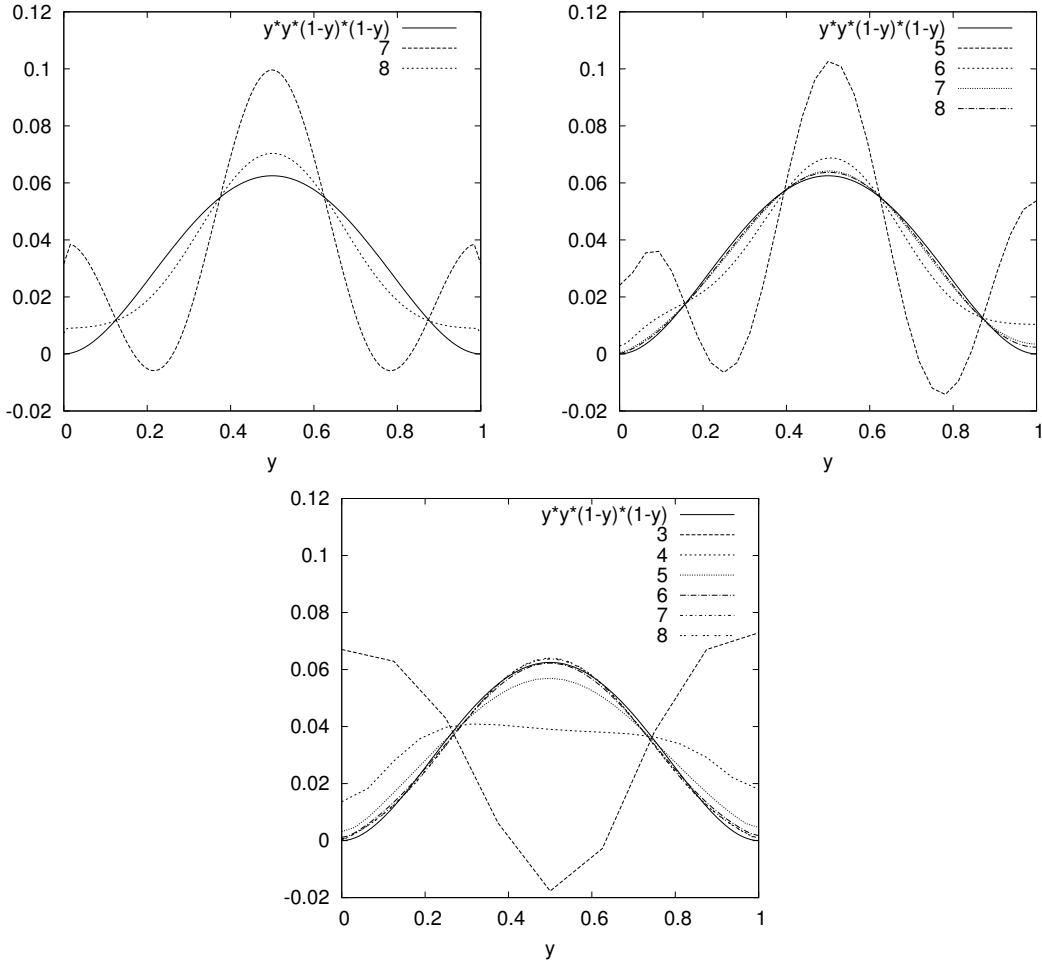
Figure 6.1: $\partial_n u|_{\Gamma_C} = y^2(1-y)^2$ and $\partial_n u_h|_{\Gamma_C}$ for different grid refinements with regularisation parameter $\alpha = 1.e-13$ calculated for searched $\partial_n u|_{\Gamma_C}$ and given $\partial_n u|_{\Gamma_O} = -y^2(1-y)^2$. Results for seven and eight refinements with $Reg = R^T R$ (top left), for five to eight grid refinements with $Reg = R_1^T R_1$ (top right) and for three to eight refinements with $Reg = R_2^T R_2$ (bottom).

We can see in all three cases that we get better results for finer grids. The unsymmetric approximation of $\partial_n u|_{\Gamma_C}$ in the case of regularising with $Reg = R_1^T R_1$ is caused by the unsymmetric matrix R_1. For the regularisation with $Reg = R_2^T R_2$ we can see that in the surrounding of $y = 0.5$ we get the best result for six refinements but near $y = 0$ and $y = 1$ we get the better results for finer grids.

For the moment we don't want to care about the error calculation because this is also dependent on the regularisation parameter as we will see later. We have seen that we have to discretise fine enough to get good results for the approximation of the control $\partial_n u|_{\Gamma_C}$. The disadvantage of this result is, if we discretise i times we have $2^i + 1$ DOF on Γ_C which is decisive for the runtime of the calculation. The question is now can we reduce the number of DOF on Γ_C for a fine grid on Ω without loosing quality of the approximation. We will analyse this for the calculation of the searched control $\partial_n u|_{\Gamma_C}$ for given Neumann measurement $\partial_n u|_{\Gamma_O} = -y^2(1 - y)^2$.

For the calculation of $\partial_n u_h|_{\Gamma_C}$ we will refine the grid eight times and set $\alpha = 1.e-13$. In Figure 6.2 we see the calculations for the different regularisation matrices with different number of DOF on Γ_C. In all graphics we present the results for 257 DOF on Γ_C which is the number of DOF for refining the grid eight times without special choice of particular DOFs.

We can see that for the regularisation with $R^T R$ (Figure 6.2 top left) and $R_2^T R_2$ (Figure 6.2 bottom) we reach good results if we reduce the number of DOF on Γ_C to 41 31 respectively. Only for the regularisation with $Reg = R_1^T R_1$ (Figure 6.2 top right) we have to use 91 DOF on Γ_C.

We have seen that we can reduce the number of DOF on Γ_C without loosing much quality of the approximation. Again we have only presented the graphical results and dispense with the error calculation caused by the dependence on the regularisation parameter. Now we will take a look on the influence of the regularisation parameter on the results of the calculation. Therefore we will discretise Ω eight times and use the reduced number of DOF on Γ_C for the calculation. Depending on the regularisation matrix we choose different regularisation parameters. In Figure 6.3

where we present the results for $\partial_n u_h|_{\Gamma_C}$ calculated with $Reg = R^T R$ and 41 DOF on Γ_C, we use regularisation parameters from $1.e - 11$ to $1.e - 07$.
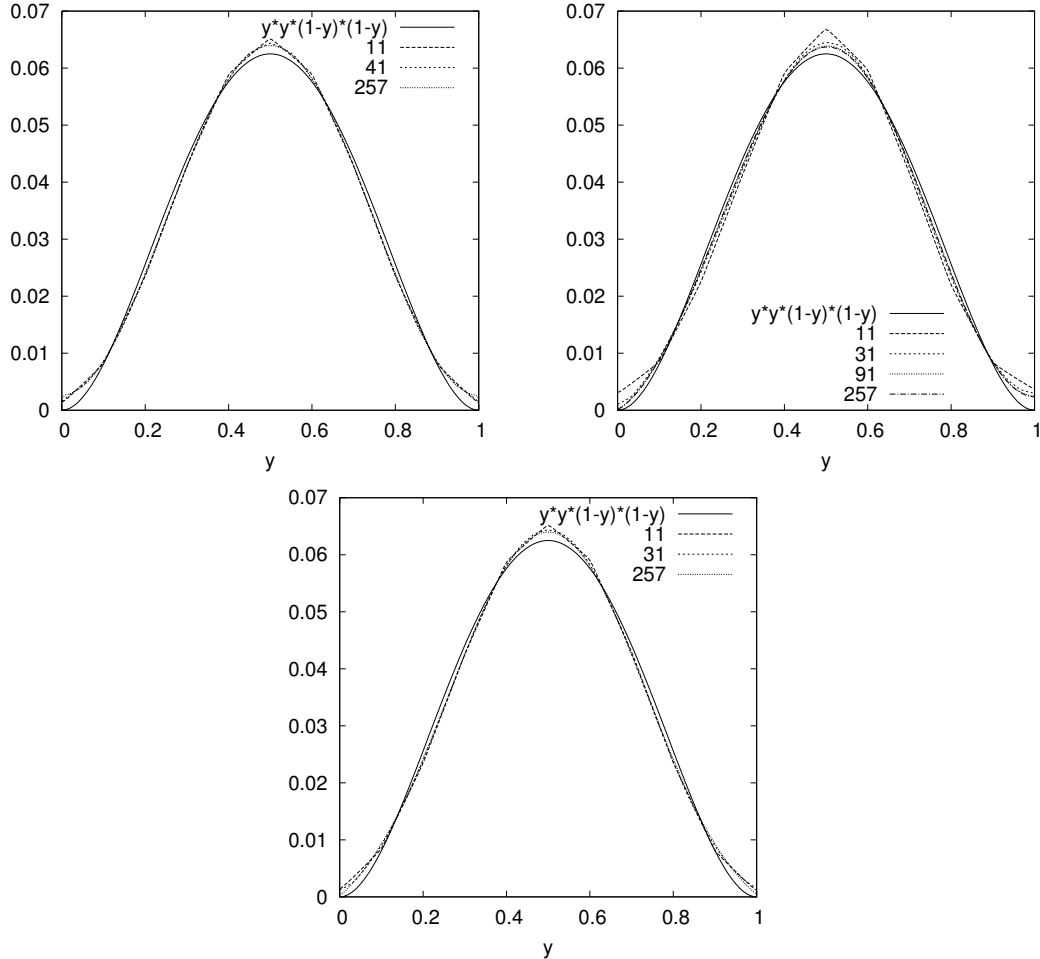
Figure 6.2: $\partial_n u|_{\Gamma_C} = y^2(1-y)^2$ and $\partial_n u_h|_{\Gamma_C}$ for different number of DOF on Γ_C with regularisation parameter $\alpha = 1.e - 13$ and refining eight times calculated for searched $\partial_n u|_{\Gamma_C}$ and given $\partial_n u|_{\Gamma_O} = -y^2(1-y)^2$. Results for 11, 41 and 257 DOF with $Reg = R^T R$ (top left), for 11, 31, 91 and 257 DOF on Γ_C with $Reg = R_1^T R_1$ (top right) and for 11, 31 and 257 DOF with $Reg = R_2^T R_2$ (bottom).

We can see that $\alpha = 1.e - 07$ is too big and we don't get a good approximation of $\partial_n u|_{\Gamma_C} = y^2(1 - y)^2$. In the surrounding of $y = 0.5$ we get the best result for $\alpha = 1.e - 08$ but near $y = 0$ and $y = 1$ we get the better results for $\alpha = 1.e - 09$

and $\alpha = 1.e - 10$. The error calculation (table 6.1) shows that with refining the grid eight times and using 41 DOF on Γ_C the optimal regularisation parameter is $\alpha = 1.e - 09$. This can also be seen in the graphical illustration (Figure 6.4).
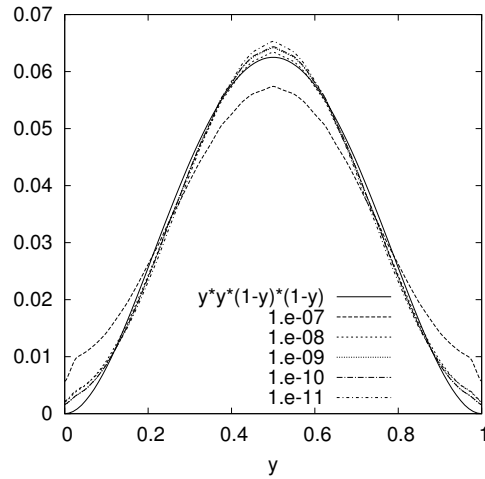
Figure 6.3: $\partial_n u|_{\Gamma_C} = y^2(1-y)^2$ and $\partial_n u_h|_{\Gamma_C}$ for different regularisation parameters using $Reg = R^T R$, refining the grid eight times, use 41 DOF on Γ_C calculated for the searched $\partial_n u|_{\Gamma_C}$ and given $\partial_n u|_{\Gamma_O} = -y^2(1-y)^2$.

Regularisationparameter	$\|\partial_n u - \partial_n u_h\|_{L^2(\Gamma_C)}$
1.e-07	4.983396e-03
1.e-08	1.455746e-03
1.e-09	1.319901e-03
1.e-10	1.387488e-03
1.e-11	2.023033e-03

Table 6.1: $\|\partial_n u - \partial_n u_h\|_{L^2(\Gamma_C)}$ for different regularisation parameters using $Reg = R^T R$, refining the grid eight times and use 41 DOF on Γ_C calculated in the case of searched $\partial_n u|_{\Gamma_C}$ for given $\partial_n u|_{\Gamma_O} = -y^2(1-y)^2$.
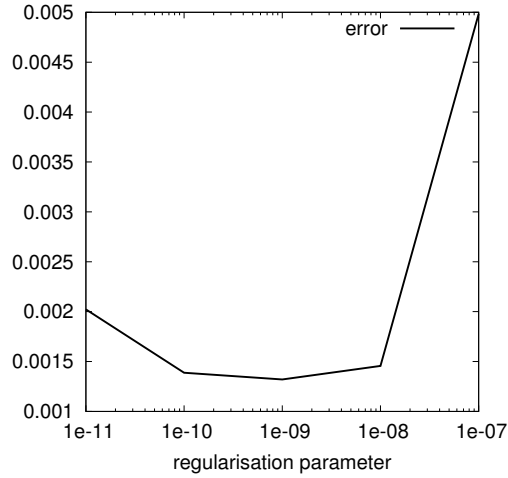
Figure 6.4: $\|\partial_n u - \partial_n u_h\|_{L^2(\Gamma_C)}$ for different regularisation parameters, using $Reg = R^T R$, refining the grid eight times, using 41 DOF on Γ_C calculated in the case of searched $\partial_n u|_{\Gamma_C}$ for given $\partial_n u|_{\Gamma_O} = -y^2(1-y)^2$.

After doing this analysis for the calculation with $Reg = R_1^T R_1$ and $Reg = R_2^T R_2$ we will analyse how good is the approximation of the other boundary data (specially of the given measurement on Γ_O) calculated with the computed control $\partial_n u_h|_{\Gamma_C}$.

Now we will analyse the influence of the regularisation parameter α on the results of the calculation of $\partial_n u|_{\Gamma_C}$ using $Reg = R_1^T R_1$. Therefore we discretise Ω eight times (66536 cells) and use 91 DOF on Γ_C. The regularisation parameter α is chosen between $\alpha = 1.e - 14$ and $\alpha = 1.e - 10$.

In table 6.2 we see the error developing of $\partial_n u_h|_{\Gamma_C}$ in dependence of the regularisation parameter α. There we can see that in this case $\alpha = 1.e - 12$ is the optimal parameter. This can also be seen in the graphical illustration of the error development in Figure 6.6. Again as in the calculation with $Reg = R^T R$ we can see the typical development of the error and the optimal regularisation parameter $\alpha = 1.e - 12$ if we refine the grid eight times, use 91 DOF on Γ_C and $Reg = R_1^T R_1$.
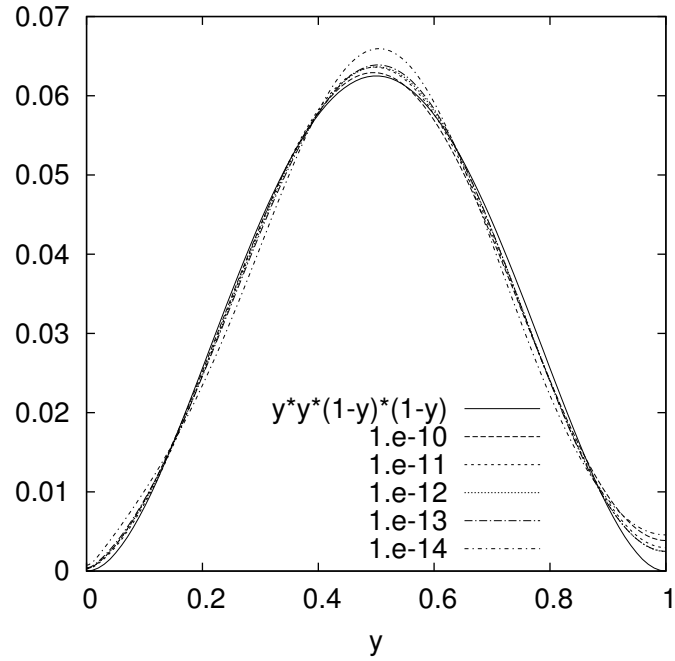
Figure 6.5: $\partial_n u|_{\Gamma_C} = y^2(1-y)^2$ and $\partial_n u_h|_{\Gamma_C}$ for different regularisation parameters, refining the grid eight times and 91 DOF on Γ_C calculated in the case of searched $\partial_n u|_{\Gamma_C} = q$ for given $\partial_n u|_{\Gamma_O} = -y^2(1-y)^2$ with $Reg = R_1^T R_1$.

Regularisationparameter	$\|\partial_n u - \partial_n u_h\|_{L^2(\Gamma_C)}$
1.e-10	1.322397e-03
1.e-11	1.137367e-03
1.e-12	1.037549e-03
1.e-13	1.176700e-03
1.e-14	2.544116e-03

Table 6.2: $\|\partial_n u - \partial_n u_h\|_{L^2(\Gamma_C)}$ for different regularisation parameters, using 91 DOF on Γ_C and refining the grid eight times with $Reg = R_1^T R_1$ calculated in the case of searched $\partial_n u|_{\Gamma_C}$ for given $\partial_n u|_{\Gamma_O} = -y^2(1-y)^2$.
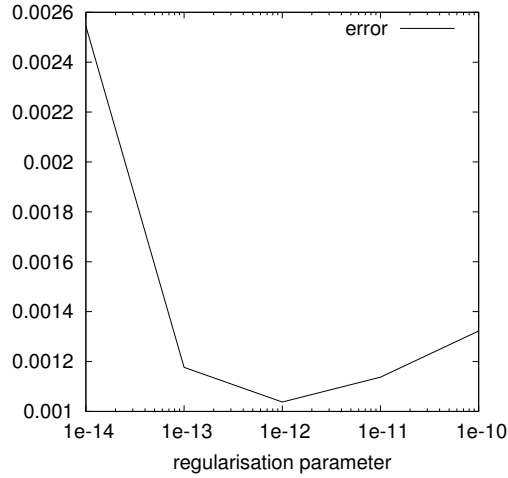
Figure 6.6: $\|\partial_n u - \partial_n u_h\|_{L^2(\Gamma_C)}$ in dependence of the regularisation parameter refining the grid eight times, using 91 DOF on Γ_C calculated in the of searched $\partial_n u|_{\Gamma_C}$ for given $\partial_n u|_{\Gamma_O} = -y^2(1-y)^2$ with $Reg = R_1^T R_1$.

At last we present the influence of the regularisation parameter α on the results of the calculation of $\partial_n u_h|_{\Gamma_C}$ for refining the grid eight times using 31 DOF on Γ_C and $Reg = R_2^T R_2$. In this case we choose α between $1.e - 15$ and $1.e - 10$.

In Figure 6.7 we can see that $\alpha = 1.e-10$ is too big for reaching a good approximation of $\partial_n u|_{\Gamma_C} = y^2(1-y)^2$. In the surrounding of $y = 0.5$ we get the best results for $\alpha = 1.e - 11$ and $\alpha = 1.e - 15$ but near $y = 0$ and $y = 1$ we get the better results for parameters between these two. Table 6.3 shows that the optimal parameter is again, as in the calculation with $Reg = R_1^T R_1$ $\alpha = 1.e - 12$. This can also be seen in Figure 6.8 where we illustrate $\|\partial_n u - \partial_n u_h\|_{L^2(\Gamma_C)}$ in dependence of the regularisation parameter.

We have seen that we have to discretise the grid fine enough to get a good approximation of the searched control $\partial_n u|_{\Gamma_C}$ but we can reduce the number of DOF on Γ_C without loosing quality of the approximation. Also we have determined the optimal regularisation parameters for the three regularisation matrices. For the calculation with $Reg = R^T R$ we can reduce the number of DOF on Γ_C to 41 and set $\alpha = 1.e-09$. If we regularise by $Reg = R_1^T R_1$ we use 91 DOF on Γ_C and set $\alpha = 1.e - 12$ and for

$Reg = R_2^T R_2$ we use 31 DOF and set $\alpha = 1.e - 12$.
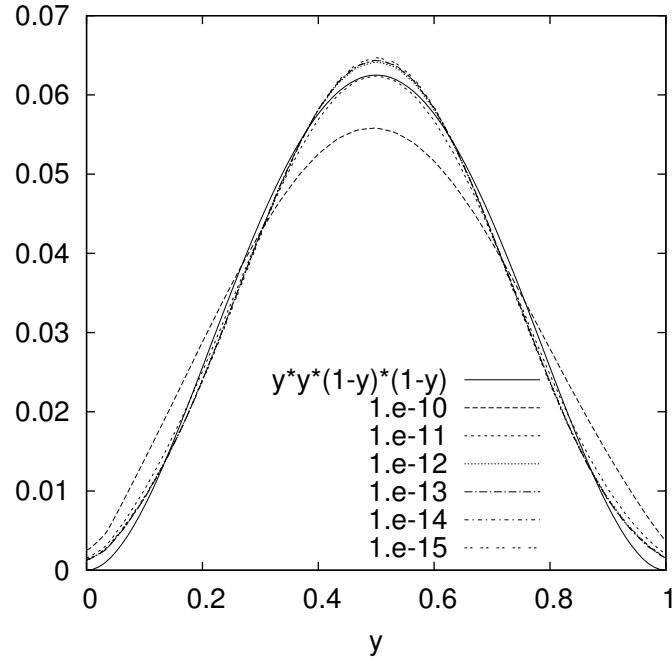
Figure 6.7: $\partial_n u|_{\Gamma_C} = y^2(1-y)^2$ and $\partial_n u_h|_{\Gamma_C}$ for different regularisation parameters, refining the grid eight times and 31 DOF on Γ_C calculated in the case of searched $\partial_n u|_{\Gamma_C} = q$ for given $\partial_n u|_{\Gamma_O} = -y^2(1-y)^2$ with $Reg = R_2^T R_2$.

Regularisationparameter	$\|\partial_n u - \partial_n u_h\|_{L^2(\Gamma_C)}$
1.e-10	4.768183e-03
1.e-11	1.535472e-03
1.e-12	1.403576e-03
1.e-13	1.435991e-03
1.e-14	1.455051e-03
1.e-15	1.632803e-03
1.e-16	3.043793e-03

Table 6.3: $\|\partial_n u - \partial_n u_h\|_{L^2(\Gamma_C)}$ for different regularisation parameters using 31 DOF on Γ_C and refining the grid eight times with $Reg = R_2^T R_2$ calculated in the case of searched $\partial_n u|_{\Gamma_C}$ for given $\partial_n u|_{\Gamma_O} = -y^2(1-y)^2$.
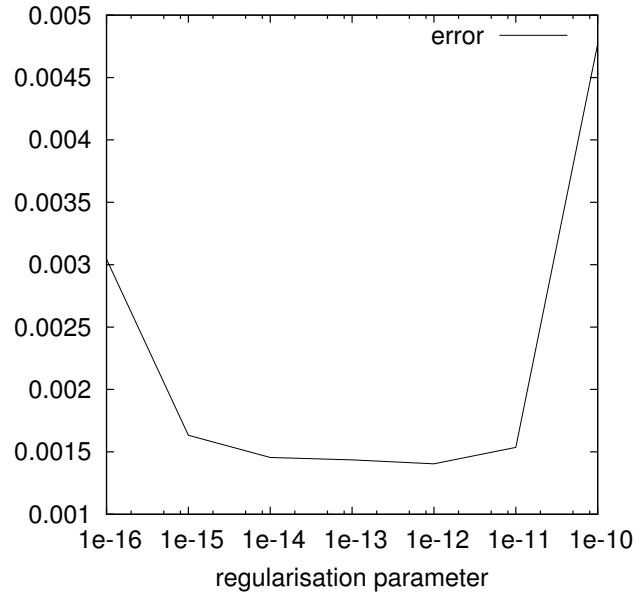
Figure 6.8: $\|\partial_n u - \partial_n u_h\|_{L^2(\Gamma_C)}$ in dependence of the regularisation parameter, refining the grid eight times using 101 DOF on Γ_C calculated with the searched $\partial_n u|_{\Gamma_C}$ and given $\partial_n u|_{\Gamma_O} = -y^2(1-y)^2$ with $Reg = R_2^T R_2$.

Now we want to compare the results for the three regularisation matrices and want to analyse how good is the approximation of the given Neumann data on Γ_O ($\partial_n u|_{\Gamma_O} = -y^2(1-y)^2$), the Dirichlet data on Γ_O we know from the underlying PDE constraint ($u|_{\Gamma_O} = 0$) and $u|_{\Gamma_C} = y^2(1-y)^2$ we know from our analytic solution computed with the calculated $\partial_n u_h|_{\Gamma_C}$.

In Figure 6.9 we can see that near $y = 0$ we reach the best approximation of the control $\partial_n u|_{\Gamma_C} = y^2(1-y)^2$ with $Reg = R_1^T R_1$ but in the surrounding of $y = 0.5$ we get the best results with $Reg = R_2^T R_2$.

Table 6.4 shows the error $\|\partial_n u - \partial_n u_h\|_{L^2(\Gamma_C)}$ for the three regularisation matrices calculated with the reduced number of DOF on Γ_C and the optimal regularisation parameters. There can be seen that the approximation of $\partial_n u|_{\Gamma_C}$ calculated with $Reg = R_1^T R_1$, 91 DOF on Γ_C and $\alpha = 1.e-12$ devoted the best result.
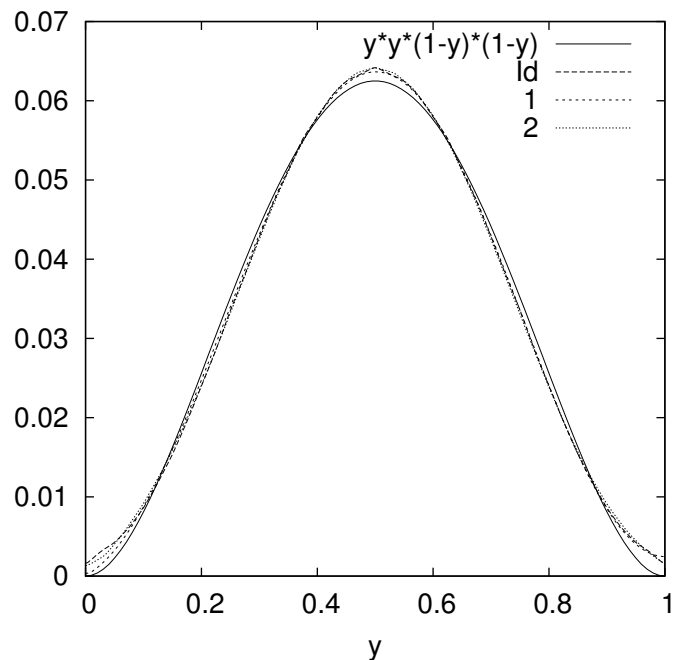
Figure 6.9: $\partial_n u|_{\Gamma_C} = y^2(1-y)^2$ and $\partial_n u_h|_{\Gamma_C}$ refining the grid eight times calculated with $Reg = R^T R$ (Id), 41 DOF on Γ_C and $\alpha = 1.e - 09$, $Reg = R_1^T R_1$ (1), 91 DOF on Γ_C and $\alpha = 1.e - 12$ and $Reg = R_2^T R_2$ (2), 31 DOF on Γ_C and $\alpha = 1.e - 12$.

Regularisation / DOF / α	$\|\partial_n u - \partial_n u_h\|_{L^2(\Gamma_C)}$
$R^T R$ / 41 / $1.e - 09$	1.319901e-03
$R_1^T R_1$ / 91 / $1.e - 12$	1.037549e-03
$R_2^T R_2$ / 31 / $1.e - 12$	1.403576e-03

Table 6.4: $\|\partial_n u - \partial_n u_h\|_{L^2(\Gamma_C)}$ for the different regularisation matrices, refining the grid eight times with reduced number of DOF on Γ_C and the optimal regularisation parameters.

Now we want to analyse how good is the approximation of the other sets of boundary data: We have given measurements $\partial_n u|_{\Gamma_O} = -y^2(1 - y)^2$ from our optimal control problem, we know $u|_{\Gamma_O} = 0$ from the underlying PDE-constraint and from the analytic solution (Equation (6.2)) we know $u|_{\Gamma_C} = y^2(1 - y)^2$.

We start with the presentation of the results for the given measurements $\partial_n u|_{\Gamma_O}$. In Figure 6.10 (left) we can see the results of calculation for the three regularisation matrices with reduced number of DOF on Γ_C and optimal regularisation parameters. The results of calculation for different grid refinements, different number of DOF on Γ_C and different regularisation parameters calculated with the computed control $\partial_n u_h|_{\Gamma_C}$ for the three regularisations can be seen in appendix A. We can see that there is graphically no obvious difference between the approximations for the different calculations and the analytic solution $\partial_n u|_{\Gamma_O} = -y^2(1-y)^2$.

Also for the approximations of $u|_{\Gamma_C} = y^2(1-y)^2$ (Figure 6.10 right) and $u|_{\Gamma_O} = 0$ (Figure 6.11) there are graphically no obvious discrepancies.

We have seen, that we get the best approximation of the control $\partial_n u|_{\Gamma_C}$ for given $\partial_n u|_{\Gamma_O} = -y^2(1-y)^2$ and reduced number of DOF with $Reg = R_1^T R_1$ using $\alpha = 1.e{-}12$. For the calculation of the other boundary data ($\partial_n u|_{\Gamma_O}$, $u|_{\Gamma_C}$ and $u|_{\Gamma_O}$) there is graphically no obvious discrepancy between the calculations with the different regularisation matrices.
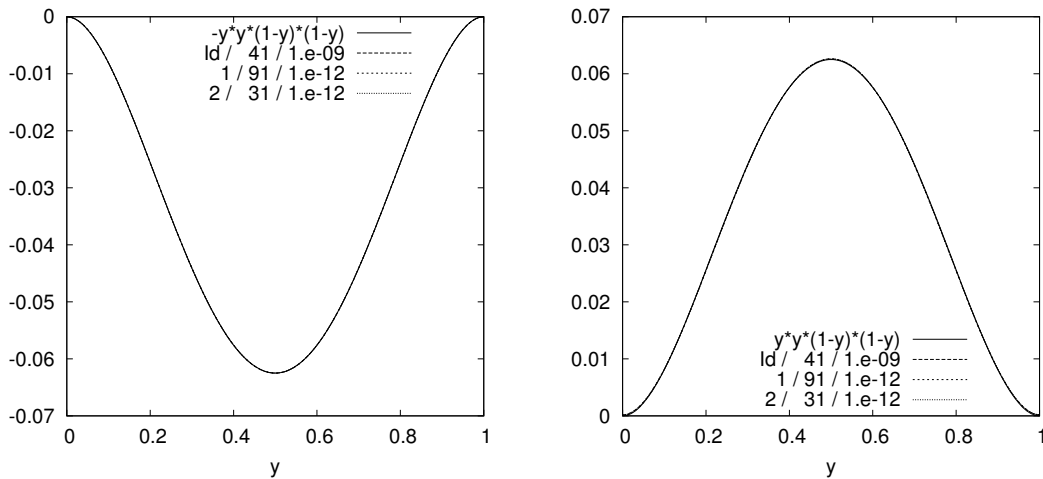
Figure 6.10: $\partial_n u|_{\Gamma_O} = -y^2(1-y)^2$ and $\partial_n u_h|_{\Gamma_O}$ (left), $u|_{\Gamma_C} = y^2(1-y)^2$ and $u_h|_{\Gamma_C}$ (right) for the three regularisation matrices with reduced number of DOF on Γ_C and optimal regularisation parameters refining the grid eight times.
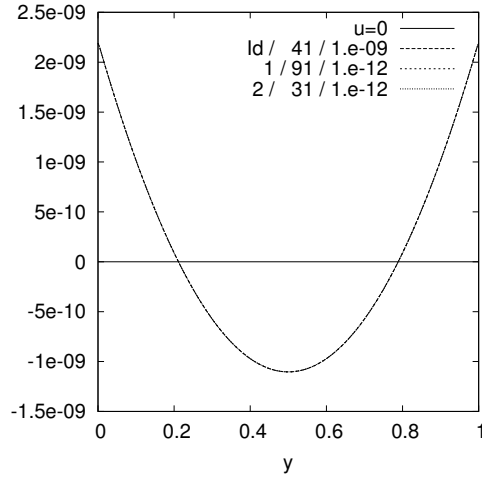
Figure 6.11: $u|_{\Gamma_O} = 0$ and $u_h|_{\Gamma_O}$ for the three regularisation matrices with reduced number of DOF on Γ_C and optimal regularisation parameters refining the grid eight times.

As can also be seen in appendix A, we have to discretise fine enough to get good approximations of the control $\partial_n u|_{\Gamma_C}$. If we have a good approximation of the control the choice of the number of DOF on Γ_C and the regularisation parameter is not decisive for the approximation of the other boundary data.

6.2 Neumann measurements on Γ_O and Dirichlet control on Γ_C

Now we take a look on the results for the second problem to be solved, i.e. we search the Dirichlet control $q = u|_{\Gamma_C}$ for given Neumann measurements $\partial_n u|_{\Gamma_O}$ such that

$$J(u, q) \to \min, \qquad J(w, \tau) = \frac{1}{2}\|\partial_n w - f\|_{\Gamma_O}^2 \tag{6.6}$$

under the PDE-constraint

$$
\begin{aligned}
-\Delta u &= g && \text{on} \quad \Omega\,, \\
\partial_n u &= 0 && \text{on} \quad \Gamma_N\,, \\
u &= 0 && \text{on} \quad \Gamma_O\,, \\
u &= q && \text{on} \quad \Gamma_C\,.
\end{aligned}
\tag{6.7}
$$

As for Neumann control and Neumann measurements in the last Section we present the results of calculation for the control $u|_{\Gamma_C}$ for different grid refinements, different DOF on Γ_C and different regularisation parameters for the three regularisation matrices ($R^T R$, $R_1^T R_1$ and $R_2^T R_2$). As in the previous Section we reduce the number of DOF and determine for this calculations the optimal regularisation parameter. After that we compare the results for the three regularisations and analyse how good the approximation of the other boundary conditions is, given from measurements, the PDE-constraint and the analytic solution.

First we analyse the results for the searched control $u|_{\Gamma_C}$ for different grid refinements and the three regularisation matrices. We discretise Ω up to eight (65536 cells) times and have $2^i + 1$ DOF on each boundary if we discretise Ω i times.

In Figure 6.12 (top left) we see the numerical results if we discretise Ω six to eight times with $Reg = R^T R$ and $\alpha = 1.e - 10$. As in the previous Section we can see that we get better results for finer grids. Again we don't make an error analysis at this point caused by the dependence on the regularisation parameter.

Figure 6.12 (top right) shows the development of $\partial_n u_h|_{\Gamma_C}$ calculated with $Reg = R_1^T R_1$ as regularisation matrix and $\alpha = 1.e - 13$. We can see that the results are unsymmetric caused by the unsymmetric R_1 and that we get the better results for finer grids.

If we regularise by $Reg = R_2^T R_2$ (Figure 6.12 bottom), we see that we get earlier better results and the discrepancy between the calculations for seven and eight grid refinements is smaller than for the other regularisation matrices. This can also be caused by the regularisation parameter which we choose here as $\alpha = 1.e - 13$.

In general we get the better results for finer grids in all three cases. As in the previous Section this is bad for the runtime of the program. A reduction of the number of DOF on Γ_C will have a positive effect on the runtime. Now we want to analyse if we can reduce the number of DOF on Γ_C for this problem (Dirichlet control for given Neumann measurement) without loosing quality of the approximation.
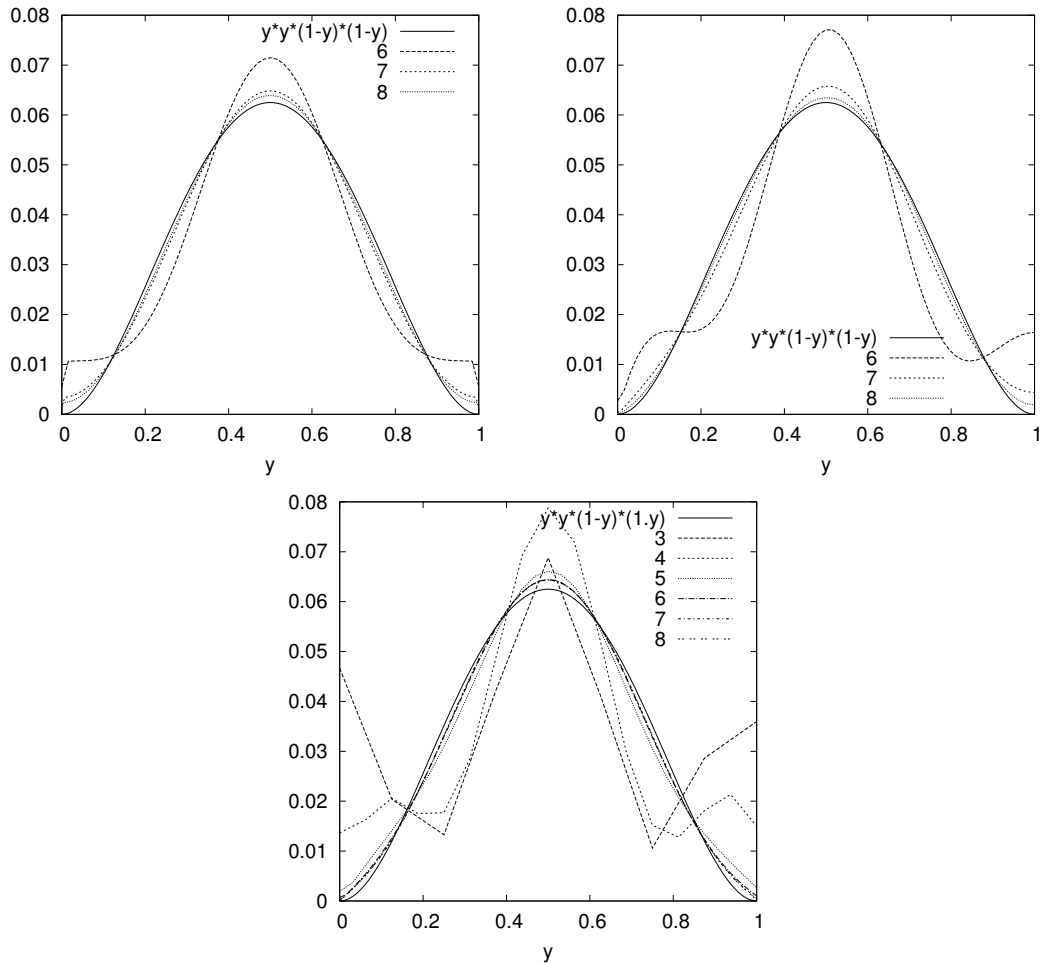
Figure 6.12: $u|_{\Gamma_C} = y^2(1-y)^2$ and $u_h|_{\Gamma_C}$ for different grid refinements calculated for searched control $u|_{\Gamma_C}$ and given $\partial_n u|_{\Gamma_O} = -y^2(1-y)^2$. Results calculated with $Reg = R^T R$ and regularisationparameter $\alpha = 1.e - 10$ (top left) with $Reg = R_1^T R_1$ and $\alpha = 1.e - 13$ (top right) with $Reg = R_2^T R_2$ and $\alpha = 1.e - 13$ (bottom).

In Figure 6.13 (left) we see the results for 11, 41 and 257 DOF on Γ_C if we refine the grid eight times, using $Reg = R^T R$ and $\alpha = 1.e - 10$. Here we can see that we get better results if we reduce the number of DOF on Γ_C. As for the calculation in the case of searched Neumann control on Γ_C (Section 6.1) we get good approximations if we reduce the number of DOF on Γ_C to 41.
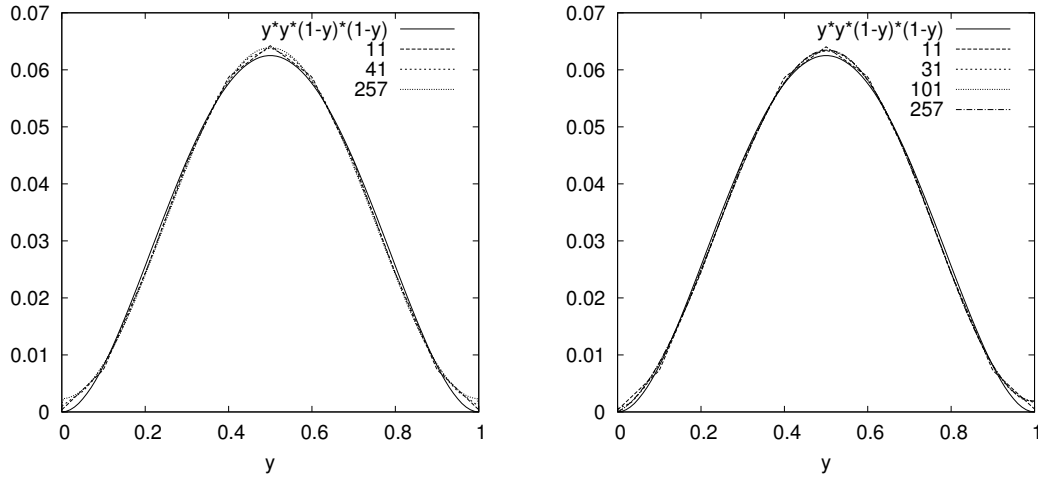
Figure 6.13: $u|_{\Gamma_C} = y^2(1 - y)^2$ and $u_h|_{\Gamma_C}$ for different number of DOFs on Γ_C for refining the grid eight times calculated for searched $u|_{\Gamma_C}$ and given $\partial_n u|_{\Gamma_O} = -y^2(1 - y)^2$. Result for 11, 41 and 257 DOF with regularisation parameter $\alpha = 1.e - 10$ and $Reg = R^T R$ (left), for 11, 31, 101 and 257 DOF, $\alpha = 1.e - 13$ and $Reg = R_1^T R_1$ (right).

We have the same effect if we use $Reg = R_1^T R_1$ as regularisation matrix (see Figure 6.13 (right)). 11 DOF on Γ_C is a too small but for 31 DOF we reach good results. In this case we can reduce the number of DOF more than in the calculation for searched Neumann control (Section 6.1) where we reduce the number of DOF on Γ_C to 91. Anyway we do the calculations in the following for 101 DOF on Γ_C. This is caused by the calculation of the other boundary data computed with this calculated control $u_h|_{\Gamma_C}$. We will analyse this later.

Also for $Reg = R_2^T R_2$ as regularisation matrix we can see, that we can reduce the number of DOF on Γ_C without loosing much quality of the results (Figure 6.14).

There we choose 11, 31, 91 and 257 DOF on Γ_C. As for $Reg = R_1^T R_1$ we enlarge the number of DOF in the following calculations to 91 although we get good results for 31 DOF again caused by the other boundary conditions.
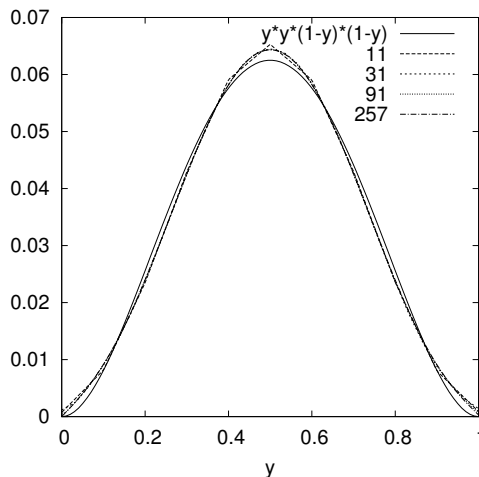
Figure 6.14: $u|_{\Gamma_C} = y^2(1-y)^2$ and $u_h|_{\Gamma_C}$ for 11, 31, 91 and 257 DOF on Γ_C using $\alpha = 1.e - 13$ and refining the grid eight times calculated for searched $u|_{\Gamma_C}$ and given $\partial_n u|_{\Gamma_O} = -y^2(1-y)^2$ with $Reg = R_2^T R_2$.

Now we want to analyse the influence of the regularisation parameter on the results of the calculation of the searched control $u|_{\Gamma_C}$. For the regularisation with $Reg = R^T R$ we choose parameters between $\alpha = 1.e - 13$ and $\alpha = 1.e - 10$. We can see (Figure 6.15) that $\alpha = 1.e - 13$ is too small and $\alpha = 1.e - 10$ is too big. For $1.e - 11$ and $1.e - 12$ there are only small differences.

The error calculation (table 6.5) where we additionally calculate the error for $\alpha = 1.e - 09$ to $\alpha = 1.e - 07$ shows that $\alpha = 1.e - 11$ is the optimal regularisation parameter if we discretise eight times, use 41 DOF on Γ_C and regularise by $Reg = R^T R$. This can also be seen in Figure 6.16.

In comparison with the results for searched Neumann control where we have for the calculation with $Reg = R^T R$ $\alpha = 1.e - 09$ as optimal parameter (see Section 6.1) we can choose a smaller parameter if we search Dirichlet control on Γ_C.
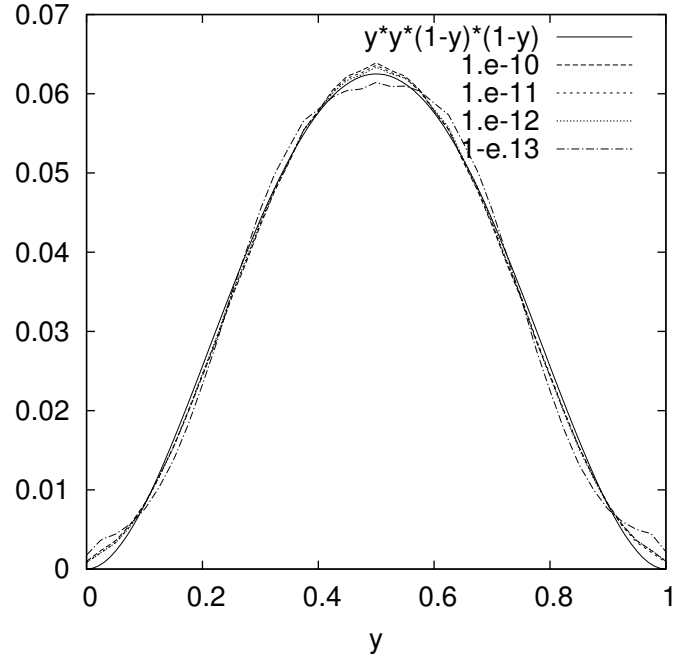
Figure 6.15: $u|_{\Gamma_C} = y^2(1-y)^2$ and $u_h|_{\Gamma_C}$ for different regularisation parameters with $Reg = R^T R$ for refining the grid eight times and 41 DOF on Γ_C calculated for the searched $u|_{\Gamma_C}$ and given $\partial_n u|_{\Gamma_O} = -y^2(1-y)^2$.

Regularisationparameter	$\|u - u_h\|_{L^2(\Gamma_C)}$
1.e-07	1.348695e-03
1.e-08	1.331564e-03
1.e-09	1.245377e-03
1.e-10	9.388004e-04
1.e-11	7.602756e-04
1.e-12	7.971643e-04
1.e-13	1.858937e-03

Table 6.5: $\|u - u_h\|_{L^2(\Gamma_C)}$ for different regularisation parameters with $Reg = R^T R$ using 41 DOF on Γ_C and refining the grid eight times.
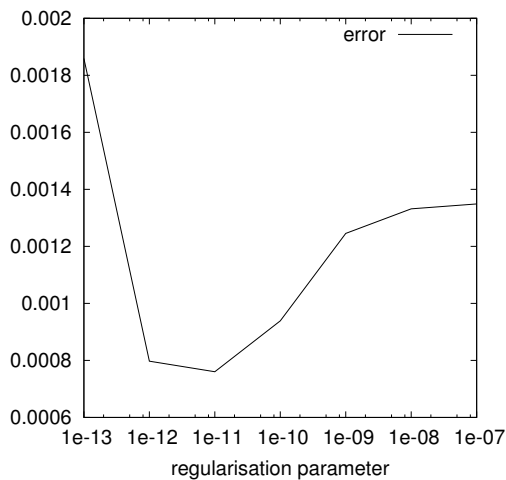
Figure 6.16: $\|u - u_h\|_{L^2(\Gamma_C)}$ in dependence of the regularisation parameter, refining the grid eight times using 41 DOF on Γ_C calculated with the searched $u|_{\Gamma_C}$ and given $\partial_n u|_{\Gamma_O} = -y^2(1-y)^2$ and $Reg = R^T R$.

In the case where we regularise by $Reg = R_1^T R_1$ refining the grid eight times and using 101 DOF on Γ_C we choose parameters between $\alpha = 1.e - 16$ and $\alpha = 1.e - 10$. The error calculation (table 6.6) and Figure 6.18, which illustrates the error development in dependence of the regularisation parameter shows clearly that the optimal regularisation parameter for regularising with $Reg = R_1^T R_1$ refining the grid eight times and using 101 DOF is $\alpha = 1.e - 14$.

In this case, where we regularise by $Reg = R_1^T R_1$, we have a smaller optimal regularisation parameter as in the calculation for searched Neumann control.

At last we want to analyse the influence of the regularisation parameter on the calculation with $Reg = R_2^T R_2$ as regularisation matrix. For this case we choose the parameters between $\alpha = 1.e - 19$ and $\alpha = 1.e - 11$, refine the grid eight times and use 91 DOF on Γ_C. For the sake of clarity in Figure 6.19 we can see only five of these parameters. Graphically $\alpha = 1.e - 17$ seems to be the optimal parameter. This is verified in table 6.7 and Figure 6.20 where we illustrate the development of $\|u - u_h\|_{L^2(\Gamma_C)}$ in dependence of the regularisation parameter.
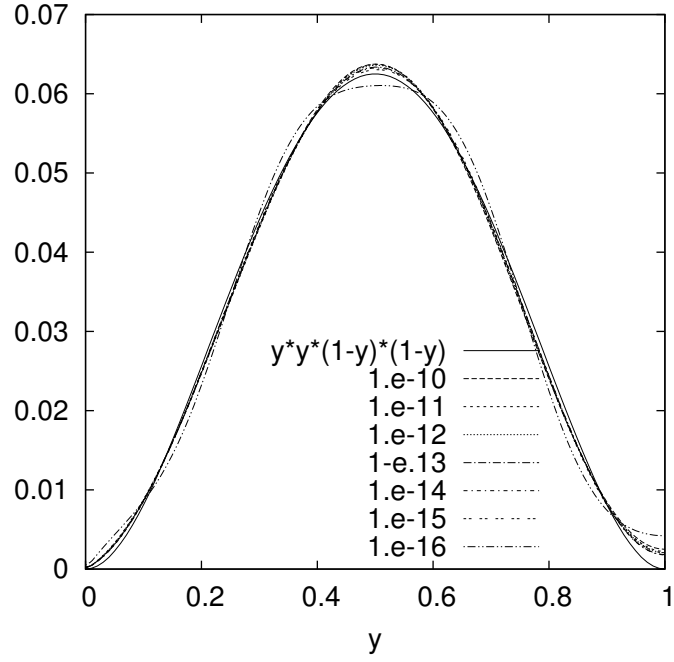
Figure 6.17: $u|_{\Gamma_C}$ and $u_h|_{\Gamma_C}$ for different regularisation parameters for refining eight times and 101 DOF on Γ_C calculated for the searched $u|_{\Gamma_C}$ and given $\partial_n u|_{\Gamma_O} = -y^2(1-y)^2$ with $Reg = R_1^T R_1$.

Regularisationparameter	$\|u - u_h\|_{L^2(\Gamma_C)}$
1.e-10	1.061429e-03
1.e-11	1.013701e-03
1.e-12	9.391228e-04
1.e-13	7.864336e-04
1.e-14	7.383610e-04
1.e-15	7.938105e-04
1.e-16	1.845287e-03

Table 6.6: $\|u - u_h\|_{L^2(\Gamma_C)}$ in dependence of the regularisation parameter, refining the grid eight times using 101 DOF on Γ_C calculated for the searched $u|_{\Gamma_C}$ and given $\partial_n u|_{\Gamma_O} = -y^2(1-y)^2$ with $Reg = R_1^T R_1$.
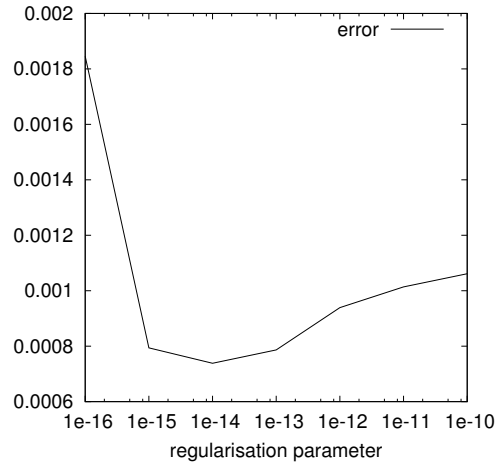
Figure 6.18: $\|u - u_h\|_{L^2(\Gamma_C)}$ in dependence of the regularisation parameter refining the grid eight times using 101 DOF on Γ_C calculated with the searched $u|_{\Gamma_C}$ and given $\partial_n u|_{\Gamma_O} = -y^2(1-y)^2$ with $Reg = R_1^T R_1$.

If we compare the results for searched Dirichlet control and searched Neumann control (from the previous Section) we have seen, that in both cases we can choose 31 DOF on Γ_C to get good approximations. In the case of the Dirichlet control we set the number of DOF to 91 caused by the calculation of the other boundary data which we will analyse in the following. But therefore we can set $\alpha = 1.e - 17$ instead of $\alpha = 1.e - 12$ in the case of searched Neumann control.

Regularisation-parameter	$\|u - u_h\|_{L^2(\Gamma_C)}$	Regularisation parameter	$\|u - u_h\|_{L^2(\Gamma_C)}$
1.e-10	3.169159e-04	1.e-15	1.957752e-04
1.e-11	2.711583e-04	1.e-16	1.489964e-04
1.e-12	2.768743e-04	1.e-17	1.434415e-04
1.e-13	2.756781e-04	1.e-18	1.687428e-04
1.e-14	2.602671e-04	1.e-19	5.699224e-04

Table 6.7: $\|u - u_h\|_{L^2(\Gamma_C)}$ for different regularisation parameters refining the grid eight times using 91 DOF on Γ_C calculated for the searched $u|_{\Gamma_C}$ and given $\partial_n u|_{\Gamma_O} = -y^2(1-y)^2$ with $Reg = R_2^T R_2$.
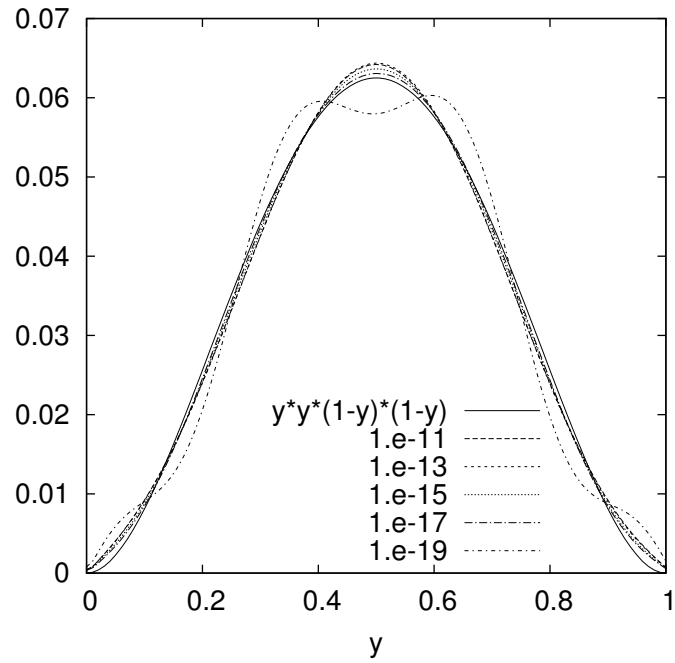
Figure 6.19: $u|_{\Gamma_C} = y^2(1-y)^2$ and $u_h|_{\Gamma_C}$ for different regularisation parameters using 91 DOF on Γ_C and refining eight times calculated for searched $u|_{\Gamma_C}$ and given $\partial_n u|_{\Gamma_O} = -y^2(1-y)^2$ with $Reg = R_2^T R_2$.
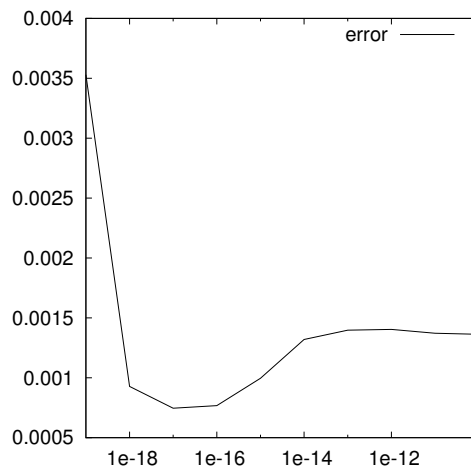
Figure 6.20: $\|u - u_h\|_{L^2(\Gamma_C)}$ in dependence of the regularisation parameter refining the grid eight times using 91 DOF on Γ_C calculated with the searched $u|_{\Gamma_C}$ and given $\partial_n u|_{\Gamma_O} = -y^2(1-y)^2$ with $Reg = R_2^T R_2$.

As in the previous Section we have seen that we have to discretise fine enough on the domain Ω to get a good approximation of the searched control $u|_{\Gamma_C}$ for given $\partial_n u|_{\Gamma_O} = -y^2(1-y)^2$. But we can reduce the number of DOF on Γ_C (depending on the regularisation matrix) for saving runtime. And we have estimated the optimal regularisation parameters for refining the grid eight times and the number of DOF on Γ_C depending on the used regularisation matrix. Now we want to compare the results for the three regularisation matrices and want to analyse how good is the approximation of the given measured data $\partial_n u|_{\Gamma_O} = -y^2(1-y)^2$, of $u|_{\Gamma_O} = 0$ which we know from the underlying PDE-constraint and of $\partial_n u|_{\Gamma_C} = y^2(1-y)^2$ which we know from our analytic solution (Equation (6.2)). We start with the comparison of the searched control $u|_{\Gamma_C}$ (Figure 6.21).
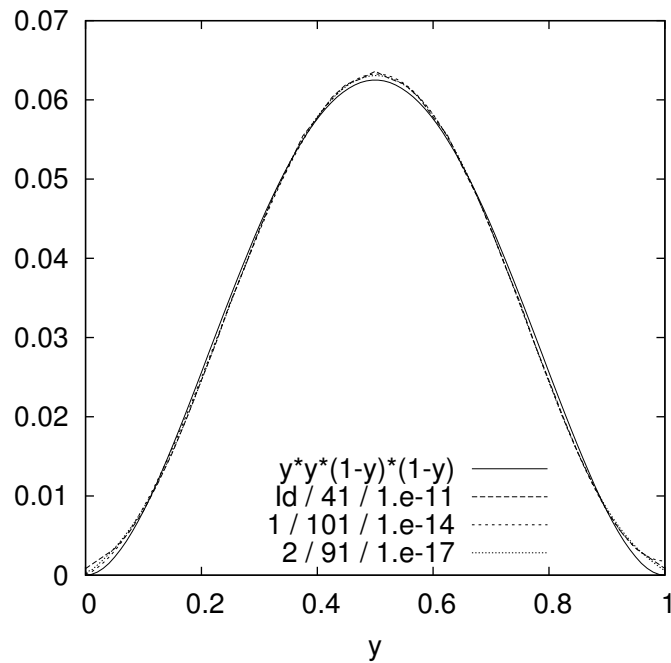
Figure 6.21: $u|_{\Gamma_C} = y^2(1-y)^2$ and $u_h|_{\Gamma_C}$ refining eight times calculated with $Reg = R^T R$, 41 DOF on Γ_C and $\alpha = 1.e-11$; $Reg = R_1^T R_1$ (1), 101 DOF on Γ_C and $\alpha = 1.e-14$ and $Reg = R_2^T R_2$ (2), 91 DOF on Γ_C and $\alpha = 1.e-17$.

Therefore we discretise eight times. For the calculation with $Reg = R^T R$ we choose 41 DOF on Γ_C and set $\alpha = 1.e - 11$. In the case where we regularise by $Reg = R_1^T R_1$ we choose 101 DOF on Γ_C and set $\alpha = 1.e - 14$ and for the regularisation with $Reg = R_2^T R_2$ we choose 91 DOF on Γ_C and set $\alpha = 1.e - 17$. We can see that there are small discrepancies between the calculations specially near $y = 0$ and $y = 1$.

Table 6.8 shows that we get the best results for the calculation with $Reg = R_2^T R_2$, $\alpha = 1.e - 17$ and 91 DOF on Γ_C. For the calculation of the searched Neumann control (previous Section) we get the best results for the regularisation with $Reg = R_1^T R_1$.

Regularisation / DOF / α	$\|u - u_h\|_{L^2(\Gamma_C)}$
$R^T R$ / 41 / 1.e-11	7.602756e-04
$R_1^T R_1$ / 101 / 1.e-14	7.383610e-04
$R_2^T R_2$ / 91 / 1.e-17	1.434415e-04

Table 6.8: $\|u - u_h\|_{L^2(\Gamma_C)}$ for the different regularisation matrices, refining the grid eight times with reduced number of DOF on Γ_C and the optimal regularisation parameters.

Now we want to analyse how good the approximation of the other boundary data is, calculated with the computed control $u_h|_{\Gamma_C}$. We start with the given measurement $\partial_n u|_{\Gamma_O} = -y^2(1 - y)^2$ (see Figure 6.22 left).

As in the case of searched Neumann control there is graphically no obvious difference between the three calculations. This is also the case for the calculation of the given boundary constraint $u|_{\Gamma_O} = 0$ (Figure 6.22 right). For the calculation of $\partial_n u|_{\Gamma_C}$ we have differences between the calculations (Figure 6.23), which is very obvious. We get oscillations in the calculation with $Reg = R^T R$ as regularisation matrix. Also without reducing the number of DOF on Γ_C we are not able to eliminate this oscillations (see appendix A.2). In the cases where we regularise by $Reg = R_1^T R_1$ and $Reg = R_2^T R_2$ we have seen that we can reduce the number of DOF to 31 to get a good approximation of the searched control $u|_{\Gamma_C}$ but we have chosen 101 91

respectively DOF in the following calculations. This is caused in the results of the calculation for $\partial_n u|_{\Gamma_C}$ with the computed control $u_h|_{\Gamma_C}$. If we set the number of DOF on Γ_C to 31, we also get oscillations in the calculation of $\partial_n u_h|_{\Gamma_C}$ (see Figure 6.24) if we regularise by $Reg = R_1^T R_1$ or $R_2^T R_2$.
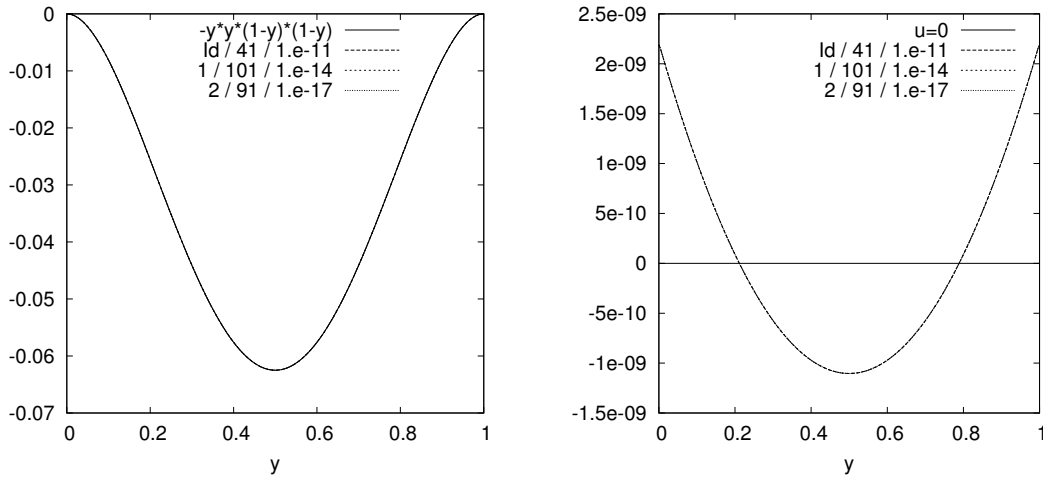
Figure 6.22: $\partial_n u|_{\Gamma_O} = -y^2(1-y)^2$ and $\partial_n u_h|_{\Gamma_O}$ (left), $u|_{\Gamma_O} = 0$ and $u_h|_{\Gamma_O}$ (right) for the three regularisation matrices with reduced number of DOF on Γ_C and optimal regularisation parameters for refining the grid eight times.

In the case of the searched Neumann control we get good approximations of $\partial_n u|_{\Gamma_C}$ but with this we also get good approximations of the other boundary data ($u|_{\Gamma_C}$, $\partial_n u|_{\Gamma_O}$, $u|_{\Gamma_O}$). If we search $u|_{\Gamma_C}$ and calculate with this $\partial_n u|_{\Gamma_C}$, $\partial_n u|_{\Gamma_O}$ and $u|_{\Gamma_O}$ now we get good approximations of the boundary data on Γ_O but for $\partial_n u|_{\Gamma_C}$ we can see a great discrepancy between the approximations and the analytic solution $\partial_n u|_{\Gamma_C} = y^2(1-y)^2$ even if we avoid oscillations. We will compare the results in detail later on.
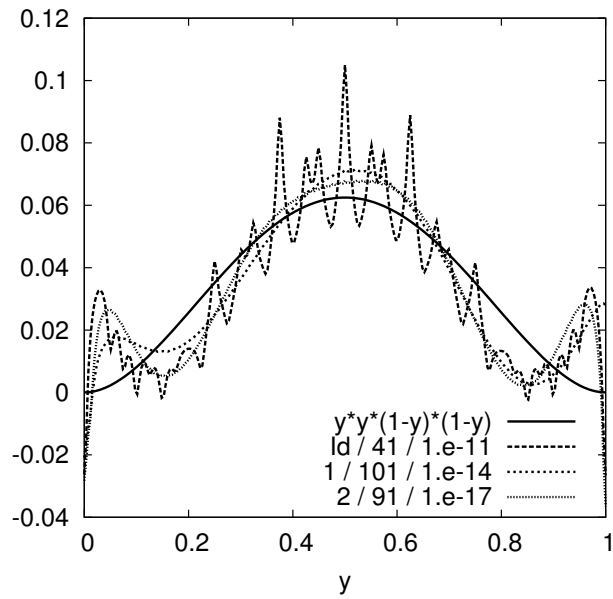
Figure 6.23: $\partial_n u|_{\Gamma_C} = y^2(1-y)^2$ and $\partial_n u_h|_{\Gamma_C}$ for the three regularisation matrices with reduced number of DOF on Γ_C and optimal regularisation parameter for refining the grid eight times.
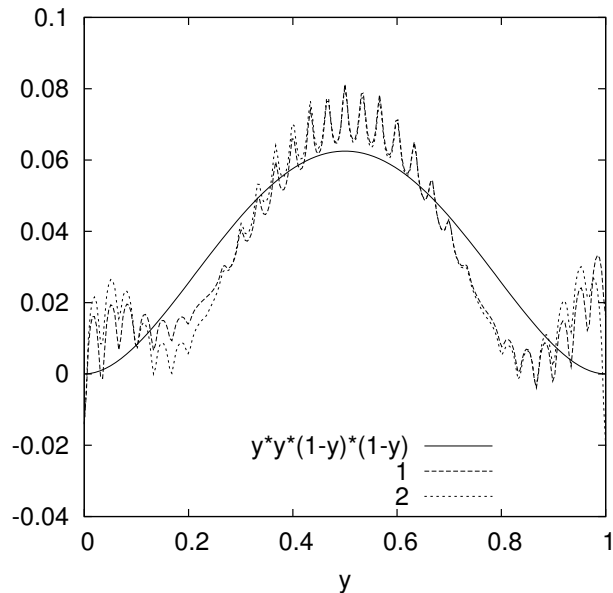
Figure 6.24: $\partial_n u|_{\Gamma_C} = y^2(1-y)^2$ and $\partial_n u_h|_{\Gamma_C}$ for eight gridrefinements, 31 DOF on Γ_C for $Reg = R_1^T R_1$ (1) and $Reg = R_2^T R_2$ (2).

6.3 Dirichlet measurements on Γ_O and Dirichlet control on Γ_C

In this Section we want to find the Dirichlet control $u|_{\Gamma_C} = q$ for given Dirichlet measurements $u|_{\Gamma_O} = 0$ such that

$$J(u, q) \rightarrow \min, \quad J(w, \tau) = \frac{1}{2} \|w\|^2_{\Gamma_O} \tag{6.8}$$

under the PDE-constraint

$$\begin{aligned} -\Delta u &= g && \text{on} \quad \Omega\,, \\ \partial_n u &= 0 && \text{on} \quad \Gamma_N\,, \\ \partial_n u &= f && \text{on} \quad \Gamma_O\,, \\ u &= q && \text{on} \quad \Gamma_C\,. \end{aligned} \tag{6.9}$$

As before we first want to analyse the results for the searched control $u|_{\Gamma_C} = q$ for different grid refinements calculated with different regularisation matrices. As in the previous Sections we use for Reg $R^T R$, $R_1^T R_1$ and $R_2^T R_2$. We discretise Ω up to eight times (65536 cells) and have $2^i + 1$ DOF on every boundary if we refine Ω i times.

In Figure 6.25 (top left) we see the results for six to eight gridrefinements in the case where we regularise by $R^T R$ and set $\alpha = 1.e - 11$. We can see, that six refinements are not sufficient and we get the best results for seven refinements. That the result for eight refinements is worse is caused by the regularisation parameter. We will see later that we get also good results for the calculation on 65536 cells.
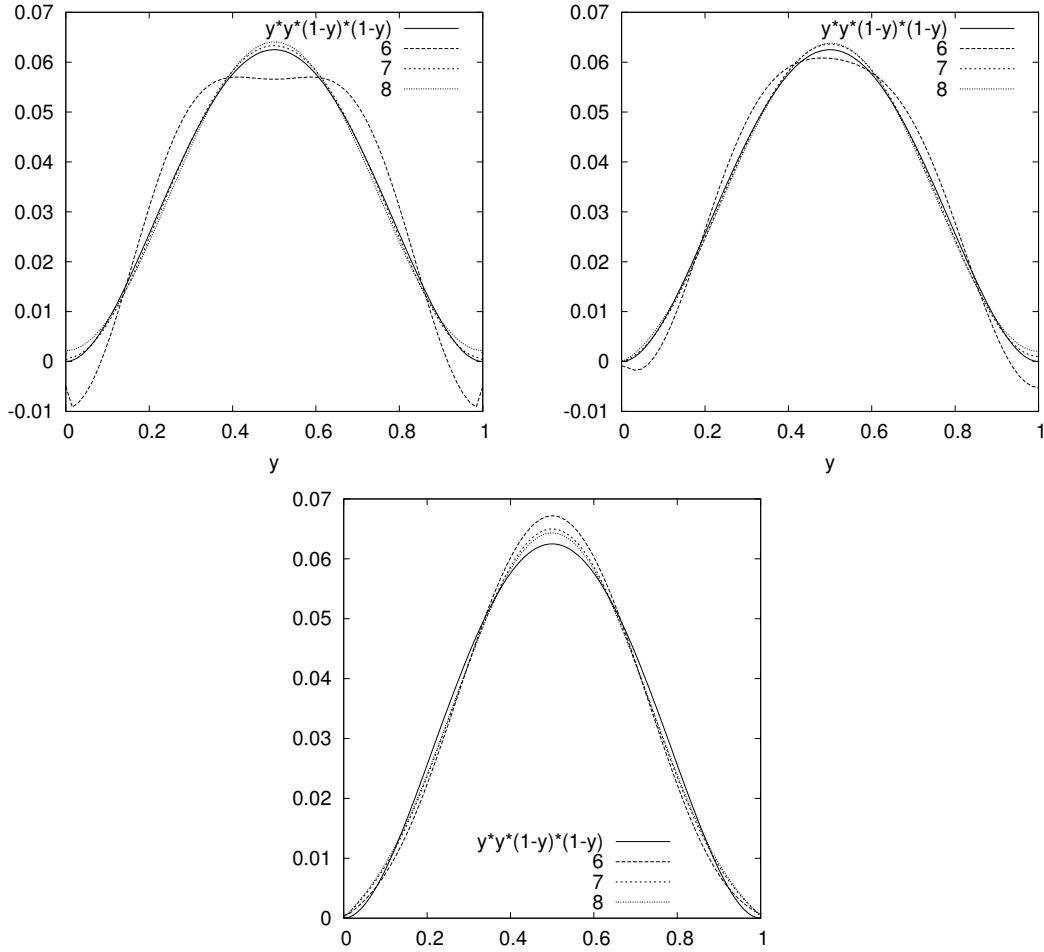
Figure 6.25: $u|_{\Gamma_C} = y^2(1-y)^2$ and $u_h|_{\Gamma_C}$ for refining the grid six to eight times calculated for searched $u|_{\Gamma_C}$ and given $u|_{\Gamma_O} = 0$ with $Reg = R^T R$ with regularisation parameter $\alpha = 1.e-11$ (top left), $Reg = R_1^T R_1$ with $\alpha = 1.e-13$ (top right) and $Reg = R_2^T R_2$ with $\alpha = 1.e-13$ (bottom).

For the unsymmetric regularisation with $Reg = R_1^T R_1$ (Figure 6.25 top right) we reach an unsymmetric result of the searched control $u_h|_{\Gamma_C}$ but we can see that we get better results for fine grids. As for $Reg = R^T R$ the better results for seven refinements than for eight are caused by the regularisation parameter. We will correct this result later with the reduction of the number of DOF on Γ_C and the choice of the regularisation parameter. As before we can see for the results with $Reg = R_2^T R_2$ (Figure 6.25 bottom) as regularisation matrix, that we get better

results for finer grids. As in the previous Sections we reach the better results for finer grids for all three regularisation matrices.

Now we want to analyse if we can reduce the number of DOF on Γ_C without loosing the quality of the approximation as in the calculations for searched Neumann control or if we have the effect as in the calculations for searched Dirichlet control and given Neumann measurements that we get oscillations if we choose the number of DOF too small. We start again with the calculation where we set $Reg = R^T R$ (Figure 6.26 top left). As number of DOF we choose 11, 31 , 101 and 257, we discretise eight times and set $\alpha = 1.e - 11$. Here we have the effect that we reach a better approximation for reducing the number of DOF to 31 instead of 257 DOF. For 101 DOF on Γ_C we get oscillations in the calculation of the searched control $u|_{\Gamma_C}$ what may be caused by the regularisation parameter. I.e. as in the previous Section we can reduce the number of DOF for the calculation with $Reg = R^T R$.

As in the previous case we choose 11, 31 101 and 257 DOF on Γ_C for the calculation of $u|_{\Gamma_C}$ with $Reg = R_1^T R_1$ as regularisation matrix and $\alpha = 1.e - 13$ (see Figure 6.26 top right). Even though we reach a good approximation of $u|_{\Gamma_C}$ with 31 DOF we will use in the following 101 DOF on Γ_C for avoiding oscillations in the calculation of $\partial_n u_h|_{\Gamma_C}$. (Compare the results for searched Dirichlet control and given Neumann measurements.)

For the calculation with $Reg = R_2^T R_2$ as regularisation matrix we discretise Ω eight times, set $\alpha = 1.e - 13$ and do the calculation for 11, 31, 101 and 257 DOF on Γ_C. We can see (Figure 6.26 bottom) that there are only small differences between the computations and that we get a good approximation for 31 DOF on Γ_C. Caused by the calculation of the other boundary conditions we have to enlarge the number of DOF a bit and use in the following 101 DOF on Γ_C.

As in the previous Section where we searched Dirichlet control for given Neumann measurement we can reduce the number of DOF on Γ_C. Caused by the calculation of the other boundary data with the computed control $u_h|_{\Gamma_C}$ we have to enlarge the number of DOF for the calculation with $Reg = R_1^T R_1$ and $R_2^T R_2$.
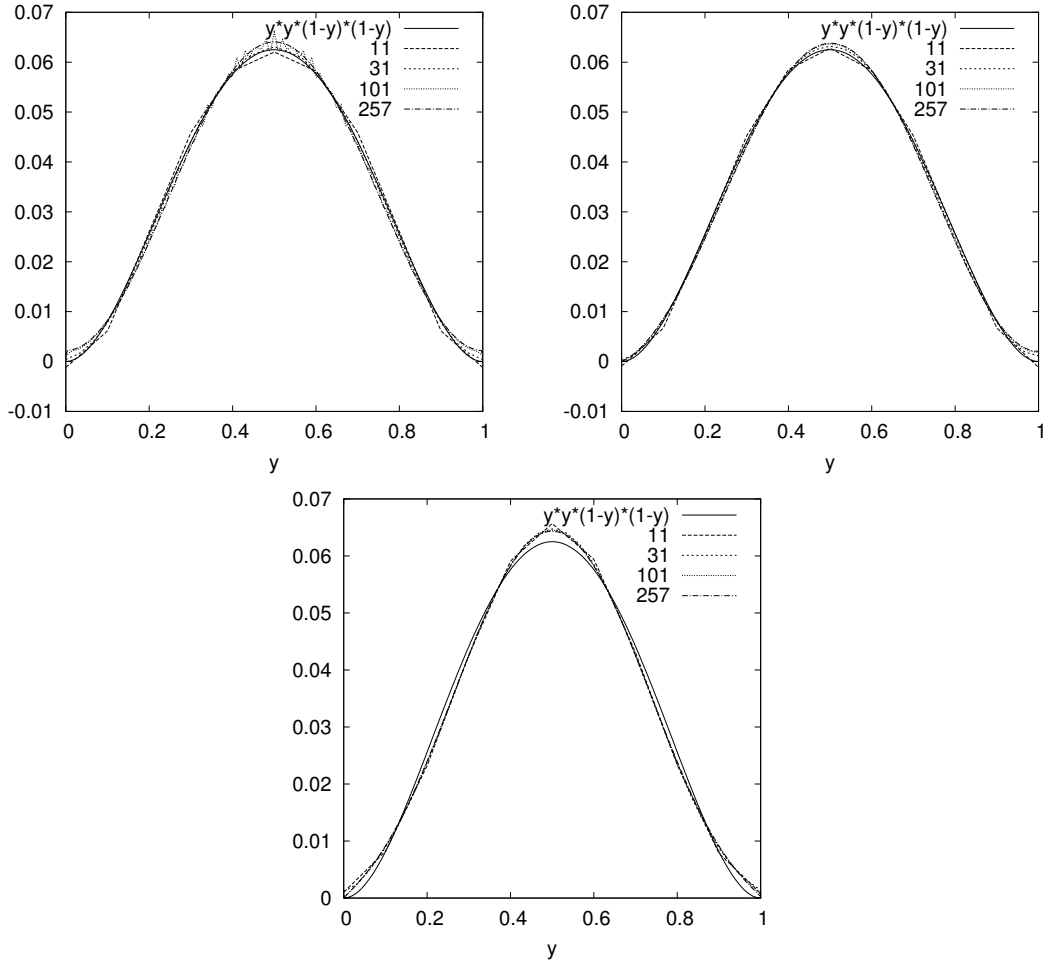
Figure 6.26: $u|_{\Gamma_C}$ and $u_h|_{\Gamma_C}$ for different DOF on Γ_C and refining the grid eight times calculated for searched $u|_{\Gamma_C}$ and given $u|_{\Gamma_O} = 0$. Results calculated with $Reg = R^T R$ and $\alpha = 1.e - 11$ (top left), with $Reg = R_1^T R_1$ and $\alpha = 1.e - 13$ (top right) and with $Reg = R_2^T R_2$ and $\alpha = 1.e - 13$ (bottom).

Before we want to analyse how good the approximation of the other boundary conditions with the computed control $u|_{\Gamma_C}$ is and what problems appear we want to estimate the optimal regularisation parameter. First we do the calculations with $Reg = R^T R$ if we refine the grid eight times and use 31 DOF on Γ_C (see Figure 6.27). We do the calculation for $\alpha = 1.e - 13$ to $\alpha = 1.e - 10$. It is obvious that we get the best result for $\alpha = 1.e - 11$. This is verified in table 6.9 and Figure 6.28

where we can see $\|u - u_h\|_{L^2(\Gamma_C)}$ in dependence of the regularisation parameter. It's the same parameter if we regularise by $R^T R$ and search Dirichlet control on Γ_C for given Neumann measurements on Γ_O.
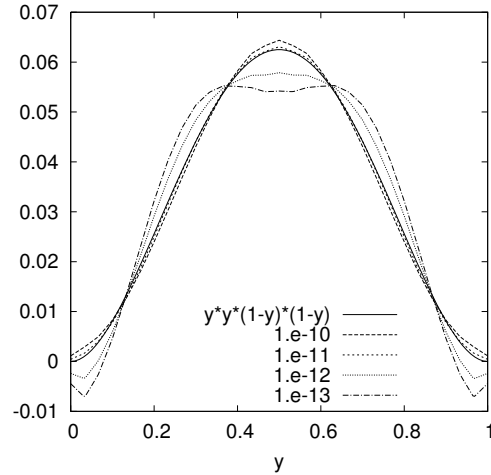
Figure 6.27: $u|_{\Gamma_C} = y^2(1-y)^2$ and $u_h|_{\Gamma_C}$ for different regularisation parameters, $Reg = R^T R$, refining the grid eight times using 31 DOF on Γ_C calculated for searched $u|_{\Gamma_C}$ and given $u|_{\Gamma_O} = 0$.
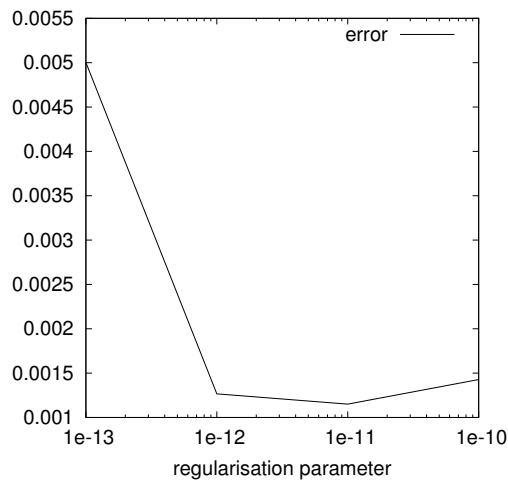
Figure 6.28: $\|u - u_h\|_{L^2(\Gamma_C)}$ in dependence of the regularisation parameter with $Reg = R^T R$ for refining the grid eight times and use 31 DOF on Γ_C.

Regularisationparameter	$\|u - u_h\|_{L^2(\Gamma_C)}$
1.e-10	1.427001e-03
1.e-11	1.150256e-03
1.e-12	1.266659e-03
1.e-13	5.002099e-03

Table 6.9: $\|u - u_h\|_{L^2(\Gamma_C)}$ for different regularisation parameters refining the grid eight times, $Reg = R^T R$ and 31 DOF on Γ_C.

If we regularise by $Reg = R_1^T R_1$, we use 101 DOF on Γ_C and choose parameters between $\alpha = 1.e - 15$ and $\alpha = 1.e - 11$ (Figure 6.29). Table 6.10 and Figure 6.30 shows, that $\alpha = 1.e - 14$ is the optimal regularisation parameter for refining the grid eight times and using 101 DOF on Γ_C. This is the same parameter as in the calculation of searched Dirichlet control for given Neumann measurements and regularise by $Reg = R_1^T R_1$ (see Section 6.2).
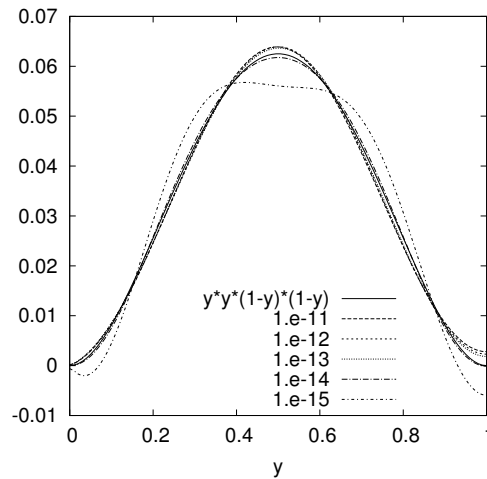
Figure 6.29: $u|_{\Gamma_C} = y^2(1 - y)^2$ and $u_h|_{\Gamma_C}$ for different regularisation parameters refining the grid eight times using 101 DOF on Γ_C and regularise by $Reg = R_1^T R_1$ calculated for searched $u|_{\Gamma_C}$ and given $u|_{\Gamma_O} = 0$.

Regularisationparameter	$\|u - u_h\|_{L^2(\Gamma_C)}$
1.e-11	1.170204e-03
1.e-12	1.058646e-03
1.e-13	8.749769e-04
1.e-14	5.156368e-04
1.e-15	4.300165e-03
1.e-16	6.205671e-03

Table 6.10: $\|u - u_h\|_{L^2(\Gamma_C)}$ for different regularisation parameters refining the grid eight times and use 101 DOF on Γ_C regularise by $Reg = R_1^T R_1$.
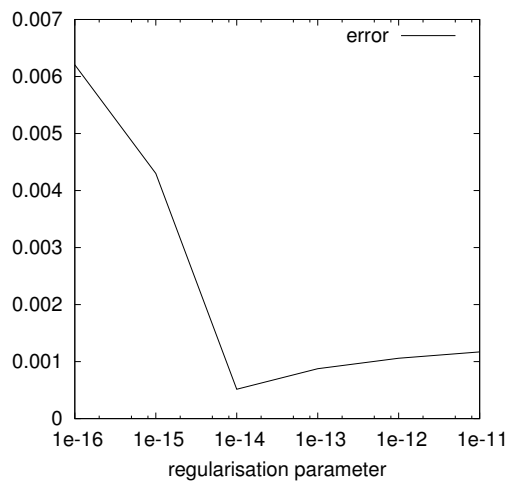
Figure 6.30: $\|u - u_h\|_{L^2(\Gamma_C)}$ in dependence of the regularisation parameter refining the grid eight times and using 101 DOF on Γ_C regularise by $Reg = R_1^T R_1$.

For the regularisation with $Reg = R_2^T R_2$ we use 101 DOF on Γ_C and choose parameters between $\alpha = 1.e - 18$ and $\alpha = 1.e - 10$. For the sake of clarity we see in Figure 6.31 the lines of only five of these parameters. It can be seen that $\alpha = 1.e - 10$ is too big and $\alpha = 1.e - 18$ is too small. Table 6.11 where we listed all parameters shows that the optimal parameter in this case is $\alpha = 1.e - 16$. This can also be seen in Figure 6.32.
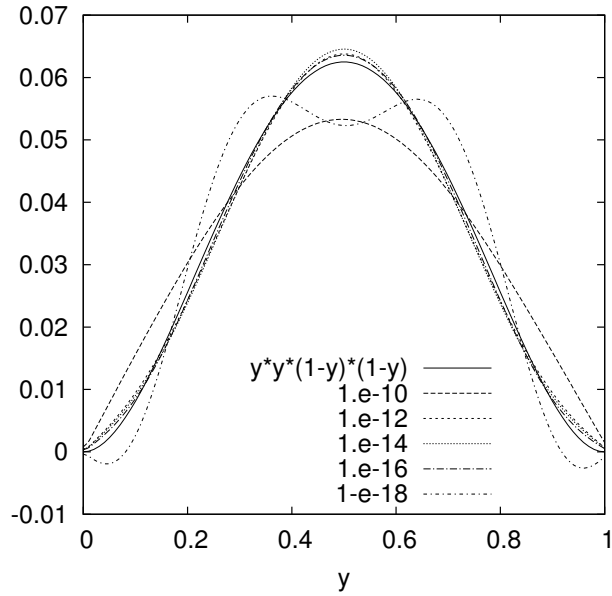
Figure 6.31: $u|_{\Gamma_C} = y^2(1-y)^2$ and $u_h|_{\Gamma_C}$ for different regularisation parameters for refining the grid eight times and 101 DOF on Γ_C calculated for the searched $u|_{\Gamma_C}$ and given $u|_{\Gamma_O} = 0$ with $Reg = R_2^T R_2$.
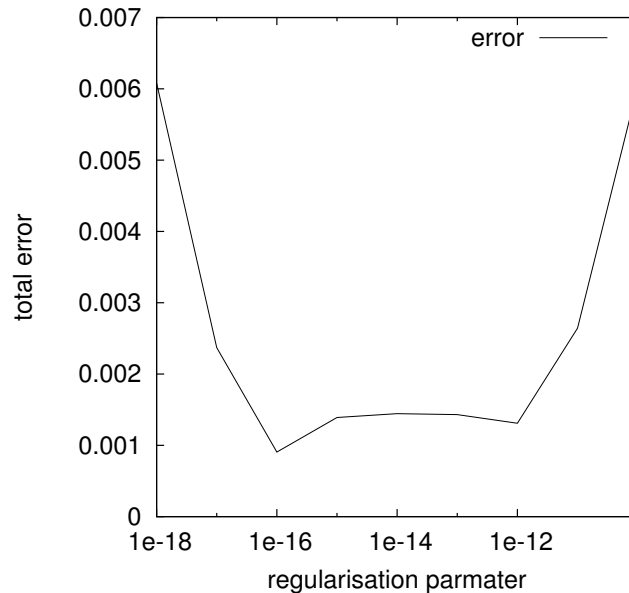
Figure 6.32: $\|u - u_h\|_{L^2(\Gamma_C)}$ in dependence of the regularisation parameter for refining the grid eight times, 101 DOF on Γ_C and $Reg = R_2^T R_2$.

Regularisationparameter	$\|u - u_h\|_{L^2(\Gamma_C)}$
1.e-10	6.027712e-03
1.e-11	2.643012e-03
1.e-12	1.309626e-03
1.e-13	1.430878e-03
1.e-14	1.443650e-03
1.e-15	1.390372e-03
1.e-16	9.057633e-04
1.e-17	2.370907e-03
1.e-18	6.082683e-03

Table 6.11: $\|u - u_h\|_{L^2(\Gamma_C)}$ for different regularisation parameters with 101 DOF on Γ_C and refining eight times (see Figure 6.31).

Now we want to compare the results with the optimal regularisation parameter for the reduced number of DOF on Γ_C for the three regularisation matrices. We start with the searched control $u|_{\Gamma_C}$ for eight grid refinements in Figure 6.33. For the regularisation with $Reg = R^T R$ we use 31 DOF on Γ_C and set $\alpha = 1.e - 11$. If we regularise by $Reg = R_1^T R_1$ we use 101 DOF on Γ_C and set $\alpha = 1.e - 14$ and with $Reg = R_2^T R_2$ we use 101 DOF on Γ_C and set $\alpha = 1.e - 16$.

For all three cases we get a good approximation of the searched control $u|_{\Gamma_C}$. Small differences are obvious in the surroundings of $y = 0$, $y = 0.5$ and $y = 1$. Table 6.12 shows, that we get the best result for the searched control $u|_{\Gamma_C}$ with $Reg = R_1^T R_1$ as regularisation matrix, 101 DOF on Γ_C and $\alpha = 1.e - 14$.

Regularisation / DOF / α	$\|u - u_h\|_{L^2(\Gamma_C)}$
$R^T R$ / 31 / 1.e-11	1.150256e-03
$R_1^T R_1$ / 101 / 1.e-14	5.156368e-04
$R_2^T R_2$ / 101 / 1.e-16	9.057633e-04

Table 6.12: $\|u - u_h\|_{L^2(\Gamma_C)}$ for the different regularisation matrices refining the grid eight times with reduced number of DOF on Γ_C and the optimal regularisation parameters.
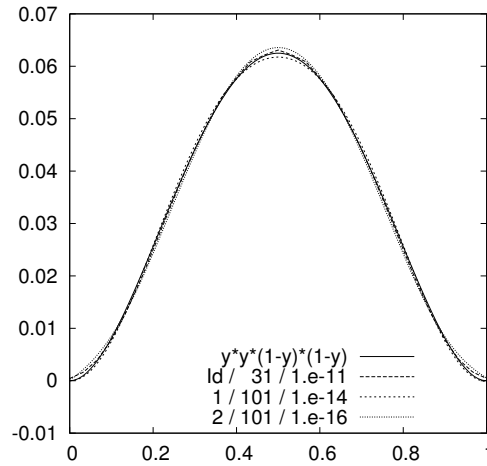
Figure 6.33: $u|_{\Gamma_C} = y^2(1-y)^2$ and $u_h|_{\Gamma_C}$ for refining the grid eight times calculated with $Reg = R^T R$, 31 DOF on Γ_C and $\alpha = 1.e-11$; $Reg = R_1^T R_1$ (1), 101 DOF on Γ_C and $\alpha = 1.e-14$; $Reg = R_2^T R_2$ (2), 101 DOF on Γ_C and $\alpha = 1.e-16$.

Now we want to know how good is the approximation of the other boundary data calculated with the computed control $u_h|_{\Gamma_C}$. We start with the given measurement $u|_{\Gamma_O} = 0$. In Figure 6.34 (left) we illustrate the results for $u_h|_{\Gamma_O}$ with $Reg = R^T R$, 31 DOF on Γ_C, $\alpha = 1.e-11$; $Reg = R_1^T R_1$, 101 DOF on Γ_C, $\alpha = 1.e-14$ and $Reg = R_2^T R_2$ with 101 DOF on Γ_C and $\alpha = 1.e-16$. We can see obvious discrepancies between the calculations but all three results are good approximations of $u|_{\Gamma_O} = 0$. Lets stay on Γ_O. We know $\partial_n u|_{\Gamma_O} = -y^2(1-y)^2$ from the underlying PDE-

constraint. In Figure 6.34 (right) we can see that there is no graphical difference between the calculations of $\partial_n u_h|_{\Gamma_O}$ for the three computations obvious. From the analytic solution we know $\partial_n u|_{\Gamma_C} = y^2(1-y)^2$ (see Figure 6.35). Again as in the calculation for searched Dirichlet control and given Neumann measurements (Section 6.2) we achieve oscillations in the calculation with $Reg = R^T R$ which we also get when we choose more DOF on Γ_C (see appendix A). If we regularise by $Reg = R_1^T R_1$ or $Reg = R_2^T R_2$ we haven't oscillations if we choose 101 DOF on Γ_C but the approximation of the analytic $\partial_n u|_{\Gamma_C} = y^2(1-y)^2$ isn't very good. If we choose fewer DOF on Γ_C we also achieve oscillations if we regularise by an approximation of the second derivative (Figure 6.36 with 31 DOF).
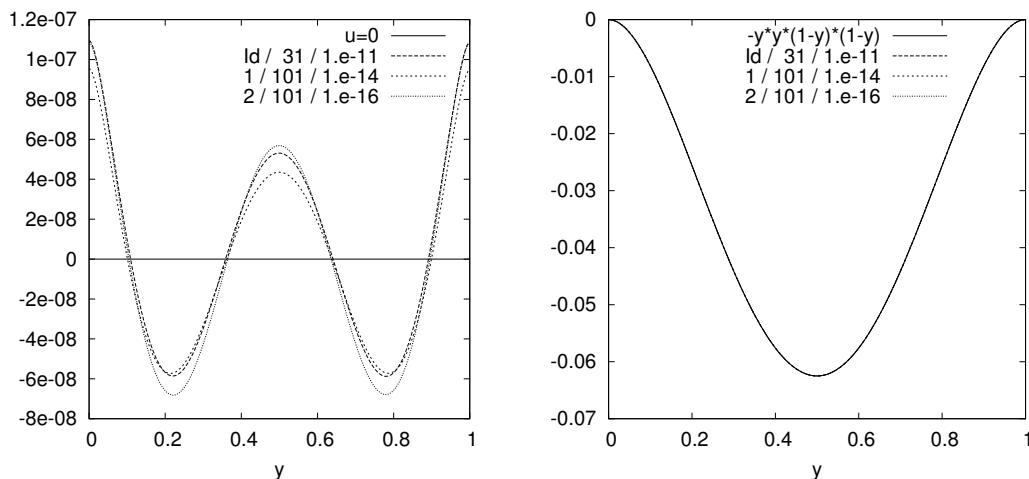
Figure 6.34: $u|_{\Gamma_O} = 0$ and $u_h|_{\Gamma_O}$ (left), $\partial_n u|_{\Gamma_O} = -y^2(1-y)^2$ and $\partial_n u_h|_{\Gamma_O}$ (right) for the three regularisation matrices with reduced number of DOF on Γ_C and optimal regularisation parameters for refining the grid eight times calculated with the computed control $u_h|_{\Gamma_C}$.

We have seen this effect in the previous Section for the calculation of $\partial_n u|_{\Gamma_C}$ with the searched Dirichlet control for given Neumann measurement regularised by $Reg = R_1^T R_1$ and $R_2^T R_2$. We have reached a good approximation of the searched control $u|_{\Gamma_C}$ for a small number of DOF on Γ_C but to avoid oscillations in the calculation of $\partial_n u|_{\Gamma_C}$ we have to enlarge the number of DOF.
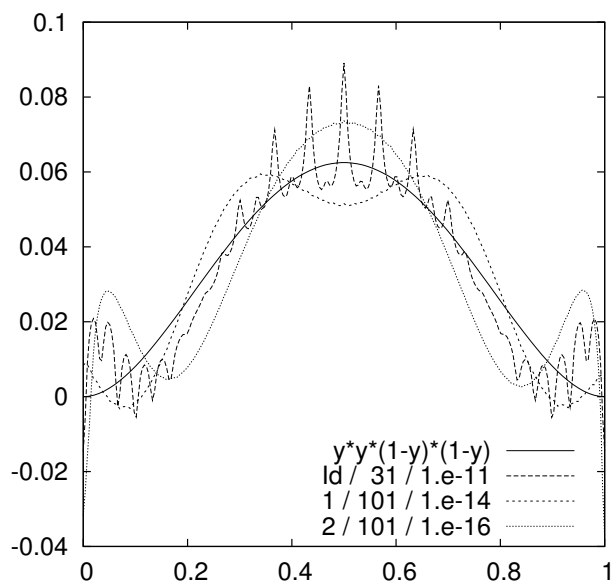
Figure 6.35: $\partial_n u|_{\Gamma_C} = y^2(1 - y)^2$ and $\partial_n u_h|_{\Gamma_C}$ for the three regularisation matrices with reduced number of DOF on Γ_C and optimal regularisation parameters for refining the grid eight times calculated with the computed control $u_h|_{\Gamma_C}$.
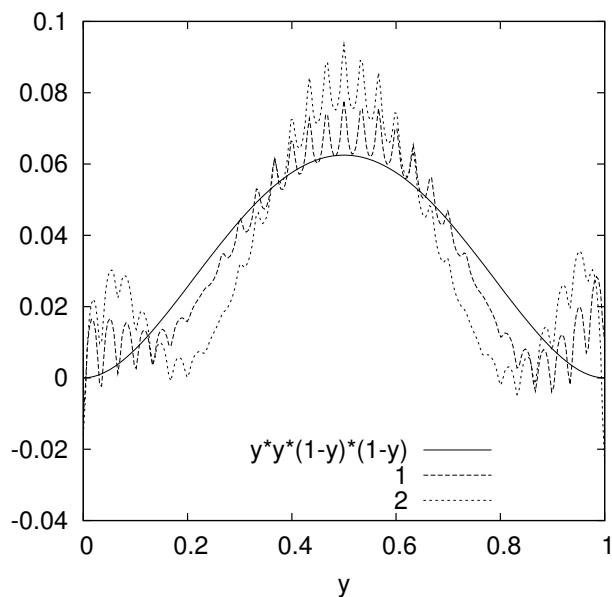
Figure 6.36: $\partial_n u|_{\Gamma_C} = y^2(1 - y)^2$ and $\partial_n u_h|_{\Gamma_C}$ for 31 DOF, refining the grid eight times and regularise by $Reg = R_1^T R_1$ (1) and $Reg = R_2^T R_2$ (2).

6.4 Comparison of the results

Now we want to compare the results for the problems, we have solved in the last three Sections. We will do this for $u_h|_{\Gamma_C}$, $\partial_n u_h|_{\Gamma_C}$, $u_h|_{\Gamma_O}$ and $\partial_n u_h|_{\Gamma_O}$. In the last Sections we have seen that with searched Neumann control for given Neumann measurements we get good approximations for all boundary data. In the case, we search Dirichlet control for given Neumann measurements, we have seen that we reach oscillations in the calculation of $\partial_n u|_{\Gamma_C}$ which we only can avoid if we use enough DOF on Γ_C and regularise by $Reg = R_1^T R_1$ or $R_2^T R_2$. For searched Dirichlet control and given Dirichlet measurements we have assert the same effect. But there we achieve discrepancies between the calculations for $u|_{\Gamma_O}$ too. For the following graphical illustration of the comparison we want to introduce the shortcuts nn for searched Neumann control and given Neumann measurements (results from Section 6.1), nd for searched Dirichlet control and given Neumann measurements (results from Section 6.2) and dd for searched Dirichlet control and given Dirichlet measurements (results from Section 6.3). We start with the results on Γ_C first with $u|_{\Gamma_C}$. For avoiding oscillations in the calculation of $\partial_n u|_{\Gamma_C}$ we use in all cases $Reg = R_2^T R_2$ as regularisation matrix and refine Ω eight times. We use 31 DOF and $\alpha = 1.e - 12$ for nn, 91 DOF and $\alpha = 1.e - 17$ for nd and 101 DOF and $\alpha = 1.e - 16$ for dd. In Figure 6.37 (left) we can see that we get the best approximation for Neumann control and Neumann measurements. For this calculation we have used the lowest number of DOF on Γ_C which is positive for the runtime of the program. We have seen in the previous Sections that we can use less DOF than we did now for searched Dirichlet control and given Neumann Dirichlet measurements respectively.

In the case of the calculation of $\partial_n u|_{\Gamma_C}$ we can see again, that we get the best result for Neumann control and Neumann measurements (Figure 6.37 (right)) and this is not only caused by the possible oscillations. For the calculation of $u|_{\Gamma_O}$ we can see in Figure 6.38 (left) only that we get the worst result for Dirichlet control and Dirichlet measurements. We put the results for Neumann measurements and Dirichlet control Neumann control respectively in Figure 6.38 (right), but anyway

there is no obvious discrepancy between the calculations. At last we have the results for the computation of $\partial_n u_h|_{\Gamma_O}$ (Figure 6.39). For all three calculations we get good approximations of the analytic $\partial_n u|_{\Gamma_O} = -y^2(1-y)^2$ and there is no graphical difference.
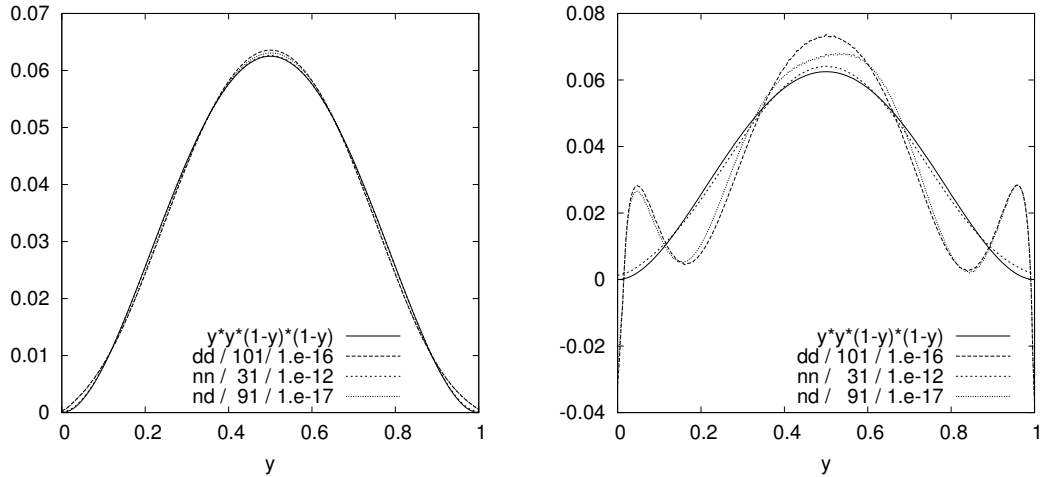
Figure 6.37: $u|_{\Gamma_C} = y^2(1-y)^2$ and $u_h|_{\Gamma_C}$ (left), $\partial_n u|_{\Gamma_C} = y^2(1-y)^2$ and $\partial_n u_h|_{\Gamma_C}$ (right) calculated for nn, nd and dd with reduced number of DOF and optimal regularisation parameter.
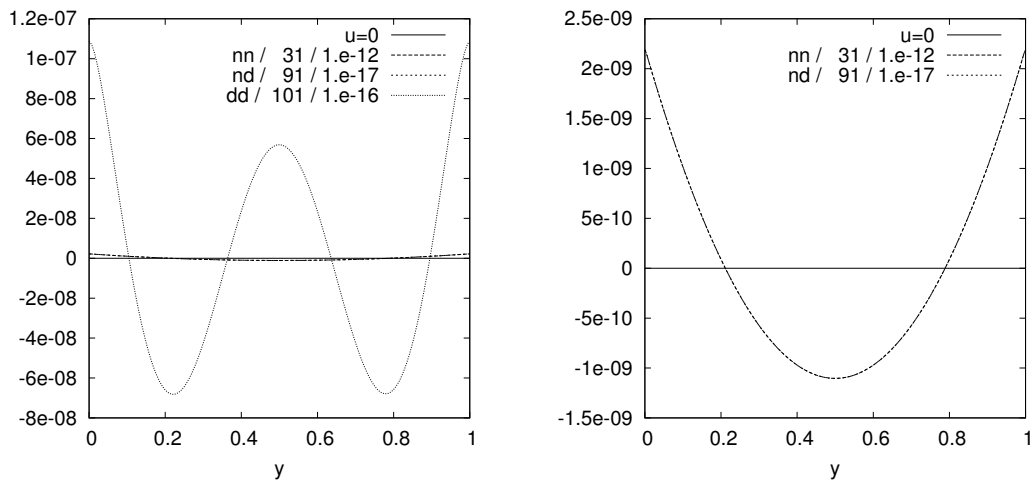
Figure 6.38: $u|_{\Gamma_O} = 0$ and $u_h|_{\Gamma_O}$ calculated for nn, nd and dd with reduced number of DOF and optimal regularisation parameters (left). And the results only for the calculation for nn and nd (right).
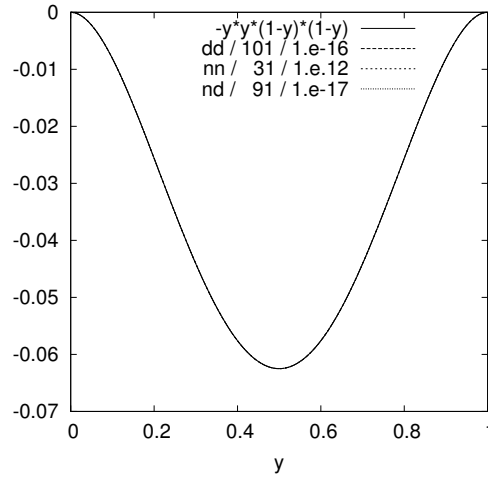
Figure 6.39: $\partial_n u|_{\Gamma_O} = -y^2(1-y)^2$ and $\partial_n u_h|_{\Gamma_O}$ calculated for nn, nd and dd with reduced number of DOF and optimal regularisation parameters.

We have seen that we get the best results for all boundary conditions for searched Neumann control and given Neumann measurements. The more Dirichlet conditions we use for our calculation the worse are the results. Another aspect is for searched Dirichlet control we have to enlarge the number of DOF on Γ_C in comparison to the calculations with searched Neumann control. And we have to take care of the regularisation matrix for avoiding oscillations.

More graphical results, calculated with the searched control for the three regularisation matrices with different grid refinements, different number of DOF on Γ_C and different regularisation matrices, can be seen in appendix A. There the results, which we have presented here, are verified.

7 Results for the Application

Now we want to present the numerical results for the application, hybrid insulation described in Section 2. In contrast to the three (four respectively) cases we had for our model problem (Section 5.1) due to technical conditions of the application here we only have the two possible cases with given Neumann measurements and searched Neumann control or given Neumann measurements and searched Dirichlet control. As we have seen in the previous Section that we get the best results for given Neumann data and searched Neumann control we consider only this case.

Instead of using the laplace equation in two dimensions for the application of hybrid insulation as it is done by I. Cherlenyak in his PhD thesis [11] we use here the three dimensional laplace equation reduced to two dimensions as described in Section 2. We have to do some modifications compared to the calculations of the model problem in the previous Sections, where we solved as direct problem the laplace equation on the unit square.
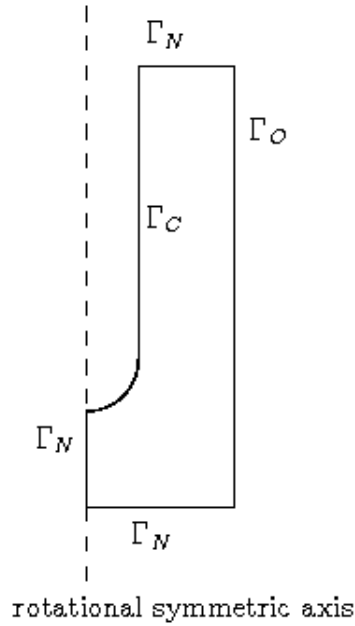
Figure 7.1: Simplified geometry of the two dimensional rotational symmetric problem of hybrid insulation.

As described in Section 2 instead of $-\Delta u = g$ we have

$$-\frac{1}{r}\frac{\partial u}{\partial r} - \frac{\partial^2 u}{\partial r^2} - \frac{\partial^2 u}{\partial z^2} = 0. \tag{7.1}$$

as underlying partial differential equation caused by the reduction from three to two dimensions on the simplified geometry (see Figure 7.1) resulting from the experimental setup (described in Section 2). This results in the following problem we want to solve:

Find $\partial_n u|_{\Gamma_C} = q$ for given measurement $\partial_n u|_{\Gamma_O} = f$ such that

$$J(u, q) \rightarrow \min, \ J(w, \tau) := \frac{1}{2}\|\partial_n w - f\|_{\Gamma_O}^2 \tag{7.2}$$

under the PDE-constraint

$$
\begin{aligned}
-\frac{1}{r}\frac{\partial u}{\partial r} - \frac{\partial^2 u}{\partial r^2} - \frac{\partial^2 u}{\partial z^2} &= 0 && \text{on } \ \Omega \,, \\
\partial_n u &= 0 && \text{on } \ \Gamma_N \,, \\
u &= 0 && \text{on } \ \Gamma_O \,, \\
\partial_n u &= q && \text{on } \ \Gamma_C \,.
\end{aligned}
\tag{7.3}
$$

As we only do the calculations for searched Neumann control we don't need Nitsches method and can use the classical variational formulation of the direct problem where the Dirichlet boundary condition on Γ_O is hidden in the function space i.e. we have $u \in V = \{\varphi \in H^1(\Omega) \mid \varphi = 0 \text{ on } \Gamma_O\}$. Again we can write the direct problem (see Section 5) after discretisation as

$$
\begin{aligned}
J(u_h, q) &\rightarrow \min \\
A u_h &= Bq
\end{aligned}
\tag{7.4}
$$

With A regular this leads to

$$
J(u_h, q) = J(A^{-1}Bq, q) \rightarrow \min
\tag{7.5}
$$

Then we have to solve the regularised normal equation as for the model problem:

$$
(B^T A^{-T} C A^{-1} B + \alpha \ Reg) \, q = B^T A^{-T} C f.
\tag{7.6}
$$

For the discretisation we use bilinear elements on quadrilaterals. In the case we have n vertices on Ω and Nq vertices on Γ_C we have:

B is the $(n \times Nq)$- matrix corresponding to $(\varphi, \ \psi \in V_h)$:

$$
(\psi, \varphi)_{0,\Gamma_O}
$$

C is the $(n \times n)$-matrix corresponding to

$$
(\partial_n \psi, \partial_n \varphi)_{0,\Gamma_O}
$$

and Cf corresponding to $(f, \partial_n\varphi)_{\Gamma_O}$.

In contrast to the model problem we have here:

A is the $(n \times n)$-matrix corresponding to:

$$(\nabla\psi, \nabla\varphi)_{0,\Omega} - \left(\frac{1}{r}\partial_r\psi, \varphi\right)_{0,\Omega}.$$

As mentioned before we have another geometry (see Figure 7.1) as for the model problem where we use the unit square as underlying geometry. We have given measuring data $f = \partial_n u|_{\Gamma_O}$ in equidistant measuring points which we interpolate linear instead of a given function. From the reduction from three to two dimensions we have the supplementary term $-\left(\frac{1}{r}\partial_r\psi, \varphi\right)_{0,\Omega}$ in the matrix A and we use the classical variational formulation of the direct problem instead of Nitsche's method.

Caused by the term $-\left(\frac{1}{r}\partial_r\psi, \varphi\right)_{0,\Gamma}$ we have an unsymmetric problem to be solved. For this we use the bicgstab-method (see e.g. [34], [15] or [31]) instead of the pcg-method, described in the following with $Ax = b$ as underlying problem :

Algorithm 7.1. *(BICGstab)*

> *Given $\bar{x}_0 \in \mathbb{R}^n$ with $\bar{r}_0 := b - A\bar{x}_0 \neq 0$. Choose $\hat{r}_0 \in \mathbb{R}^n$ such that $(\hat{r}_0, \bar{r}_0) \neq 0$,*
> *set $\bar{p}_0 := \bar{r}_0$.*
> *For $k = 0, 1, \dots$*
>
> *1) $a_k := \dfrac{(\hat{r}_0, \bar{r}_k)}{(\hat{r}_0, A\bar{p}_k)}$*
>
> $v := A\bar{p}_k, \quad t := As$
>
> *2) $\omega_{k+1} := \dfrac{(s, t)}{(t, t)}$*
>
> $\bar{x}_{k+1} := \bar{x}_k + a_k\bar{p}_k + \omega_{k+1}s$
>
> $\bar{r}_{k+1} := s - \omega_{k+1}$
>
> *if*
>
> > $\|\bar{r}_{k+1}\|$ *is small enough stop*
>
> *else*

$$b_k := \frac{(\hat{r}_0, \bar{r}_{k+1})}{(\hat{r}_0, \bar{r}_k)} \frac{a_k}{\omega_{k+1}}$$

$$\bar{p}_{k+1} := \bar{r}_{k+1} + b_k(\bar{p}_k - \omega_{k+1}v)$$

We do the calculations for different cases of measuring data. The regularisation parameter is chosen by tried and error as in the previous Sections, as regularisation matrix we choose an approximation of the second derivative but we didn't reduce the number of DOF on Γ_C.

In the first two cases we present we have given negative data on Γ_O. Figure 7.2 shows the calculated control $q = \partial_n u_h|_{\Gamma_C}$ projected on the z-axis (left) for the given data ($f = \partial_n u|_{\Gamma_O}$, right) and the computed normal derivative $\partial_n u_h|_{\Gamma_O}$ (right) for refining the grid six times (24576 cells, 321 DOF on Γ_C) and $\alpha = 1.e - 06$.
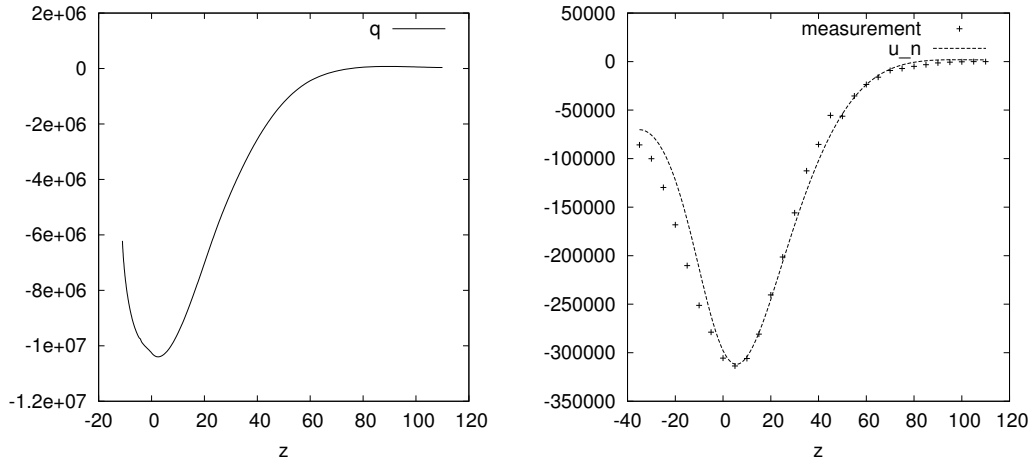
Figure 7.2: The calculated control $q = \partial_n u_h|_{\Gamma_C}$ (left), the given measurements and the calculated normal derivative $\partial_n u_h|_{\Gamma_O}$ (right) for refining the grid six times and $\alpha = 1.e - 06$.

In Figure 7.3 we can see on the left a video image of the experiment and on the right the calculated u_h on Ω (the simplified rotational symmetric geometry) for the given measurements illustrated in Figure 7.2.

In both cases we reach a good approximation of the given measurements. We get better results for this approximation for smaller regularisation parameters but we

have oscillations in the calculation of the control $q = \partial_n u|_{\Gamma_C}$. This can be seen in appendix B.
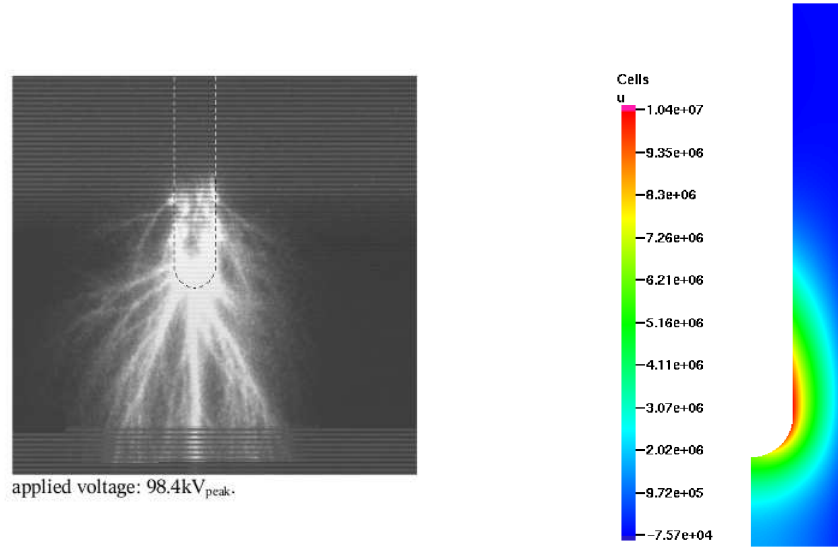
Figure 7.3: Video image (left, from F. Mauseth NTNU Trondheim) and calculated u_h on Ω for the given measurements $\partial_n u|_{\Gamma_O}$ (illustrated in Figure 7.2 right). The calculation is done for six grid refinements and $\alpha = 1.e - 06$.

In the following Figures we see the results for other negative measurements. Again we refine the grid six times (24576 cells and 321 DOF on Γ_C) and choose this time $\alpha = 1.e - 07$.

Figure 7.4 shows the calculated $q = \partial_n u_h|_{\Gamma_C}$, the given measurements and the computed normal derivative $\partial_n u_h|_{\Gamma_O}$. In Figure 7.5 we can see on the left a video image of the experiment and on the right the calculated u_h on Ω (the simplified rotational symmetric geoemtry).

Again we reach a better approximation of the given measurements by a smaller regularisation parameter but this results as in the previous calculations in oscillations in the calculation of the searched control. (see appendix B).

114
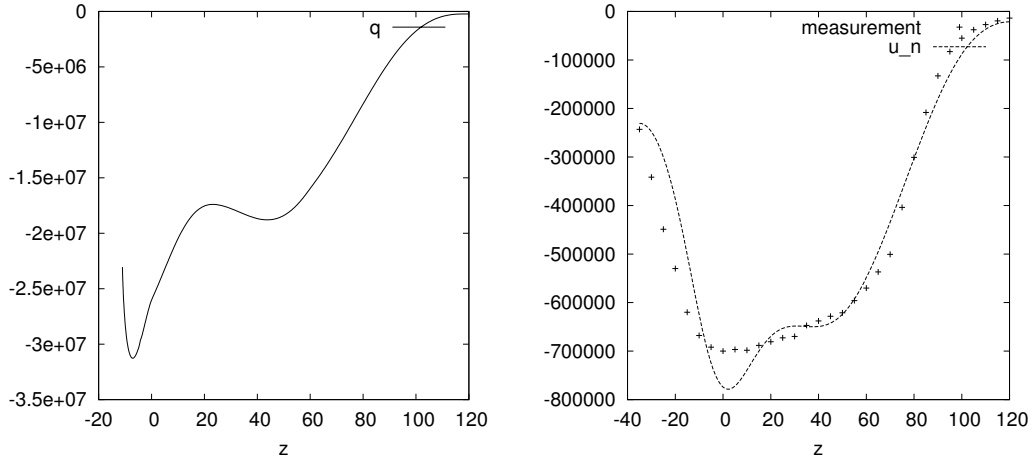
Figure 7.4: The calculated control $q = \partial_n u_h|_{\Gamma_C}$ (left), the calculated $\partial_n u_h|_{\Gamma_O}$ and the given measurements (right) for refining the grid six times and $\alpha = 1.e - 07$.
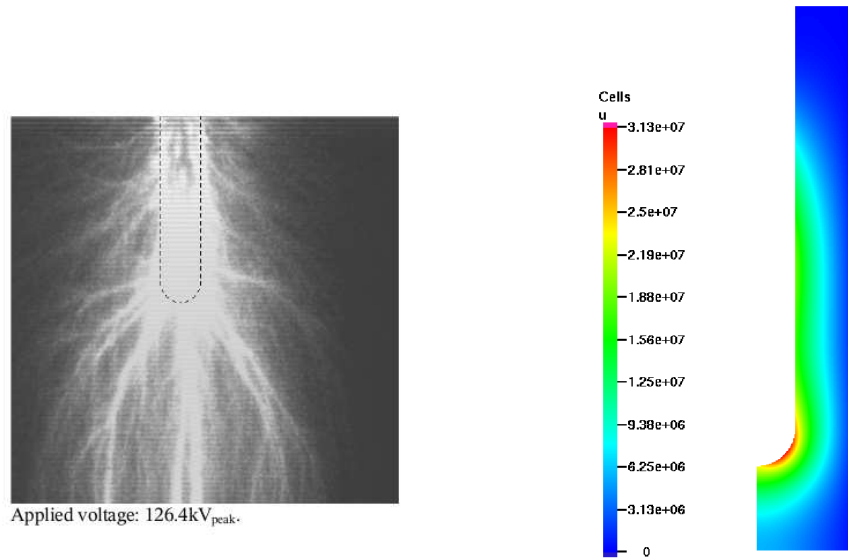
Figure 7.5: Video image (left, from F. Mauseth NTNU Trondheim) and calculated u_h on Ω for the given measurements $\partial_n u|_{\Gamma_O}$ (illustrated in Figure 7.4 right). The calculation is done for six grid refinements and $\alpha = 1.e - 07$.

Now we present the results for two cases with positive measurements. We again refine Ω six times (24576 cells and 321 DOF on Γ_C) but here we choose $\alpha = 1.e - 08$. Figure

7.6 shows the control $q = \partial_n u_h|_{\Gamma_C}$, the given Neumann measurement and $\partial_n u_h|_{\Gamma_O}$. In Figure 7.7 we can see on the left a video image of the experiment and on the right the calculated u_h on Ω.
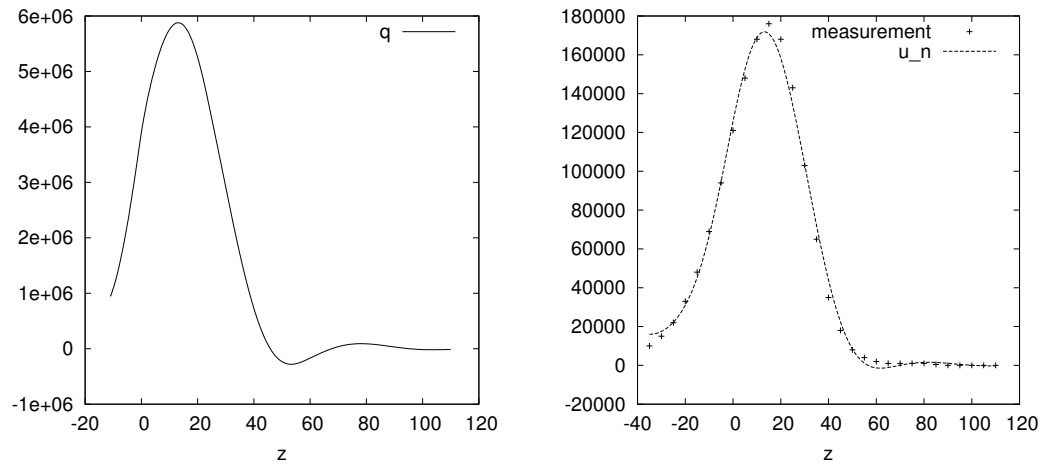
Figure 7.6: The calculated $q = \partial_n u_h|_{\Gamma_C}$ (left), the calculated $\partial_n u_h|_{\Gamma_O}$ and the given measurements (right).
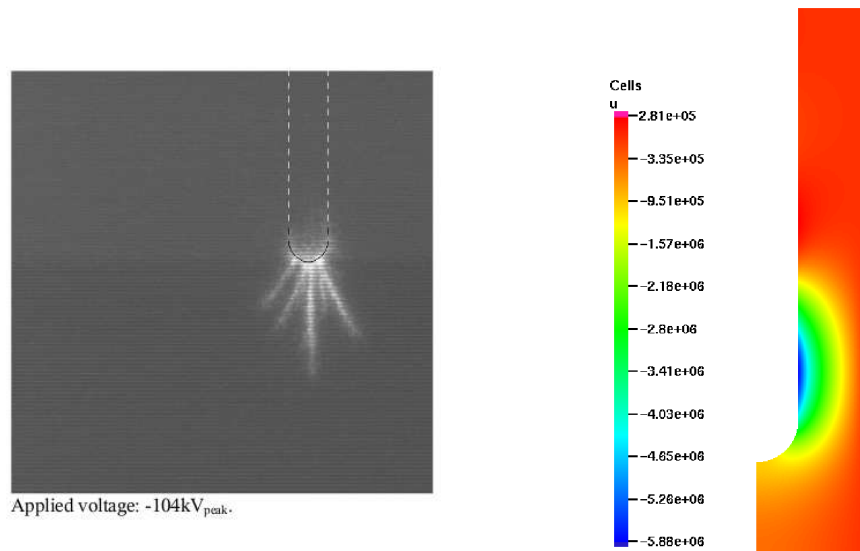
Figure 7.7: Video image (left, from F. Mauseth NTNU Trondheim) and calculated u_h on Ω for the given measurement $\partial_n u|_{\Gamma_O}$ illustrated in Figure 7.6 (right).

At last we present the results for another positive measurement. We refine therefore the grid six times and set $\alpha = 1.e - 07$. In Figure 7.8 we can see the calculated control q on Γ_C, the given measurement and the computed $\partial_n u_h|_{\Gamma_O}$. Figure 7.9 shows the video image of the experiment and the calculated u_h on Ω for the given data. More numerical results for this cases can be seen in appendix B.
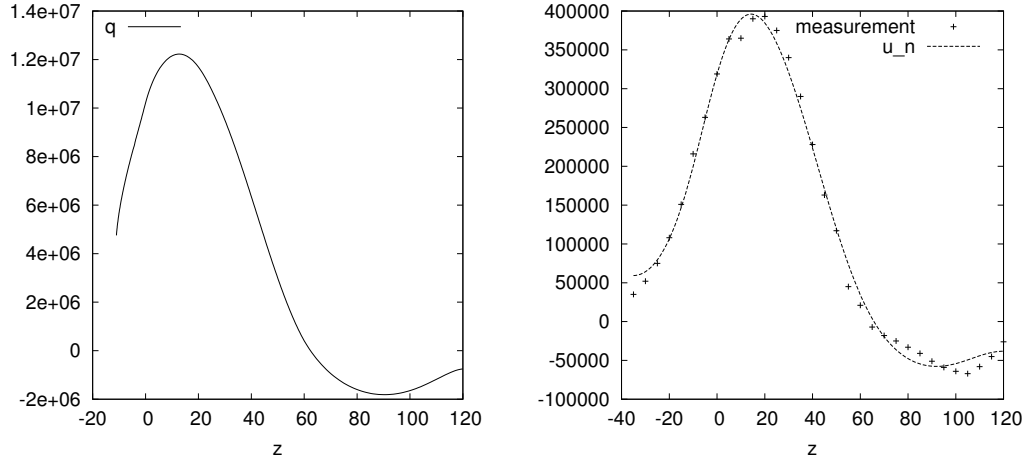
Figure 7.8: The calculated $q = \partial_n u_h|_{\Gamma_C}$ (left), the calculated $\partial_n u_h|_{\Gamma_O}$ and the given measurements (right).
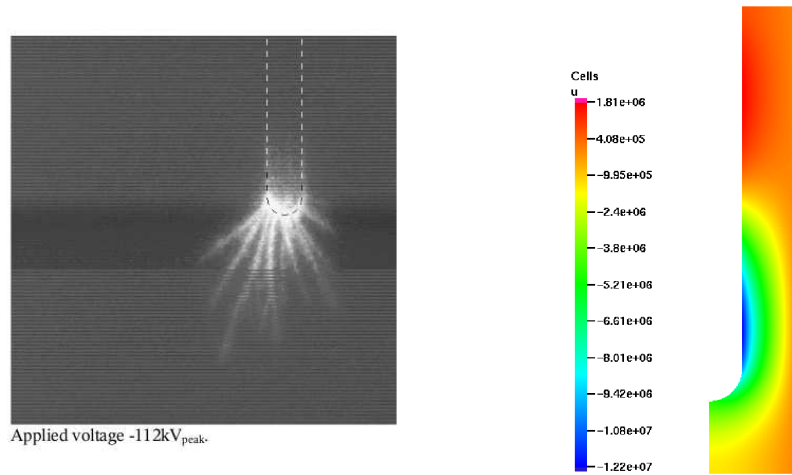
Figure 7.9: Video image (left, from F. Mauseth NTNU Trondheim) and calculated u_h on Ω for the given measurements $\partial_n u|_{\Gamma_O}$ illustrated in Figure 7.8 (right).

117

8 Conclusion and outlook

In this dissertation we have presented results for a Cauchy type problem in electrical engineering. The experimental setup for the application of hybrid insulation takes place at the NTNU Trondheim. Frank Mauseth who deals with this application in his PhD thesis [26] provided us the description of the application and the measurements we needed for solving the problem.

Caused by the rotational symmetry we have reduced the problem of hybrid insulation from three to two dimensions. As for the application it is possible to search Dirichlet or Neumann control we first presented Nitsche's method for the calculation of direct problems with Dirichlet boundary data. There the Dirichlet boundary data, achieved in the variational formulation and weren't hidden in the underlying function space. We have shown stability, consistency and have done the error estimation. We have seen that the errors in $L^2(\Omega)$- and $H^1(\Omega)$-norm are of the same order as in the classical variational formulation.

After we have introduced the basic theory of inverse problems we presented three optimal control problems, we solved on the unit square. Based on the application we searched Dirichlet or Neumann control for given Neumann measurements. We also wanted to know, what happened if we have given Dirichlet measurements and the Neumann condition is part of the underlying PDE-constraint. We only took care of the problem with searched Dirichlet control for given Dirichlet measurements. The case of searched Neumann control isn't uniquely solvable.

We have done the calculation for the three optimal control problems for three different regularisation matrices (the identity and approximations of first and second

derivative). We have noticed that we have to discretise Ω fine enough to reach good results. For saving runtime we have reduced the number of DOF on Γ_C (the boundary on which we searched the control) without loosing quality of the calculation. As a last aspect we have done the calculation for different regularisation parameters to estimate the optimal parameter in dependence of the regularisation matrix and the number of DOF on Γ_C.

In the case of searched Neumann control for given Neumann measurements we have seen, that we achieved good results for the searched control for all of the regularisation matrices. We have also seen, that we can reduce the number of DOF on Γ_C for all regularisations (41 DOF for Reg $= R^T R$, 31 DOF for Reg $= R_2^T R_2$ and 91 DOF for Reg $= R_1^T R_1$). For the calculation of the other boundary data computed by the searched control there was graphically no discrepancy obvious.

In the case of searched Dirichlet control for given Neumann measurements we also achieved good results for the searched control for all three regularisations. But in this case we had to enlarge the number of DOF (compared to the case of searched Neumann control) in the case we regularised by an approximation of first (101 DOF) or second (91 DOF) derivative caused by the calculation of the other boundary data, especially of $\partial_n u_h|_{\Gamma_C}$. There we achieved oscillations if we reduced the number of DOF too much. If we regularised by the identity we weren't able to avoid these oscillations.

A similar effect we have seen in the last case of searched Dirichlet control for given Dirichlet measurements. There again we achieved good results for the searched control but we have to enlarge the number of DOF on Γ_C compared to the results for searched and given Neumann data. Again we weren't able to avoid oscillations in the calculation of $\partial_n u_h$, if we regularise by the identity. Also in the calculation of $u_h|_{\Gamma_O}$ we have seen discrepancies between the three regularisations.

In the comparison of the three problems, where we used the approximation of the second derivative for all calculations we have seen, that we get the best results in the case of searched Neumann control and given Neumann measurement. For this case

we have used the smallest number of DOF on Γ_C and we didn't have the problem of arising oscillations if we regularise by the identity or an approximation of the first derivative. As a conclusion we can say the results are worse the more Dirichlet data (as searched control or/and given measurement) we have.

At last we have presented the results for the application of hybrid insulation. Caused by the results for the model problem, where we achieved the best results for searched Neumann control and given Neumann measurements we considered only the case of searched Neumann control. As we have no Dirichlet data to calculate, we used the classical variational formulation of the direct problem where the Dirichlet data are hidden in the function space. We have modified the geometry and the matrix A caused by the rotational symmetry. We have presented the results for four cases of given measurement. As we only know the measurement this was the only evidence for the choice of the regularisation parameter.

For the future work one can take a look on the automation of the choice of the regularisation parameter and, in connection with this, on the possible error analysis. Perhaps the choice of number of DOF on Γ_C can be optimised by doing the calculation adaptivly in the sense of refining the grid without Γ_C. Also the choice of the constant γ for Nitsche's method could be done by calculating the eigenvalue as it is mentioned by Hansbo et al. ([19] and [6]).

As hybrid insulation is a problem in three dimensions another possibility is, to do the calculation in three dimensions. But therefore we need other measurements.

Hybrid insulation isn't the only application for this problem. Another application is the control of forming processes illustrated in Figure 8.1. If we simplify this problem to the unit square we have the model problem (see Section 5) with given Neumann measurements (the designated martensite concentration).
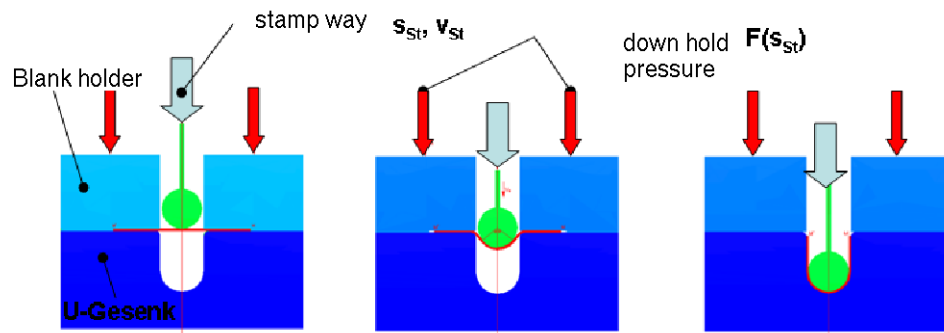
Figure 8.1: Illustration of a forming process.

For this processes the influencing values are e.g. geometry, temperature and stamp speed. The control parameters are the down hold pressure and the sheet tracking. In Figure 8.2 we could regard the down hold pressure or the sheet tracking at the left boundary as control and the martensite concentration V_M in the marked critical deformed area as observation. Here we have V_M as function of deformation $\epsilon(v)$. This means we have to find the optimal derivative in the right subarea by presettings on the left boundary.
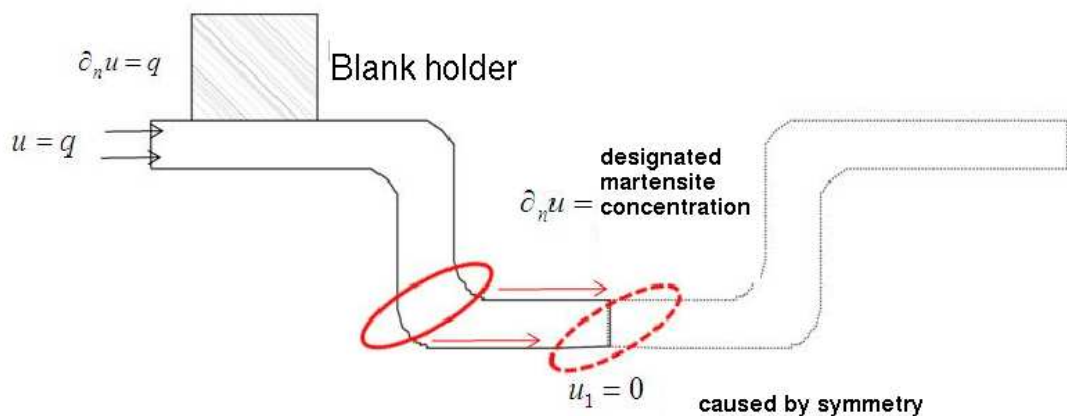
Figure 8.2: For an optimal control the hold down pressure or the sheet tracking at the left boundary could be regarded as control and the martensite concentration V_M in the marked critical deformed area as observation.

A More numerical results for the model problem

In this Section we want to present more numerical results. We will present graphical results for searched Neumann control and given Neumann measurements, searched Dirichlet control and given Neumann measurements and searched Dirichlet control and given Dirichlet measurements. Furthermore we will differ between the results for the different regularisation matrices, for different grid refinements, different number of DOFs on Γ_C and different regularisation parameters.

Later on we present more numerical results for the application of hybrid insulation. There we do the calculations in the case of searched Neumann control and given Neumann measurements for different regularisation parameters and present the results for the searched control $q = \partial_n u|_{\Gamma_C}$ and the approximation of the given measurements $\partial_n u_h|_{\Gamma_O}$.

A.1 Results for given $\partial_n u|_{\Gamma_O}$ and searched $\partial_n u|_{\Gamma_C}$
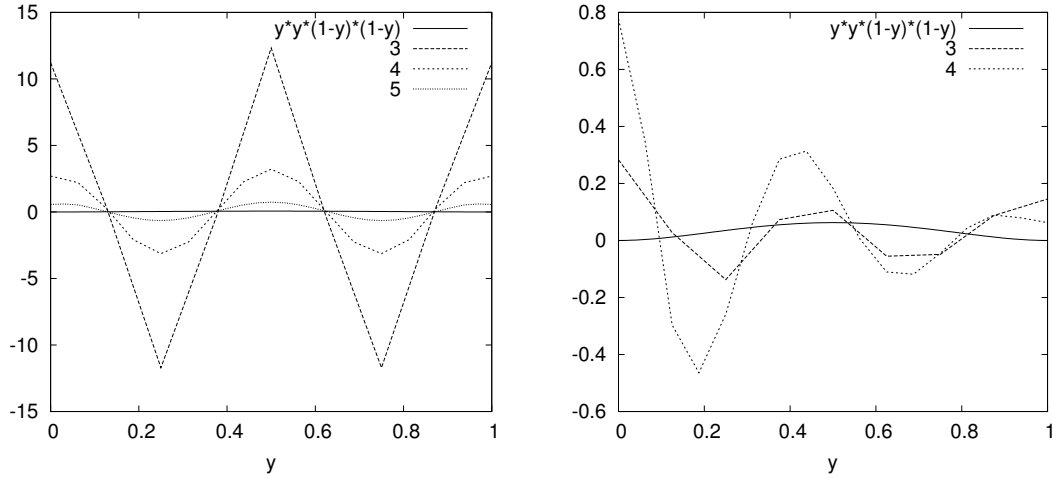
Figure A.1: $\partial_n u_h|_{\Gamma_C}$ with $\text{Reg} = R^T R$, $\alpha = 1.e - 13$ and three to five grid refinements (left) and $\partial_n u_h|_{\Gamma_C}$ with $\text{Reg} = B_1^T B_1$, $\alpha = 1.e - 10$ for three and four grid refinements (right).

As mentiond in Section 6.1 here we present the graphics for the calculation of Neumann control on Γ_C for given Neumann measurements on Γ_O. We can see in Figure A.1 the results for regularising with $\text{Reg} = R^T R$ and $\text{Reg} = R_1^T R_1$ for small grid refinements. We can see that these refinements are too small to deliver good results.

Results for searched $\partial_n u|_{\Gamma_C}$ and given $\partial_n u|_{\Gamma_O}$ with $\text{Reg} = R^T R$

Now we present the graphical results calculated with $\text{Reg} = R^T R$ for different grid refinements and $\alpha = 1.e - 13$ and without special choice of the number of DOF on Γ_C. The results for the searched control $q = \partial_n u|_{\Gamma_C}$ can be seen in Section 6.1. In the Figures (A.2 and A.3) we can see that we achieve better results for smaller grids.
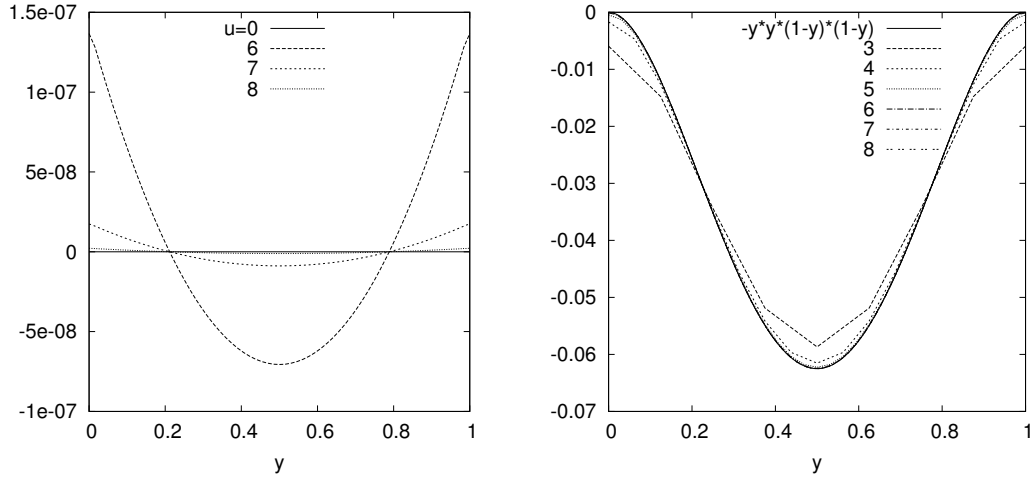
Figure A.2: Results on Γ_O: $u|_{\Gamma_O} = 0$ and $u_h|_{\Gamma_O}$ (left), $u|_{\Gamma_O} = -y^2(1-y)^2$ and $u_h|_{\Gamma_O}$ (right) for six to eight grid refinements calculated with the computed control, Reg $= R^T R$ and $\alpha = 1.e - 13$.
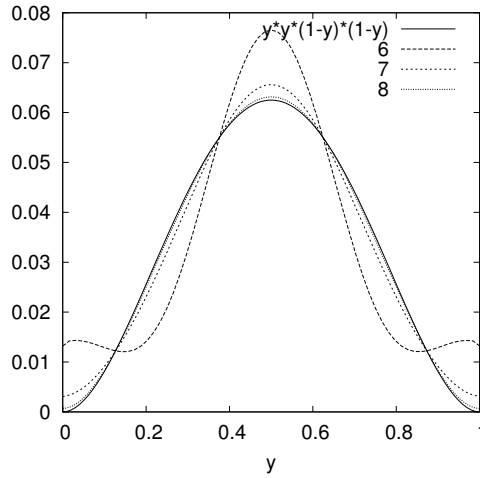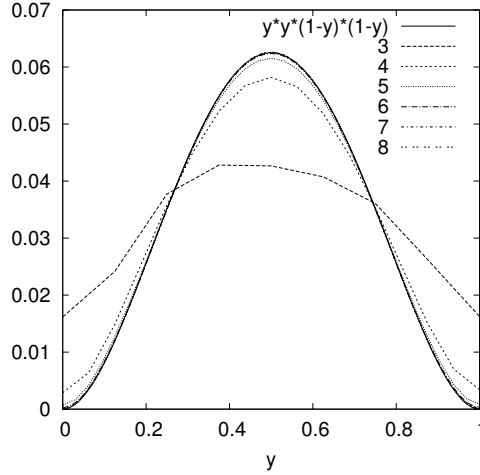

Figure A.3: $\partial_n u|_{\Gamma_C} = y^2(1-y)^2$ and $\partial_n u_h|_{\Gamma_C}$ for different grid refinements calculated with the computed control, Reg $= R^T R$ and $\alpha = 1.e - 13$.

The following graphics illustrate the results for refining the grid eight times, Reg $= R^T R$, $\alpha = 1.e - 13$ and a different number of DOF on Γ_C. As for the calculated control (see Section 6.1) we can see that we can reduce the number of DOF without loosing quality of the calculation.
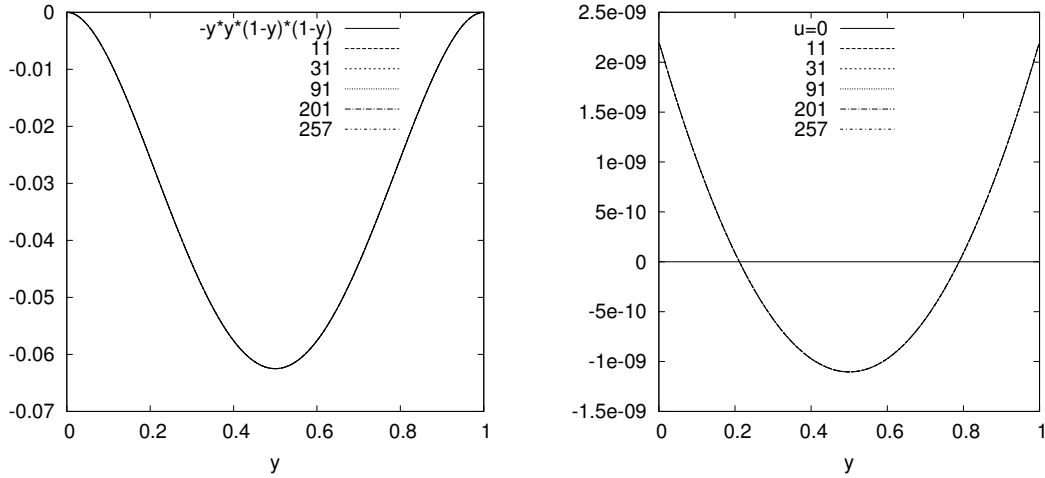
Figure A.4: Results on Γ_O: $\partial_n u|_{\Gamma_O} = -y^2(1-y)^2$ and $\partial_n u_h|_{\Gamma_O}$ (left), $u|_{\Gamma_O} = 0$ and $u_h|_{\Gamma_O}$ (right) for different DOF on Γ_C for eight grid refinements calculated with the computed control with $\mathrm{Reg} = R^T R$ and $\alpha = 1.e-13$.
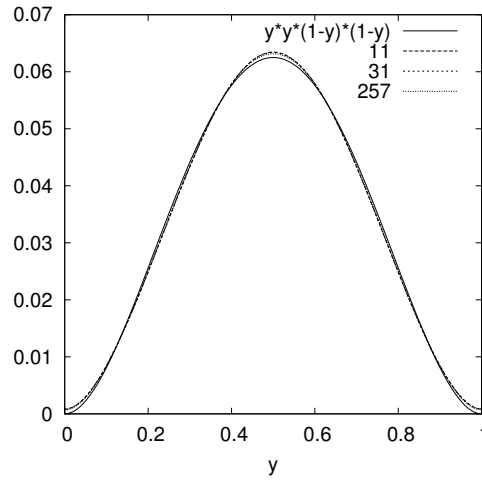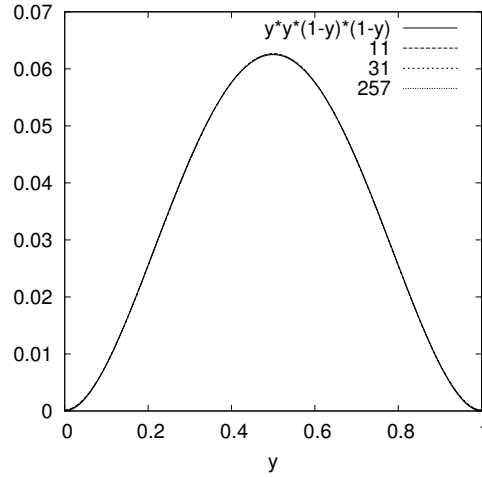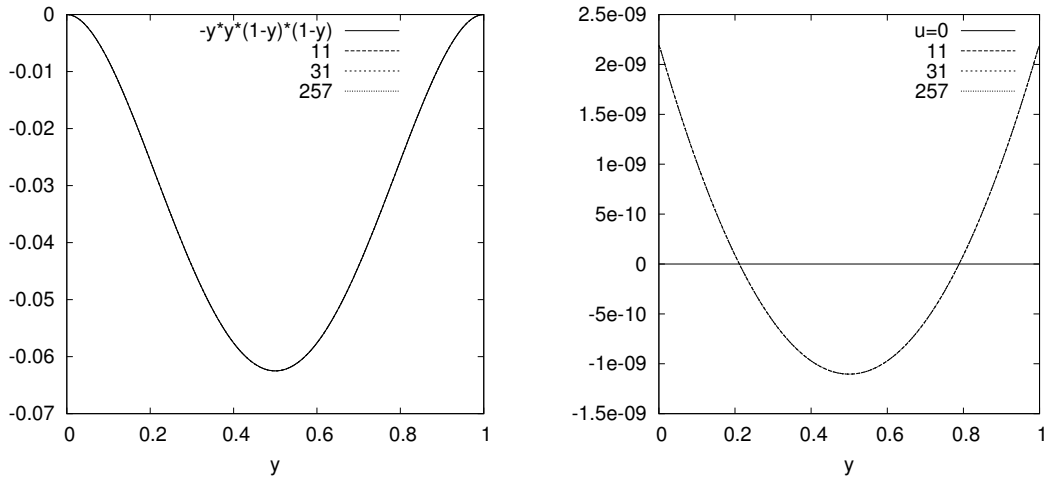

Figure A.5: $u|_{\Gamma_C} = y^2(1-y)^2$ and $u_h|_{\Gamma_C}$ for different DOF on Γ_C for eight grid refinements calculated with the computed control, $\mathrm{Reg} = R^T R$ and $\alpha = 1.e - 13$.

At last we present the results for different regularisation parameters. Therefore we discretise Ω eight times and use 41 DOF on Γ_C. We can see that the influence of the regularisation parameter in this results is small.
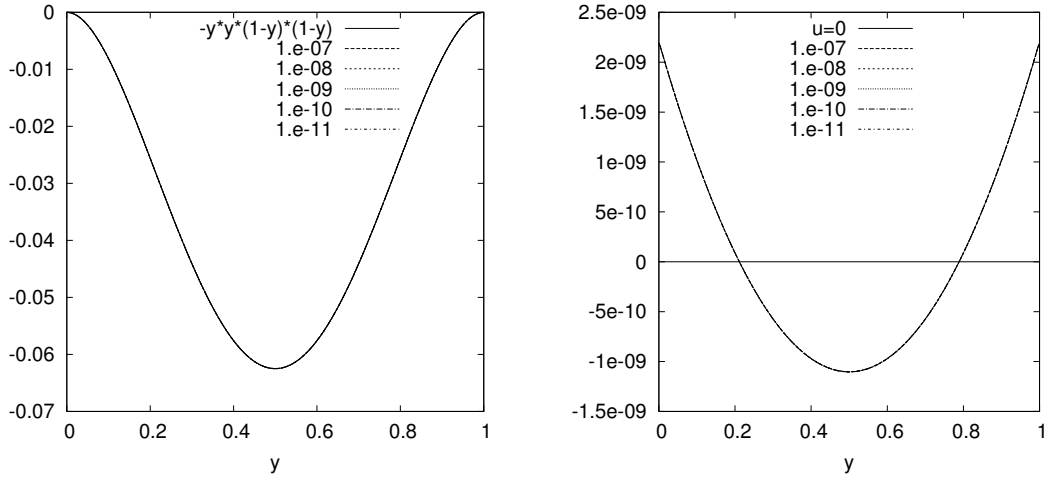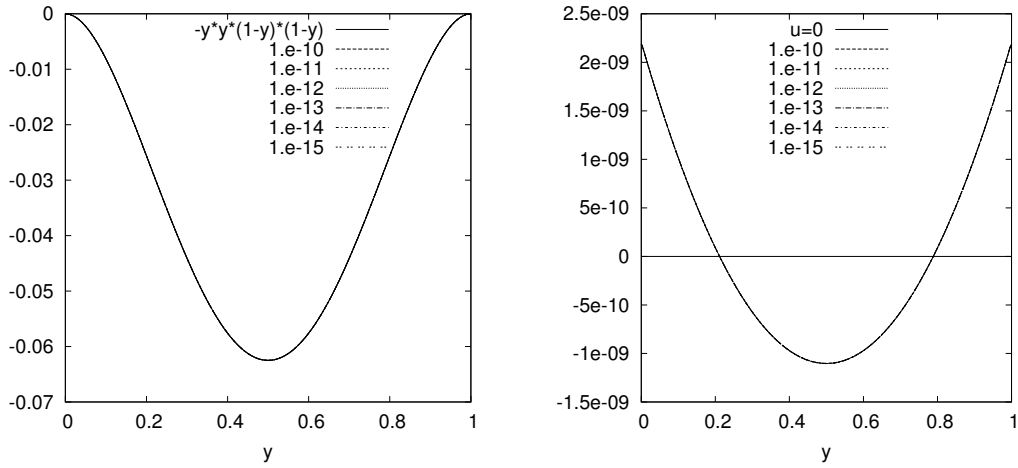
Figure A.6: Results on Γ_O: $\partial_n u|_{\Gamma_O} = -y^2(1-y)^2$ and $\partial_n u_h|_{\Gamma_O}$ (left), $u|_{\Gamma_O} = 0$ and $u_h|_{\Gamma_O}$ (right) for different regularisation parameters refining the grid eight times and 41 DOF on Γ_C calculated with the computed control.
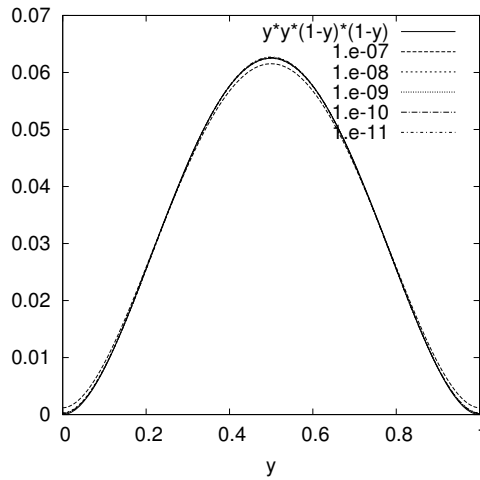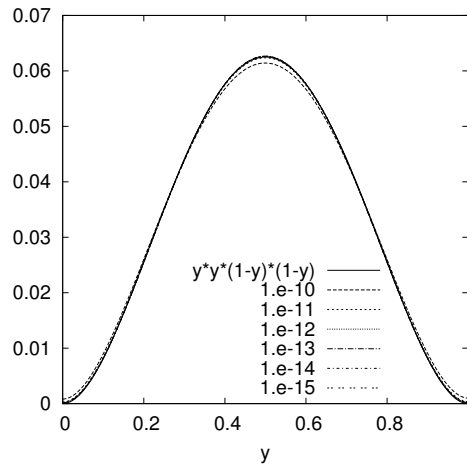

Figure A.7: $u|_{\Gamma_C} = y^2(1-y)^2$ and $u_h|_{\Gamma_C}$ for different regularisation parameters refining the grid eight times and 41 DOF on Γ_C calculated with the computed control.

Results for searched $\partial_n u|_{\Gamma_C}$ and given $\partial_n u|_{\Gamma_O}$ with $\mathrm{Reg} = R_1^T R_1$

Now we take a look on the results for searched Neumann control and given Neumann measurements calculated with $\mathrm{Reg} = R_1^T R_1$ for different grid refinements and the

regularisation parameter $\alpha = 1.e - 13$. The results for the searched control can be seen in Section 6.1. As there we can see here the better results for smaller grids.
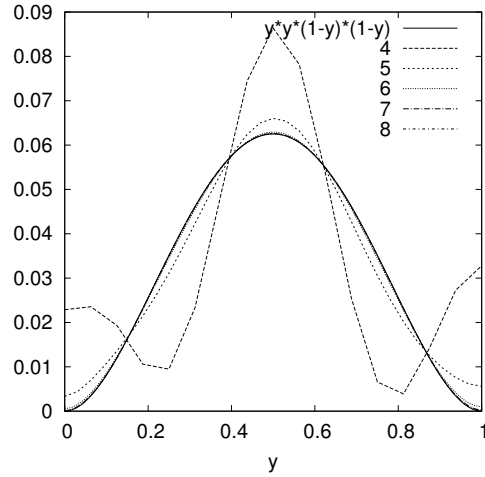
Figure A.8: $u|_{\Gamma_C} = y^2(1-y)^2$ and $u_h|_{\Gamma_C}$ for different grid refinements with Reg $= R_1^T R_1$ and $\alpha = 1.e - 13$ calculated with the computed control.
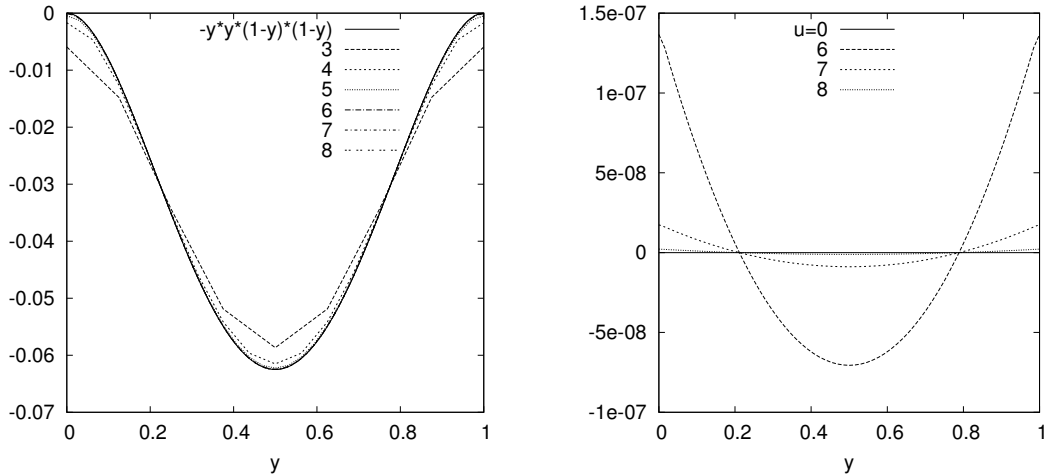
Figure A.9: Results on Γ_O: $\partial_n u|_{\Gamma_O} = -y^2(1-y)^2$ and $\partial_n u_h|_{\Gamma_O}$ (left), $u|_{\Gamma_O} = 0$ and $u_h|_{\Gamma_O}$ (right) for different grid refinements with Reg $= R_1^T R_1$ and $\alpha = 1.e - 13$ calculated with the computed control.

Now the results for different DOF on Γ_C for Reg $= R_1^T R_1$ and $\alpha = 1.e - 13$. Graphically there is no discrepancy obvious. For the results of the searched control see Section 6.1.
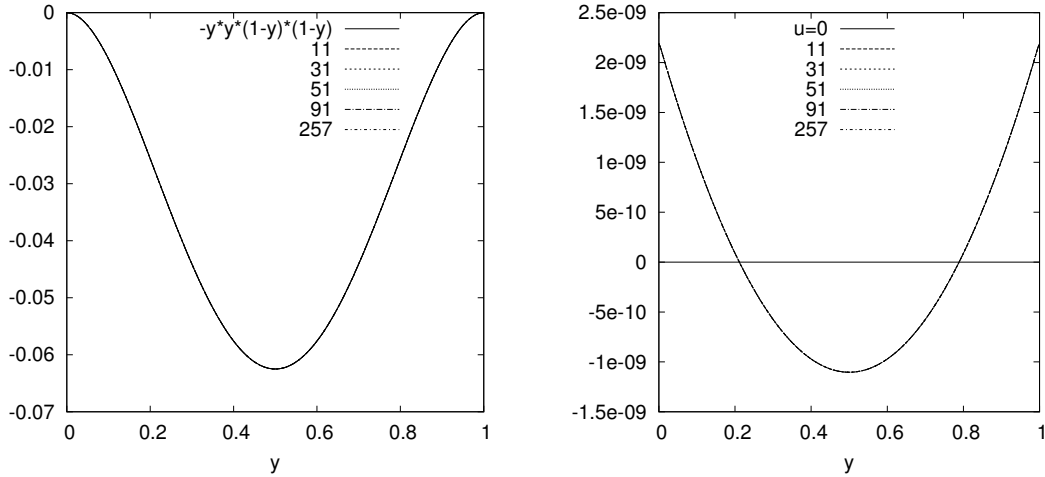
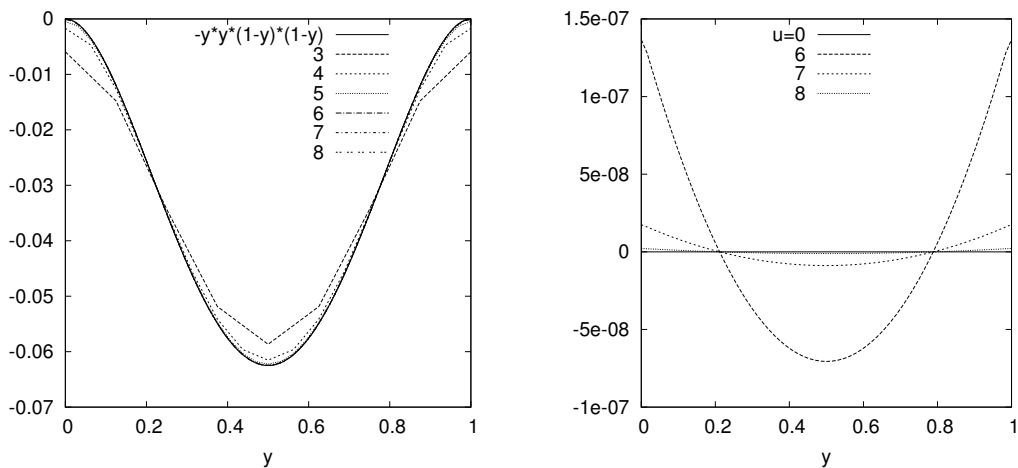Figure A.10: Results on Γ_O: $\partial_n u|_{\Gamma_O} = -y^2(1 - y)^2$ and $\partial_n u_h|_{\Gamma_O}$ (left), $u|_{\Gamma_O} = 0$ and $u_h|_{\Gamma_O}$ (right) for different DOF on Γ_C with Reg $= R_1^T R_1$ and $\alpha = 1.e - 13$ calculated with the computed control.
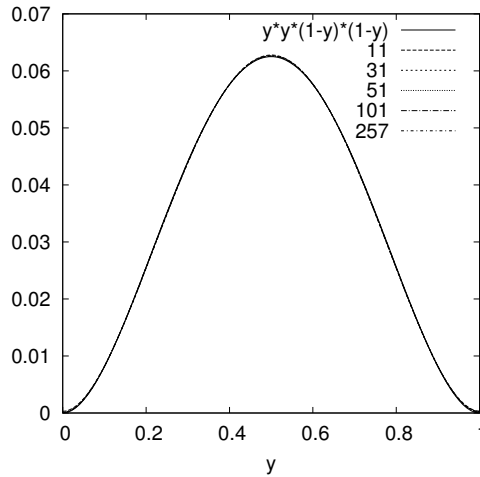
Figure A.11: $u|_{\Gamma_C} = y^2(1-y)^2$ and $u_h|_{\Gamma_C}$ for different DOF on Γ_C with Reg $= R_1^T R_1$ and $\alpha = 1.e - 13$ calculated with the computed control.

In the following we illustrate the results for different regularisation parameters discretise Ω eight times and use 101 DOF on Γ_C. Again we can see that the influence of the regularisation parameter on these results is small.
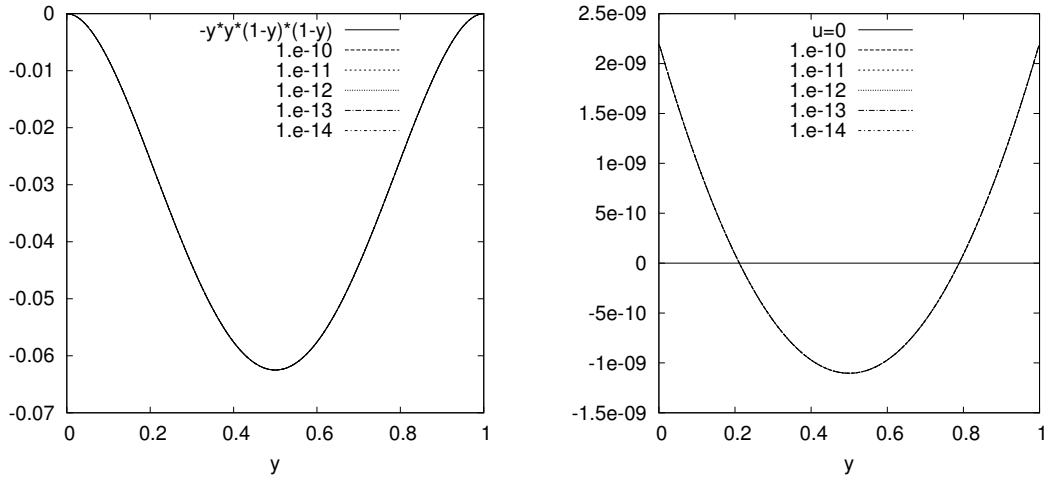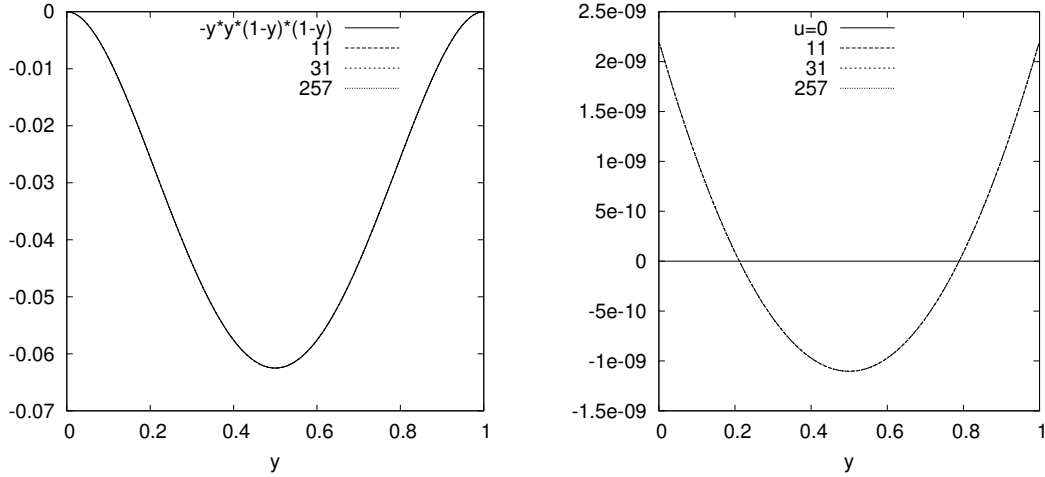

Figure A.12: Results on Γ_O: $\partial_n u|_{\Gamma_O} = -y^2(1-y)^2$ and $\partial_n u_h|_{\Gamma_O}$ (left), $u|_{\Gamma_O} = 0$ and $u_h|_{\Gamma_O}$ (right) for different regularisation parameters, refining eight times and using 101 DOF on Γ_C calculated with the computed control.
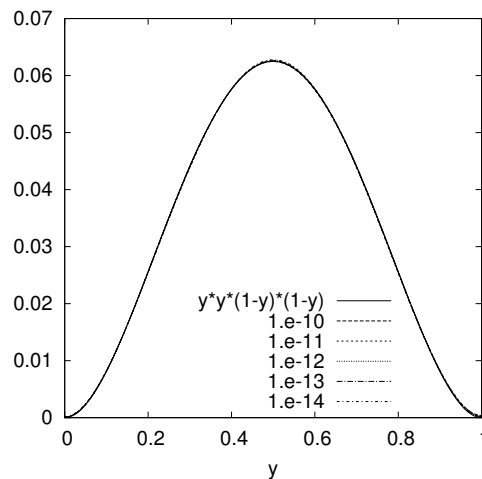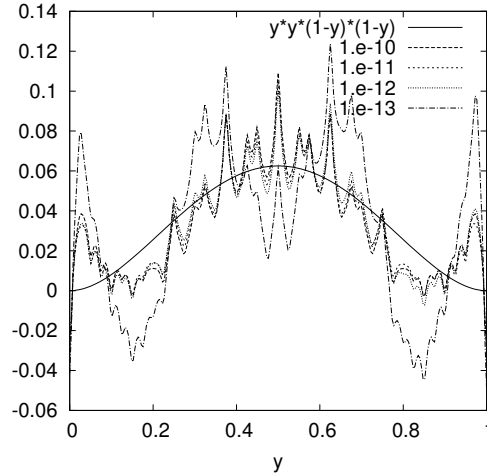

Figure A.13: $u|_{\Gamma_C} = y^2(1-y)^2$ and $u_h|_{\Gamma_C}$ for different regularisation parameter refining eight times and using 101 DOF on Γ_C calculated with the computed control.

Results for searched $\partial_n u|_{\Gamma_C}$ and given $\partial_n u|_{\Gamma_O}$ with $\text{Reg} = R_2^T R_2$

In the following we present the results for different grid refinements regularise by an approximation of the second derivative $(R_2^T R_2)$ and $\alpha = 1.e - 13$. As for the searched control (see Section 6.1) we get better results for smaller grids.

Figure A.14: $u|_{\Gamma_C} = y^2(1 - y)^2$ and $u_h|_{\Gamma_C}$ for different grid refinements calculated with the computed control, $\text{Reg} = R_2^T R_2$ and $\alpha = 1.e - 13$.
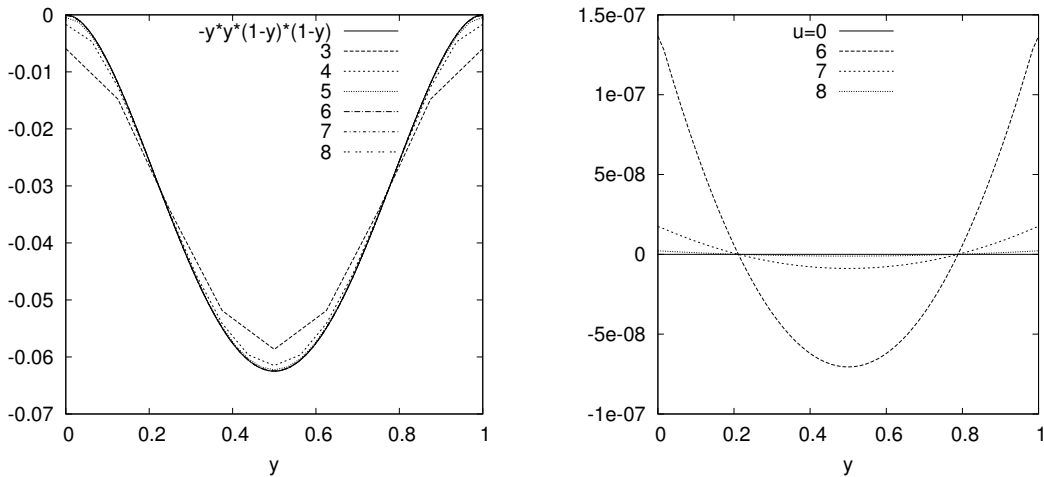
Figure A.15: $\partial_n u|_{\Gamma_O} = -y^2(1 - y)^2$ and $\partial_n u_h|_{\Gamma_O}$ (left),$u|_{\Gamma_O} = 0$ and $u_h|_{\Gamma_O}$ (right) for different grid refinements calculated with the computed control, $\text{Reg} = R_2^T R_2$ and $\alpha = 1.e - 13$.

Now we present the graphical results for different DOF on Γ_C refining Ω eight times and $\alpha = 1.e - 13$. Again we can see that we don't loose quality of the results if we reduce the number of DOF on Γ_C. For the computed control see Section 6.1.

Figure A.16: $u|_{\Gamma_C} = y^2(1-y)^2$ and $u_h|_{\Gamma_C}$ for different DOF on Γ_C refining Ω eight times calculated with the computed control, $\text{Reg} = R_2^T R_2$ and $\alpha = 1.e - 13$.
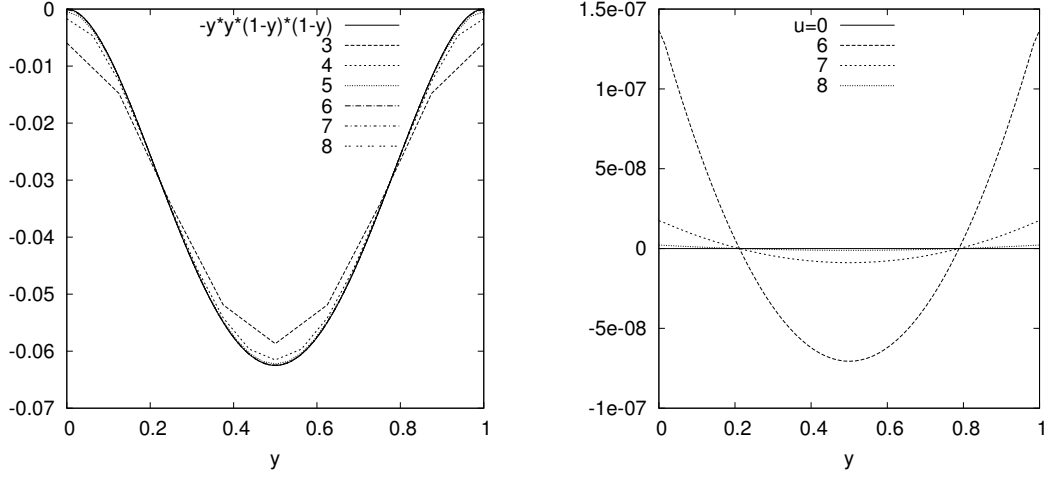

Figure A.17: Results on Γ_O: $\partial_n u|_{\Gamma_O} = -y^2(1-y)^2$ and $\partial_n u_h|_{\Gamma_O}$ (left), $u|_{\Gamma_O} = 0$ and $u_h|_{\Gamma_O}$ (right) for different DOF on Γ_C refining Ω eight times calculated with the computed control, $\text{Reg} = R_2^T R_2$ and $\alpha = 1.e - 13$.

In the following Figures we see the results for different regularisation parameters refining the grid eight times and use 31 DOF on Γ_C. As for the previous calculations we can see that the influence of the regularisation parameter on these results is very small.

Figure A.18: Results on Γ_O: $\partial_n u|_{\Gamma_O} = -y^2(1-y)^2$ and $\partial_n u_h|_{\Gamma_O}$ (left), $u|_{\Gamma_O} = 0$ and $u_h|_{\Gamma_O}$ (right) for different regularisation parameters refining Ω eight times, 31 DOF on Γ_C calculated with the computed control and Reg $= R_2^T R_2$.

Figure A.19: $u|_{\Gamma_C} = y^2(1-y)^2$ and $u_h|_{\Gamma_C}$ for different regularisation parameters refining Ω eight times, 31 DOF on Γ_C calculated with the computed control and Reg $= R_2^T R_2$.

A.2 Results for given $\partial_n u|_{\Gamma_O}$ and searched $u|_{\Gamma_C}$

Results for searched $u|_{\Gamma_C}$ and given $\partial_n u|_{\Gamma_O}$ with $\text{Reg} = R^T R$

In the following we present the results for searched Dirichlet control and given Neumann measurement calculated for different grid refinements with $\text{Reg} = R^T R$ and $\alpha = 1.e - 10$. As for the searched control (see Section 6.2) we reach better results for smaller grids.
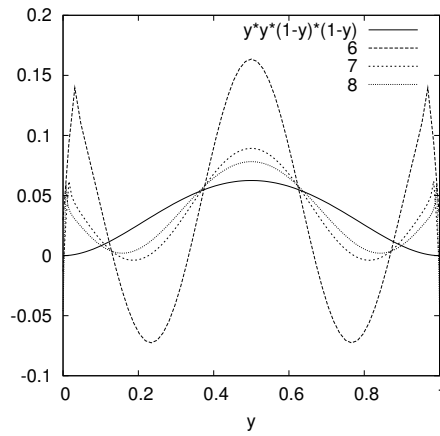
Figure A.20: $\partial_n u_h|_{\Gamma_C} = y^2(1-y)^2$ and $\partial_n u_h|_{\Gamma_C}$ for different grid refinements calculated with the computed control, $\text{Reg} = R^T R$ and $\alpha = 1.e - 10$.

Figure A.21: $\partial_n u_h|_{\Gamma_O} = -y^2(1-y)^2$ and $\partial_n u_h|_{\Gamma_O}$ (left), $u|_{\Gamma_O} = 0$ and $u_h|_{\Gamma_O}$ (right) for different grid refinements with $\text{Reg} = R^T R$ and $\alpha = 1.e - 10$.

Now we reduce the number of DOF on Γ_C. Therefore we refine eight times, use $\alpha = 1.e - 10$ and Reg $= R^T R$. Specially in Figure A.23 we can see the problems if we reduce the number of DOF on Γ_C too much.

Figure A.22: Results on Γ_O: $\partial_n u|_{\Gamma_O} = -y^2(1 - y)^2$ and $\partial_n u_h|_{\Gamma_O}$ (left), $u|_{\Gamma_O} = 0$ and $u_h|_{\Gamma_O}$ (right) for different DOF on Γ_C refining the grid eight times calculated with the computed control, Reg $= R^T R$ and $\alpha = 1.e - 10$.
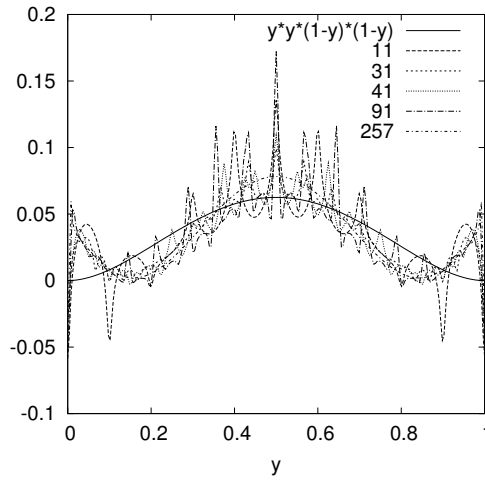
Figure A.23: $\partial_n u|_{\Gamma_C} = y^2(1 - y)^2$ and $\partial_n u_h|_{\Gamma_C}$ for different DOF on Γ_C refining the grid eight times calculated with the computed control, Reg $= R^T R$ and $\alpha = 1.e - 10$.

Now we use Reg $= R^T R$, 41 DOF on Γ_C and refine the grid eight times for different

regularisation parameters. We can see that we weren't able to avoid the oscillations in the calculation of $\partial_n u_h|_{\Gamma_C}$.
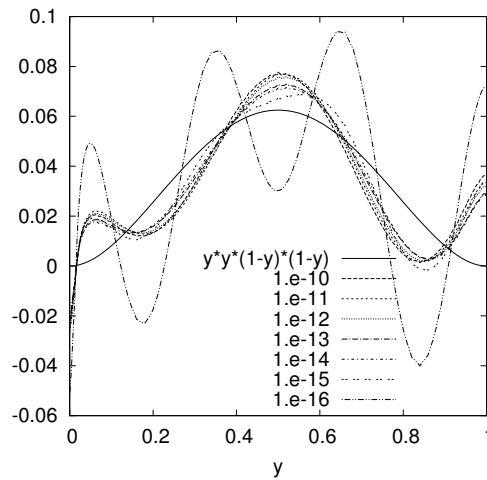

Figure A.24: $\partial_n u|_{\Gamma_C} = y^2(1-y)^2$ and $\partial_n u_h|_{\Gamma_C}$ for different regularisation parameters refining the grid eight times calculated with the computed control, 41 DOF on Γ_C and Reg $= R^T R$.
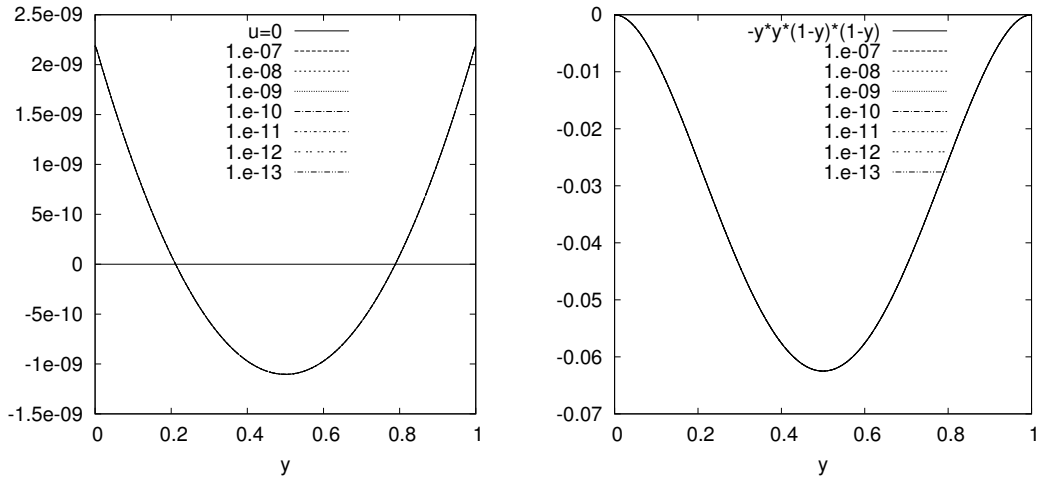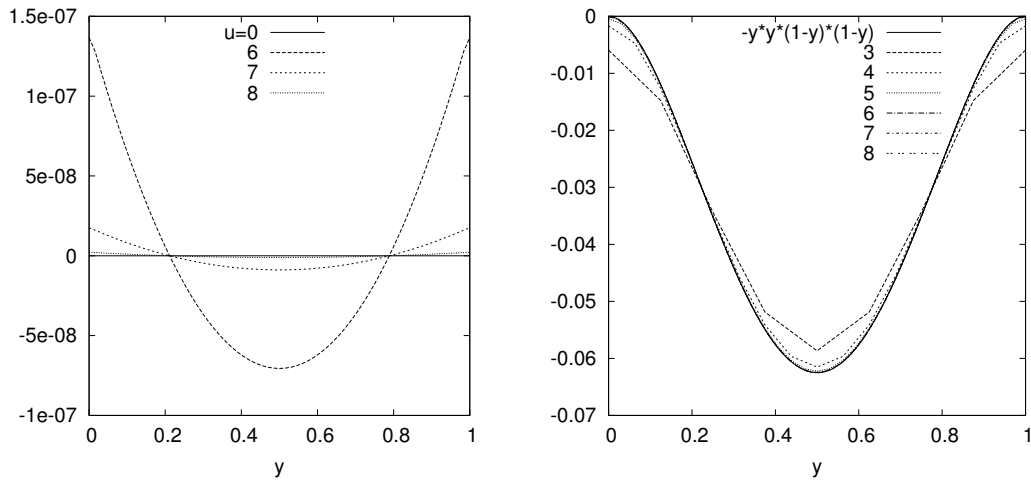

Figure A.25: Results on Γ_O: $u|_{\Gamma_O} = 0$ and $u_h|_{\Gamma_O}$ (left),$\partial_n u|_{\Gamma_O} = -y^2(1-y)^2$ and $\partial_n u_h|_{\Gamma_O}$ (right) for different regularisation parameters refining the grid eight times calculated with the computed control, 41 DOF on Γ_C and Reg $= R^T R$.

Results for searched $u|_{\Gamma_C}$ and given $\partial_n u|_{\Gamma_O}$ with $\text{Reg} = R_1^T R_1$

Figure A.26: Results on Γ_O: $\partial_n u|_{\Gamma_O} = -y^2(1-y)^2$ and $\partial_n u_h|_{\Gamma_O}$ (left), $u|_{\Gamma_O} = 0$ and $u_h|_{\Gamma_O}$ (right) for different grid refinements calculated with the computed control, $\text{Reg} = R_1^T R_1$ and $\alpha = 1.e - 13$.

Figures A.26 and A.27 show the results for searched $u|_{\Gamma_C}$ and given $\partial_n u|_{\Gamma_O}$ for different grid refinements regularise by $\text{Reg} = R_1^T R_1$ with $\alpha = 1.e - 13$. As before we get the better results for smaller grids.
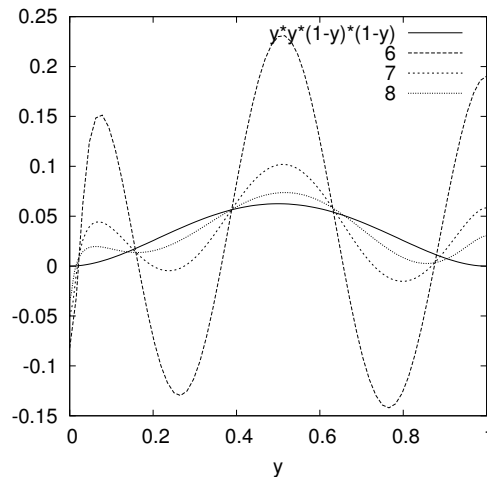
Figure A.27: $\partial_n u|_{\Gamma_C} = y^2(1-y)^2$ and $\partial_n u_h|_{\Gamma_C}$ for different grid refinements calculated with the computed control, $\text{Reg} = R_1^T R_1$ and $\alpha = 1.e - 13$.

Now we want to reduce the number of DOF on Γ_C. Therefore we discretise eight times, regularise by $\text{Reg} = R_1^T R_1$ and set $\alpha = 1.e-13$. In Figure A.29 we can see the oscillations if we reduce the number of DOF on Γ_C too much.
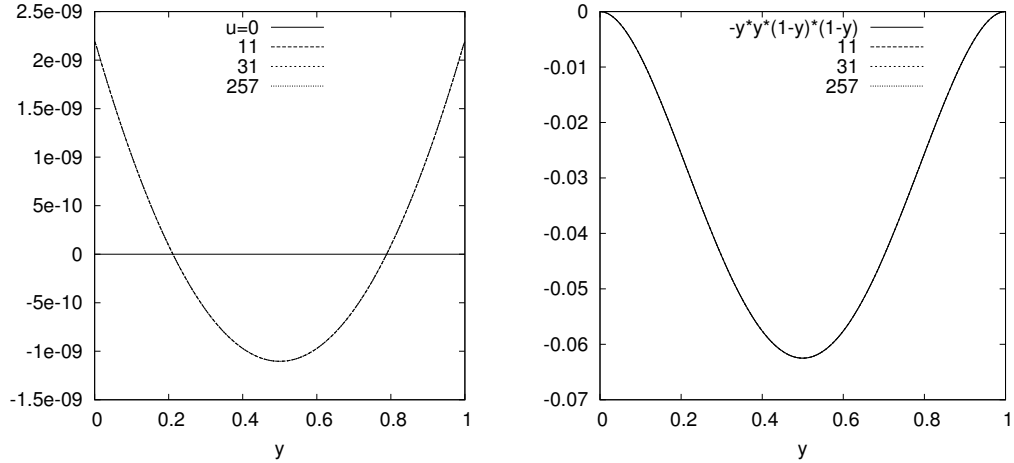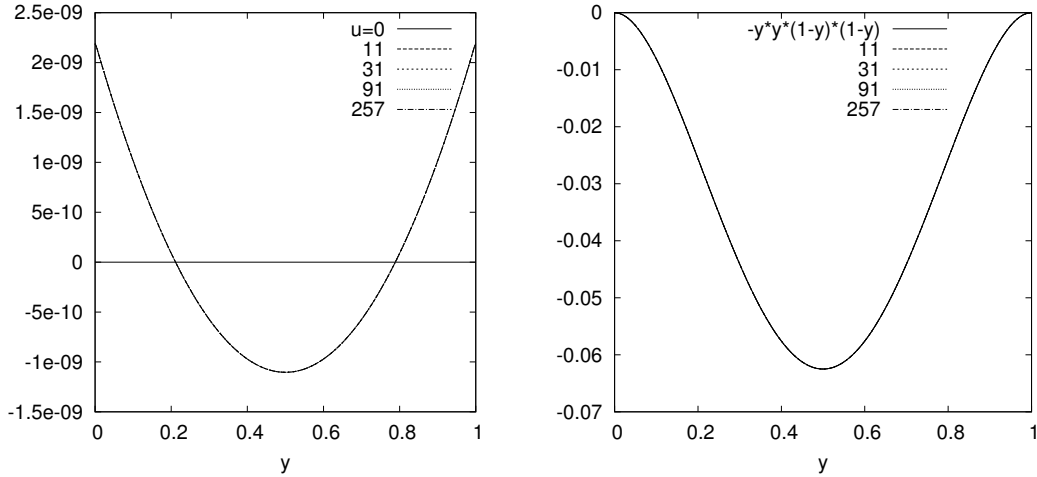

Figure A.28: Results on Γ_O: $u|_{\Gamma_O} = 0$ and $u_h|_{\Gamma_O}$ (left), $\partial_n u|_{\Gamma_O} = -y^2(1-y)^2$ and $\partial_n u_h|_{\Gamma_O}$ (right) for different DOF on Γ_C refining the grid eight times calculated with the computed control, $\text{Reg} = R_1^T R_1$ and $\alpha = 1.e-13$.
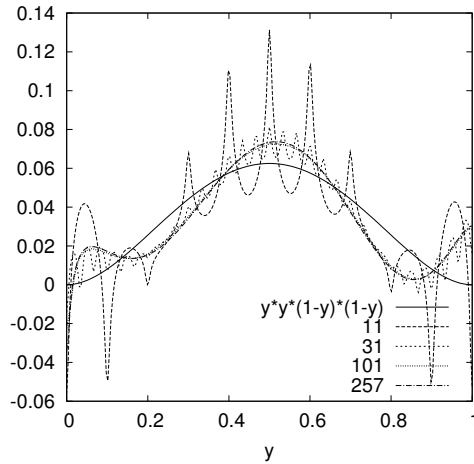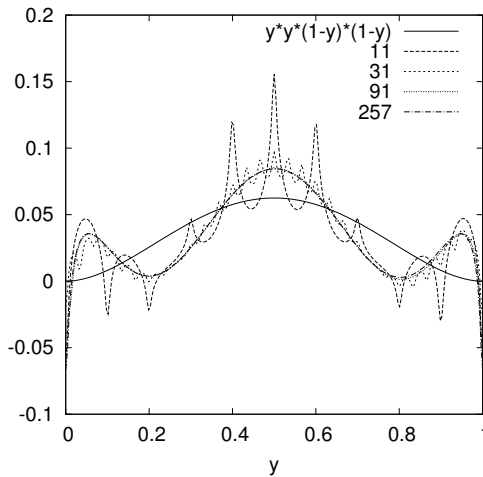

Figure A.29: $\partial_n u|_{\Gamma_C} = y^2(1-y)^2$ and $\partial_n u_h|_{\Gamma_C}$ for different DOF on Γ_C refining the grid eight times calculated with the computed control, $\text{Reg} = R_1^T R_1$ and $\alpha = 1.e-13$.

In the following we present the results for different regularisation parameters regularise by $\text{Reg} = R_1^T R_1$ refining the grid eight times and use 101 DOF on Γ_C. There are only discrepancies in the calculation of $\partial_n u_h|_{\Gamma_C}$ obvious.
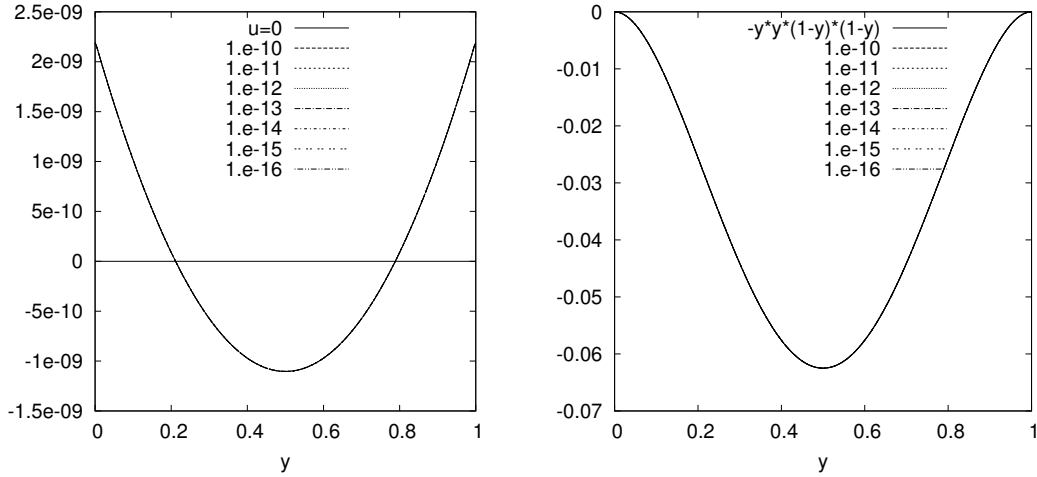
Figure A.30: Results on Γ_O: $u|_{\Gamma_O} = 0$ and $u_h|_{\Gamma_O}$ (left), $\partial_n u|_{\Gamma_O} = -y^2(1-y)^2$ and $\partial_n u_h|_{\Gamma_O}$ (right) for different regularisation parameters calculated with the computed control, $\text{Reg} = R_1^T R_1$, 101 DOF on Γ_C and refining the grid eight times.
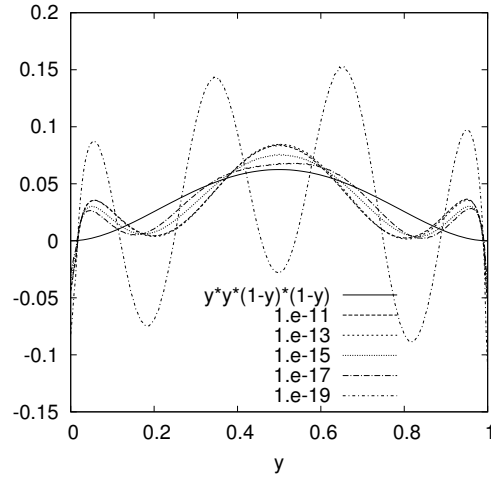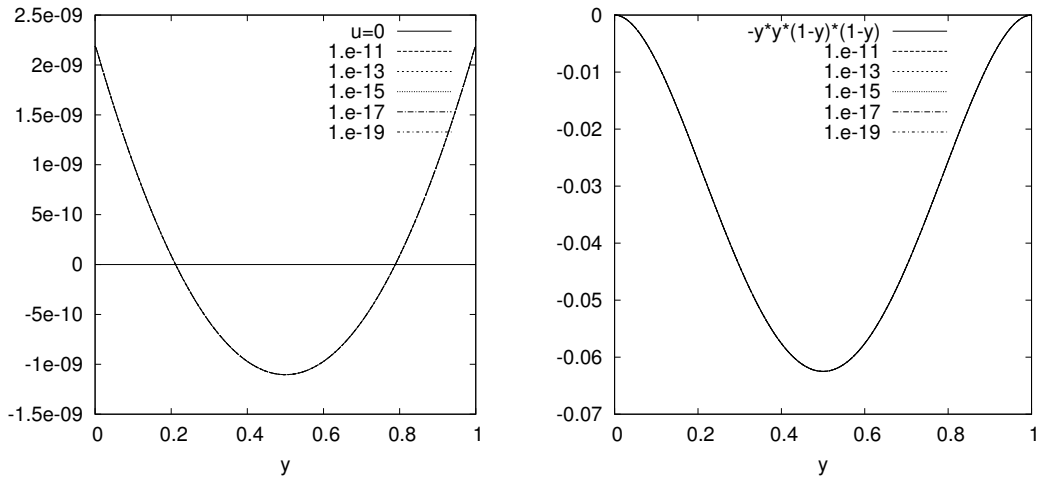

Figure A.31: $\partial_n u|_{\Gamma_C} = y^2(1-y)^2$ and $\partial_n u_h|_{\Gamma_C}$ for different regularisation parameters calculated with the computed control, $\text{Reg} = R_1^T R_1$, 101 DOF on Γ_C and refining the grid eight times.

139

Results for searched $u|_{\Gamma_C}$ and given $\partial_n u|_{\Gamma_O}$ with $\mathrm{Reg} = R_2^T R_2$

At last we analyse the results for $\mathrm{Reg} = R_2^T R_2$. We start with different grid refinements and $\alpha = 1.e - 13$. Again we can see the better results for smaller grids.
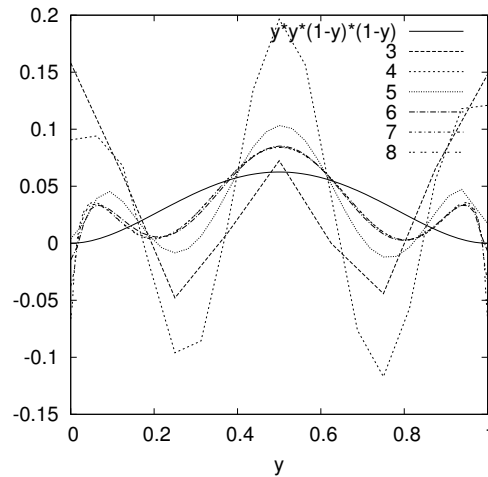
Figure A.32: $\partial_n u|_{\Gamma_C} = y^2(1-y)^2$ and $\partial_n u_h|_{\Gamma_C}$ for different grid refinements calculated with the computed control, $\alpha = 1.e - 13$ and $\mathrm{Reg} = R_2^T R_2$.

Figure A.33: Results on Γ_O: $u|_{\Gamma_O} = 0$ and $u_h|_{\Gamma_O}$ (left), $\partial_n u|_{\Gamma_O} = -y^2(1-y)^2$ and $\partial_n u_h|_{\Gamma_O}$ (right) for different grid refinements calculated with the computed control, $\alpha = 1.e - 13$ and $\mathrm{Reg} = R_2^T R_2$.

Now we present the results for reduced number of DOF on Γ_C. We discretise Ω eight times and set $\alpha = 1.e - 13$. As in the previous calculations we can see the oscillations in the calculation of $\partial_n u_h|_{\Gamma_C}$ if we reduce the number of DOF on Γ_C too much.

Figure A.34: Results on Γ_O: $u|_{\Gamma_O} = 0$ and $u_h|_{\Gamma_O}$ (left), $\partial_n u|_{\Gamma_O} = -y^2(1-y)^2$ and $\partial_n u_h|_{\Gamma_O}$ (right) for different DOF on Γ_C refining eight times calculated with the computed control, $\text{Reg} = R_2^T R_2$ and $\alpha = 1.e - 13$.
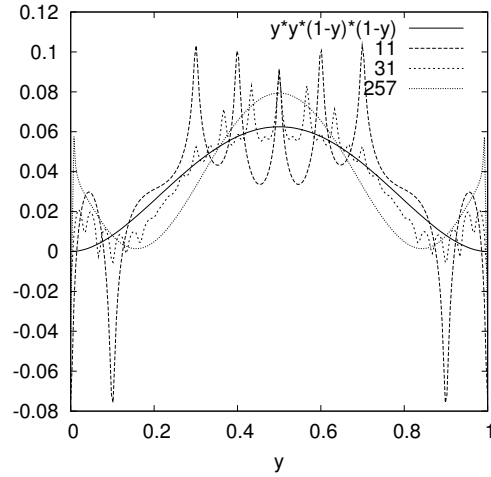

Figure A.35: $\partial_n u|_{\Gamma_C} = y^2(1-y)^2$ and $\partial_n u_h|_{\Gamma_C}$ for different DOF on Γ_C refining the grid eight times calculated with the computed control, $\text{Reg} = R_2^T R_2$ and $\alpha = 1.e - 13$.

At last we present the results for different regularisation parameters. We discretise eight times and use 91 DOF on Γ_C. We can see again that only for the calculation of $\partial_n u_h|_{\Gamma_C}$ the influence of the regularisation parameter is obvious.

Figure A.36: $\partial_n u|_{\Gamma_C} = y^2(1-y)^2$ and $\partial_n u_h|_{\Gamma_C}$ for different regularisation parameters, refining the grid eight times calculated with the computed control, 91 DOF on Γ_C and $\mathrm{Reg} = R_2^T R_2$.
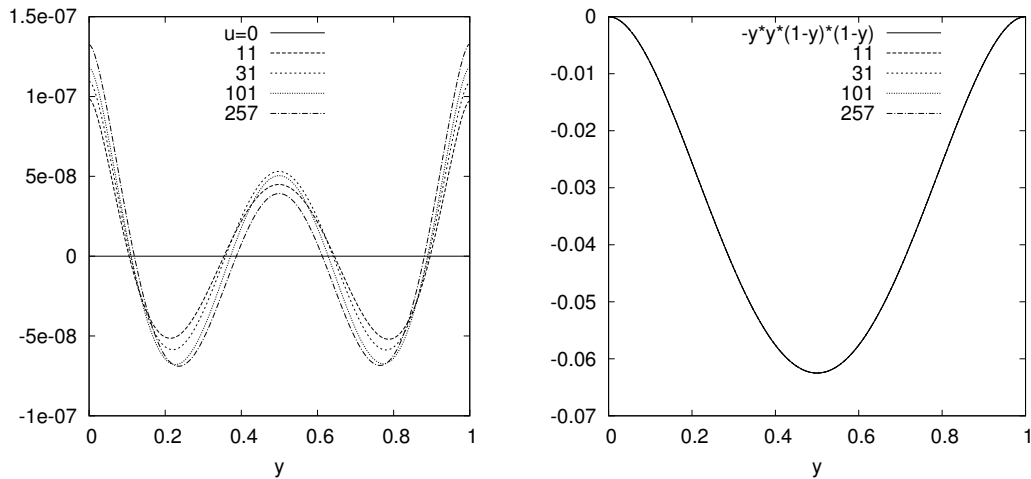

Figure A.37: Results on Γ_O: $u|_{\Gamma_O} = 0$ and $u_h|_{\Gamma_O}$ (left), $\partial_n u|_{\Gamma_O} = -y^2(1-y)^2$ and $\partial_n u_h|_{\Gamma_O}$ (right) for different regularisation parameters refining the grid eight times calculated with the computed control, 91 DOF on Γ_C and $\mathrm{Reg} = R_2^T R_2$.

A.3 Results for given $u|_{\Gamma_O}$ and searched $u|_{\Gamma_C}$

Results for searched $u|_{\Gamma_C}$ and given $u|_{\Gamma_O}$ with $\mathrm{Reg} = R^T R$

Now we present the results for searched Dirichlet control and given Dirichlet data for different grid refinements regularise by $\mathrm{Reg} = R^T R$ and $\alpha = 1.e - 11$. Again we can see the better results for smaller grids.
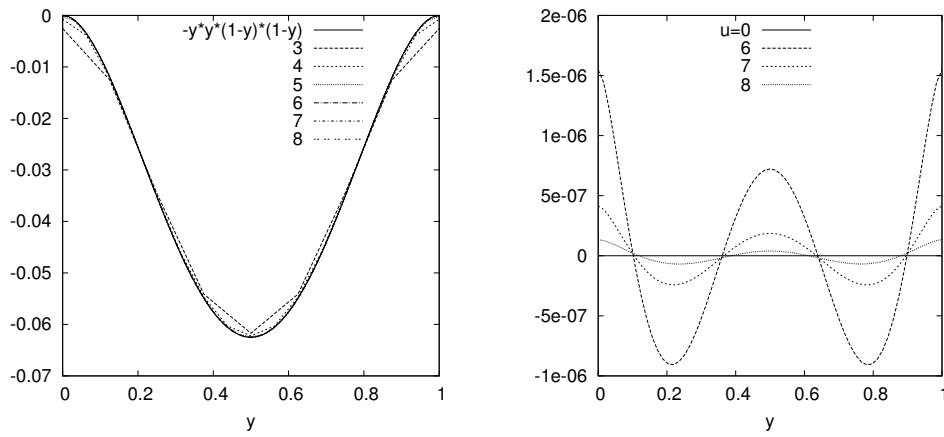
Figure A.38: Results on Γ_O: $\partial_n u|_{\Gamma_O} = -y^2(1-y)^2$ and $\partial_n u_h|_{\Gamma_O}$ (left), $u|_{\Gamma_O}$ and $u_h|_{\Gamma_O}$ (right) for different grid refinements calculated with the computed control, $\mathrm{Reg} = R^T R$ and $\alpha = 1.e - 11$.
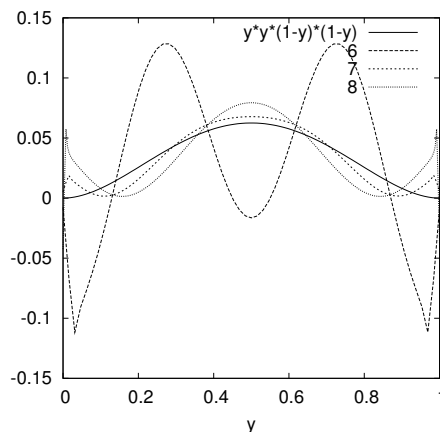
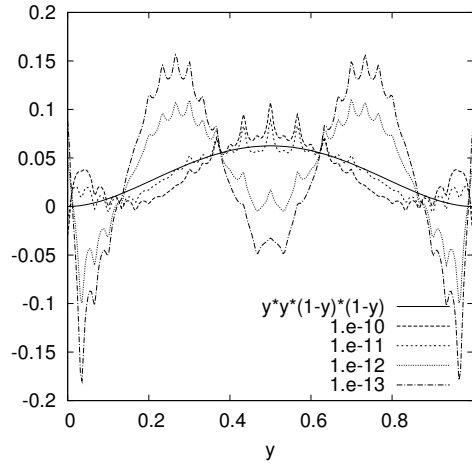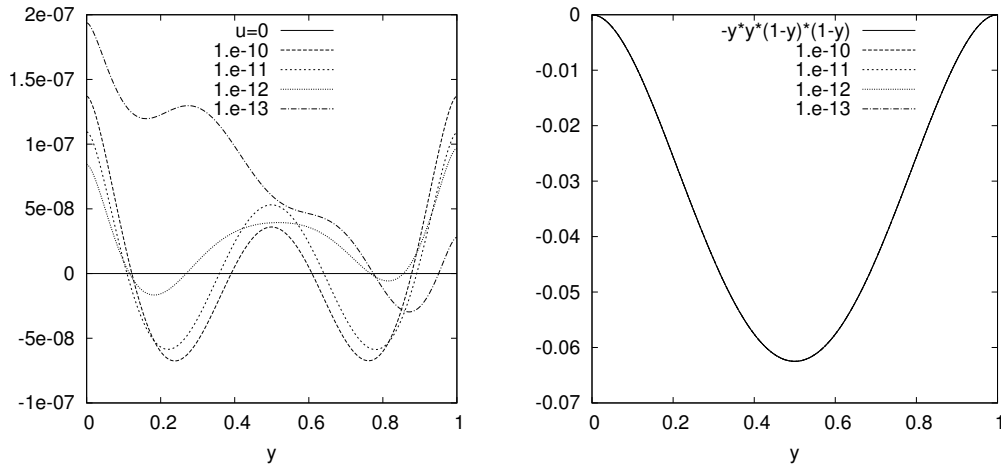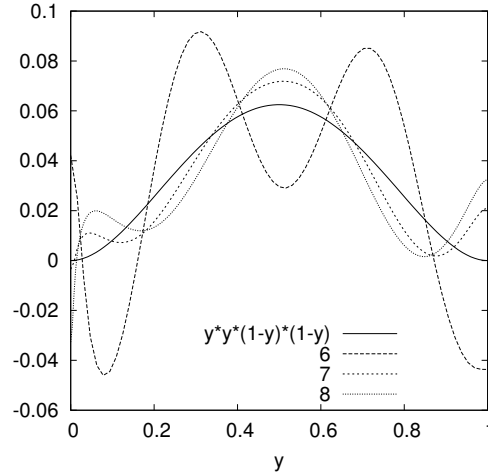

Figure A.39: $\partial_n u|_{\Gamma_C} = y^2(1-y)^2$ and $\partial_n u_h|_{\Gamma_C}$ for different grid refinements calculated with the computed control, $\mathrm{Reg} = R^T R$ and $\alpha = 1.e - 11$.

In the following we reduce the number of DOF on Γ_C refine the grid eight times and set $\alpha = 1.e - 11$. We can see the oscillations in the calculation of $\partial_n u_h|_{\Gamma_C}$ and also in the results for $u_h|_{\Gamma_O}$ we can see discrepancies.

Figure A.40: $\partial_n u|_{\Gamma_C} = y^2(1 - y)^2$ and $\partial_n u_h|_{\Gamma_C}$ for different DOF on Γ_C refining the grid eight times calculated with the computed control, Reg $= R^T R$ and $\alpha = 1.e - 11$.

Figure A.41: Results on Γ_O: $u|_{\Gamma_O} = 0$ and $u_h|_{\Gamma_O}$ (left), $\partial_n u|_{\Gamma_O} = -y^2(1 - y)^2$ and $\partial_n u_h|_{\Gamma_O}$ for different DOF on Γ_C refining the grid eight times calculated with the computed control, Reg $= R^T R$ and $\alpha = 1.e - 11$.

Now we use different regularisation parameters, discretise Ω eight times use 101 DOF on Γ_C and regularise by $\text{Reg} = R^T R$. We can see that we can't avoid the oscillations in the calculation of $\partial_n u_h|_{\Gamma_C}$ and again we have achieve discrepancies in the calculation of $u_h|_{\Gamma_O}$.

Figure A.42: $\partial_n u|_{\Gamma_C} = y^2(1-y)^2$ and $\partial_n u_h|_{\Gamma_C}$ for different regularisation parameters calculated with the computed control, $\text{Reg} = R^T R$, refining Ω eight times and use 101 DOF on Γ_C.
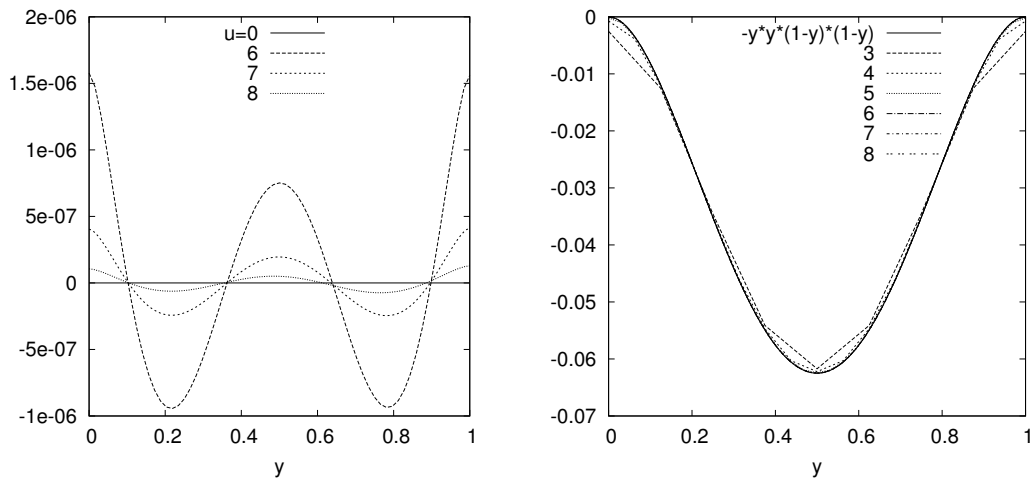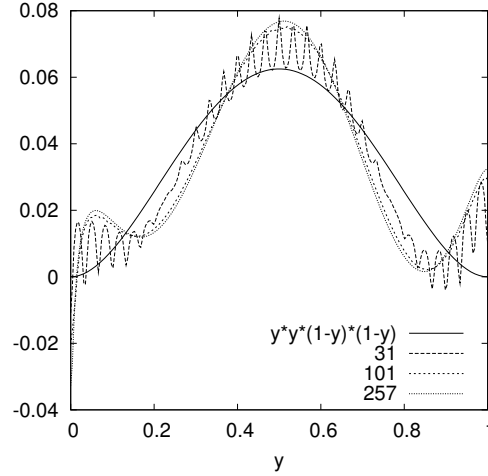
Figure A.43: Results on Γ_O: $u|_{\Gamma_O} = 0$ and $u_h|_{\Gamma_O}$ (left), $\partial_n u|_{\Gamma_O} = -y^2(1-y)^2$ and $\partial_n u_h|_{\Gamma_O}$ (right) for different regularisation parameters calculated with the computed control, $\text{Reg} = R^T R$, refining the grid eight times and use 101 DOF on Γ_C.

Results for searched $u|_{\Gamma_C}$ and given $u|_{\Gamma_O}$ with $\mathrm{Reg} = R_1^T R_1$

For the regularisation with $\mathrm{Reg} = R_1^T R_1$ we set $\alpha = 1.e - 13$ and start with the results for different grid refinements. As in the previous Sections we reach the better results for smaller grids.

Figure A.44: $\partial_n u|_{\Gamma_C} = y^2(1-y)^2$ and $\partial_n u_h|_{\Gamma_C}$ for different grid refinements calculated with the computed control, $\mathrm{Reg} = R_1^T R_1$ and $\alpha = 1.e - 13$.
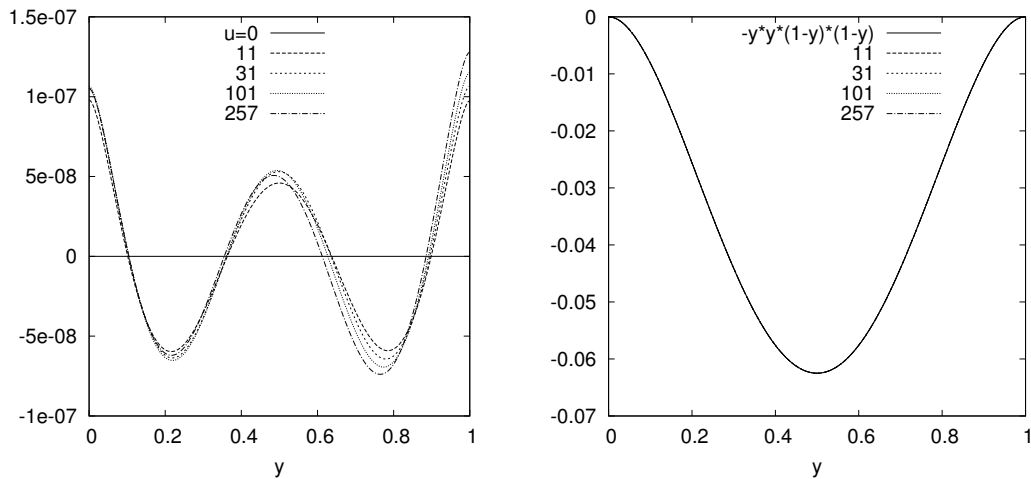

Figure A.45: Results on Γ_O: $u|_{\Gamma_O} = 0$ and $u_h|_{\Gamma_O}$ (left), $\partial_n u|_{\Gamma_O} = -y^2(1-y)^2$ and $\partial_n u_h|_{\Gamma_O}$ for different grid refinements calculated with the computed control, $\mathrm{Reg} = R_1^T R_1$ and $\alpha = 1.e - 13$.

In the following Figures we reduce the number of DOF, refine the grid eight times and regularise by Reg $= R_1^T R_1$, $\alpha = 1.e - 13$. Again we can see the problems in the calculation of $\partial_n u_h|_{\Gamma_C}$ and the discrepancies in the results for $u_h|_{\Gamma_O}$.

Figure A.46: $\partial_n u|_{\Gamma_C} = y^2(1-y)^2$ and $\partial_n u_h|_{\Gamma_C}$ for different DOF on Γ_C refining the grid eight times calculated with the computed control, Reg $= R_1^T R_1$ and $\alpha = 1.e - 13$.

Figure A.47: Results on Γ_O: $u|_{\Gamma_O} = 0$ and $u_h|_{\Gamma_O}$ (left), $\partial_n u|_{\Gamma_O} = -y^2(1-y)^2$ and $\partial_n u_h|_{\Gamma_O}$ for different DOF on Γ_C refining the grid eight times calculated with the computed control, Reg $= R_1^T R_1$ and $\alpha = 1.e - 13$.

At last we present the results for different regularisation parameters using 101 DOF on Γ_C and refining the grid eight times. Here we can see the influence of the regularisation parameter on the calculation of $\partial_n u_h|_{\Gamma_C}$ and $u_h|_{\Gamma_O}$.
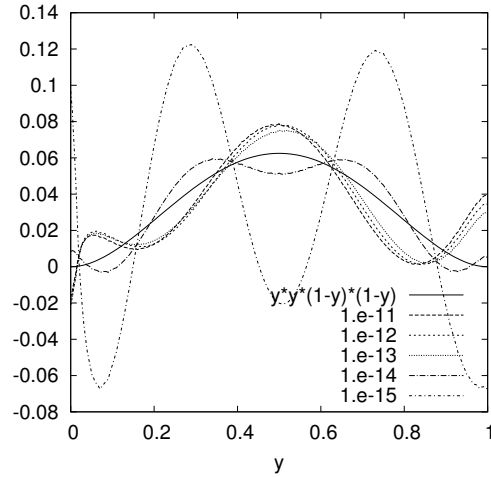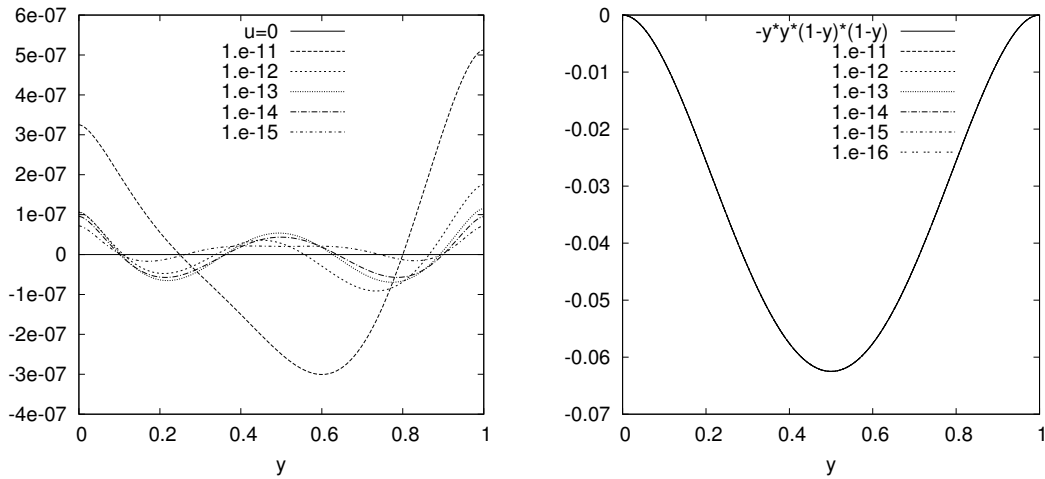

Figure A.48: $\partial_n u|_{\Gamma_C} = y^2(1-y)^2$ and $\partial_n u_h|_{\Gamma_C}$ for different regularisation parameters, refining the grid eight times calculated with the computed control, 101 DOF on Γ_C and $\mathrm{Reg} = R_1^T R_1$.

Figure A.49: Results on Γ_O: $u|_{\Gamma_O} = 0$ and $u_h|_{\Gamma_O}$ (left), $\partial_n u|_{\Gamma_O} = -y^2(1-y)^2$ and $\partial_n u_h|_{\Gamma_O}$ (right) for different regularisation parameters, refining the grid eight times calculated with the computed control, 101 DOF on Γ_C and $\mathrm{Reg} = R_1^T R_1$.

Results for searched $u|_{\Gamma_C}$ and given $u|_{\Gamma_O}$ with $\text{Reg} = R_2^T R_2$

Again we start the presentation with the results for different grid refinements with $\text{Reg} = R_2^T R_2$ as regularisation matrix and $\alpha = 1.e - 13$. As in the previous calculations we get better results for smaller grids.
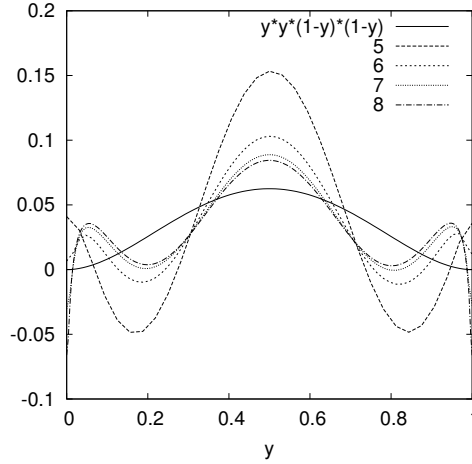

Figure A.50: $\partial_n u|_{\Gamma_C} = y^2(1-y)^2$ and $\partial_n u_h|_{\Gamma_C}$ for different grid refinements calculated with the computed control, $\text{Reg} = R_2^T R_2$ and $\alpha = 1.e - 13$.
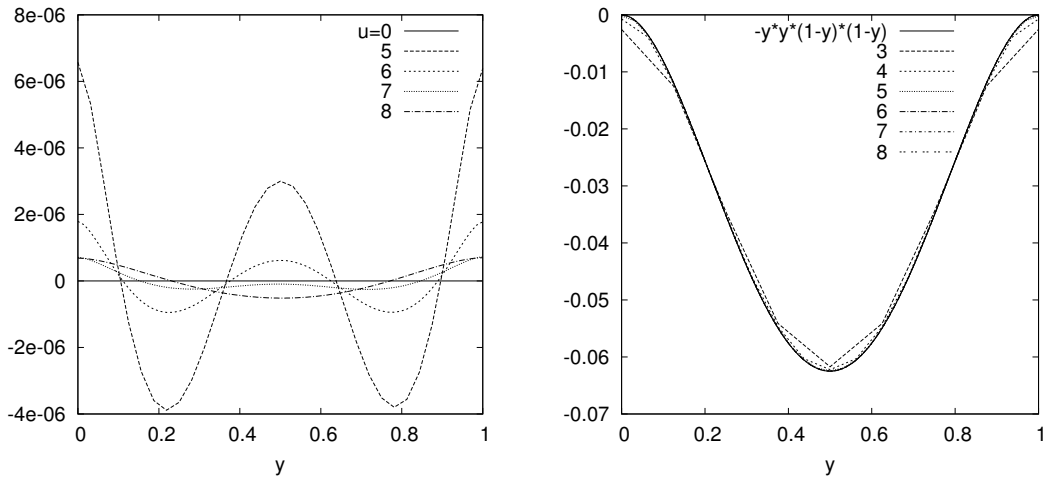

Figure A.51: Results on Γ_O: $u|_{\Gamma_O} = 0$ and $u_h|_{\Gamma_O}$ (left), $\partial_n u|_{\Gamma_O} = -y^2(1-y)^2$ and $\partial_n u_h|_{\Gamma_O}$ (right) for different grid refinements calculated with the computed control, $\text{Reg} = R_2^T R_2$ and $\alpha = 1.e - 13$.

Now we reduce the number of DOF on Γ_C refine the grid eight times and regularise by $\mathrm{Reg} = R_2^T R_2$, $\alpha = 1.e - 13$. As mentioned in Section 6.3 we achieve oscillations in the calculation of $\partial_n u_h|_{\Gamma_C}$ if we reduce the number of DOF on Γ_C too much.
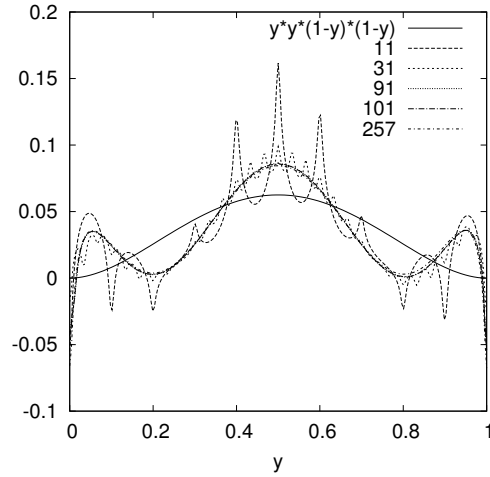

Figure A.52: $\partial_n u|_{\Gamma_C} = y^2(1-y)^2$ and $\partial_n u_h|_{\Gamma_C}$ for different numbers of DOF on Γ_C, refining the grid eight times calculated with the computed control, $\mathrm{Reg} = R_2^T R_2$ and $\alpha = 1.e - 13$.
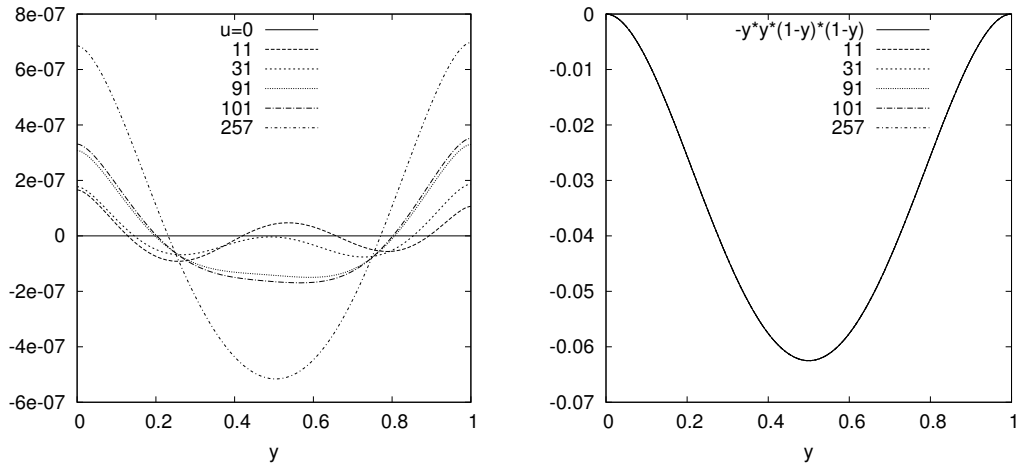

Figure A.53: $u|_{\Gamma_O} = 0$ and $u_h|_{\Gamma_O}$ (left), $\partial_n u|_{\Gamma_O} = -y^2(1-y)^2$ and $\partial_n u_h|_{\Gamma_O}$ (right) for different numbers of DOF on Γ_C, refining the grid eight times calculated with the computed control, $\mathrm{Reg} = R_2^T R_2$ and $\alpha = 1.e - 13$.

At last we refine the grid eight times use 101 DOF on Γ_C regularise with Reg $= R_2^T R_2$ and do the calculations for different regularisation parameters. As in the previous calculations we can see the influence of the regularisation parameters on the results for $\partial_n u_h|_{\Gamma_C}$ and $u_h|_{\Gamma_O}$.
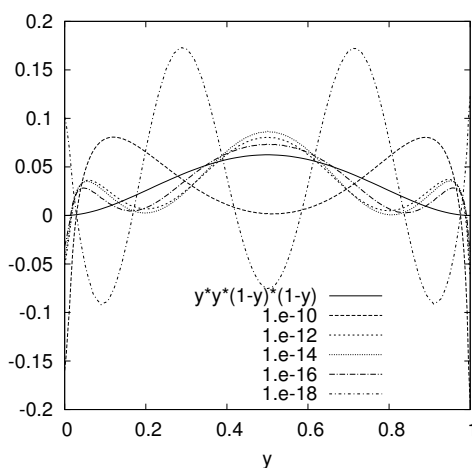

Figure A.54: $\partial_n u|_{\Gamma_C} = y^2(1-y)^2$ and $\partial_n u_h|_{\Gamma_C}$ for different regularisation parameters, refining the grid eight times calculated with the computed control, 101 DOF on Γ_C and Reg $= R_2^T R_2$.
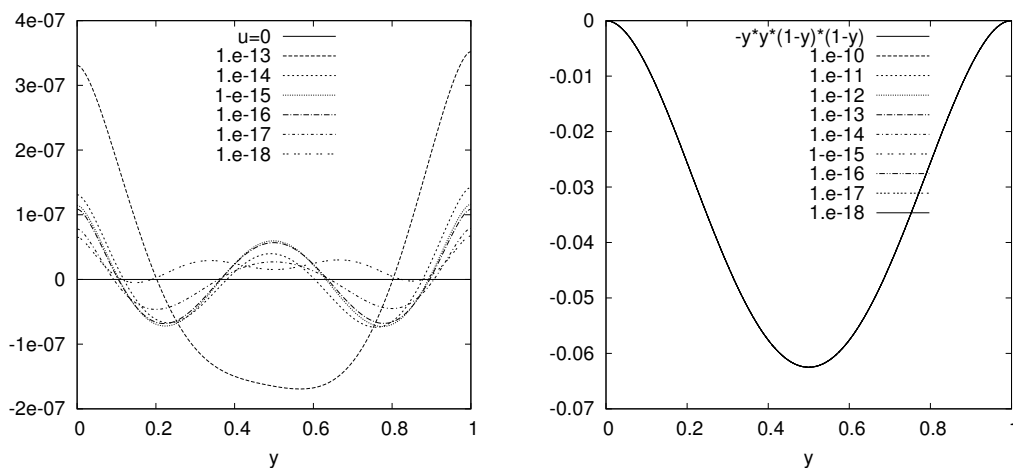

Figure A.55: $u|_{\Gamma_O} = 0$ and $u_h|_{\Gamma_O}$ (left), $\partial_n u|_{\Gamma_O} = -y^2(1-y)^2$ and $\partial_n u_h|_{\Gamma_O}$ (right) for different regularisation parameters, refining the grid eight times calculated with the computed control, 101 DOF on Γ_C and Reg $= R_2^T R_2$.

B More numerical results for hybrid insulation

In this Section we want to present more numerical results for the application of hybrid insulation. Therefore we use the same four measurements as in Section 7 but we present the results for different regularisation parameters. In all calculations we refine Ω six times (24576 cells and 321 DOF on Γ_C) and present only the results for the searched control $q = \partial_n u|_{\Gamma_C}$ and the approximation of the given measurements $\partial_n u|_{\Gamma_O}$.

We start with the first negative measurements as in Section 7 (see Figure B.1 right). For these calculations we use regularisation parameters between 10^{-9} and 10^{-4} and additionally 10^{-11}. We can see that for smaller parameter we reach the better approximations of the given measurement (see Figure B.1 (right)) but we achieve oscillations in the calculation of the searched control $q = \partial_n u|_{\Gamma_C}$. Caused of this we choose the regularisation parameter $\alpha = 1.e - 06$ in the presentation of the results in Section 7 (see Figure 7.2).
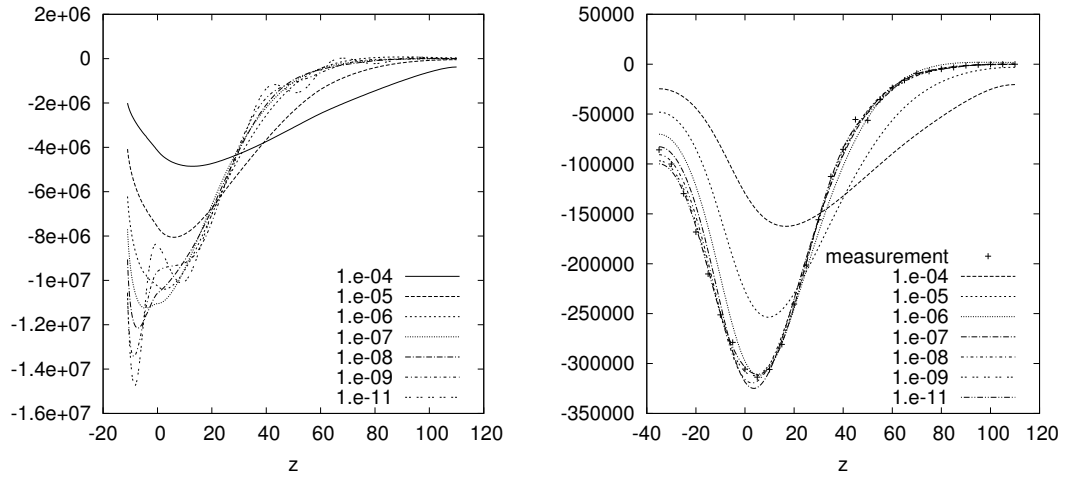
Figure B.1: $\partial_n u_h|_{\Gamma_C}$ (left), $\partial_n u_h|_{\Gamma_O}$ and the given measurement (right) calculated for different regularisation parameters and refining Ω six times.

Now we present the results for the other negative data. Here we use again regularisations between 10^{-8} and 10^{-4} and additionally 10^{-11}. As in the previous calculation we get a better approximation of the given measurements on Γ_O for smaller parameters (Figure B.2 right) but again we achieve oscillations in the calculation of the searched control $q = \partial_n u|_{\Gamma_C}$ (Figure B.2 left).
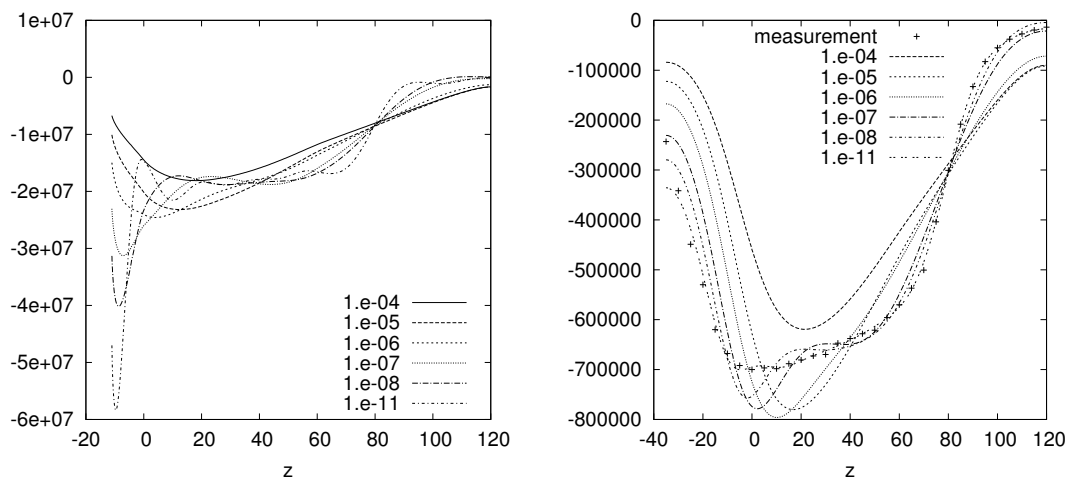

Figure B.2: $\partial_n u_h|_{\Gamma_C}$ (left), $\partial_n u_h|_{\Gamma_O}$ and the given measurement (right) calculated for different regularisation parameters and refining Ω six times.

In the following we see the results for the positive measurements (see Section 7) calculated for different regularisation parameters (Figure B.3 and Figure B.4). Here we have the same effect as in the calculations with given negative measurements. For smaller parameters we get the better approximation for the given measurements but we have oscillations in the results for the searched control $q = \partial_n u|_{\Gamma_C}$. Caused by these oscillations we have chosen the bigger parameters in the presentation of the results in Section 7.
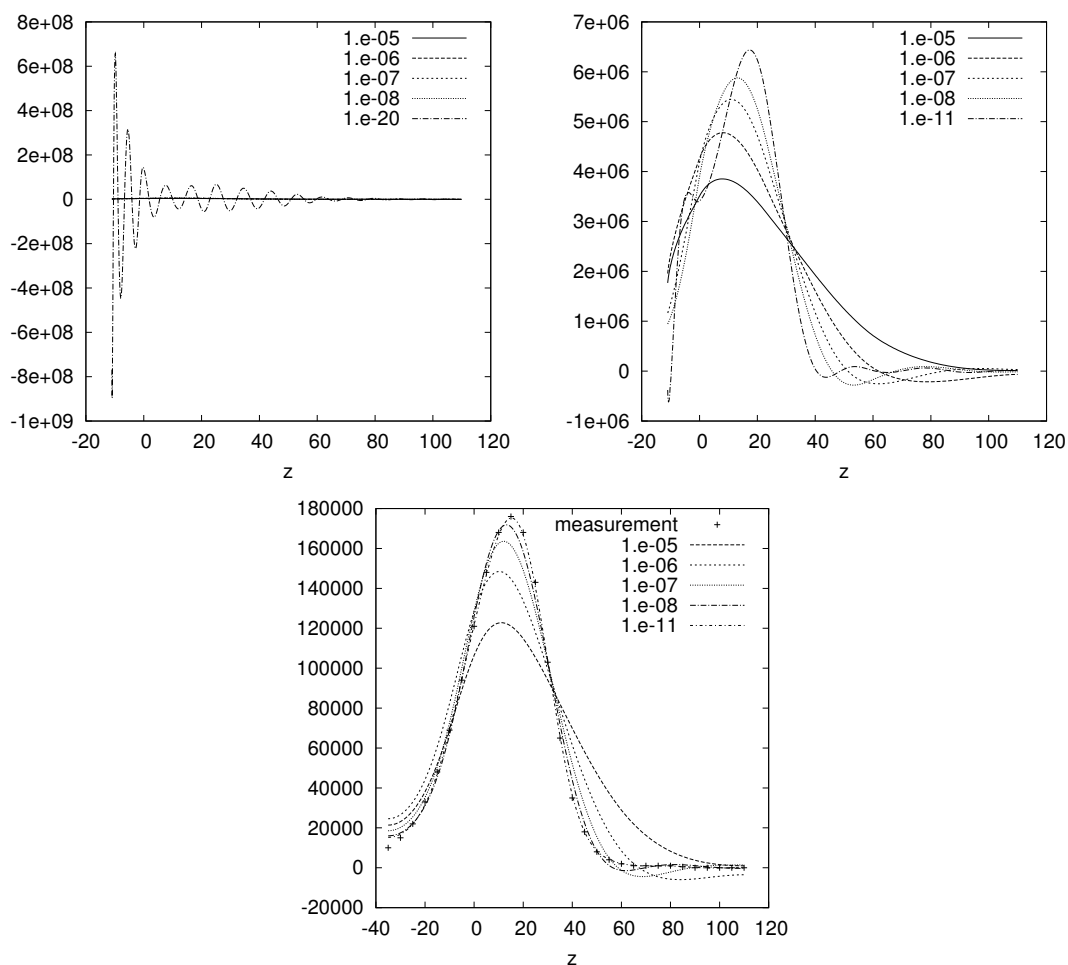

Figure B.3: $\partial_n u_h|_{\Gamma_C}$ (top left and right), $\partial_n u_h|_{\Gamma_O}$ and the given measurements for different regularisation parameters.

At last the results for the second given positive measurements calculated for different regularisation parameters.
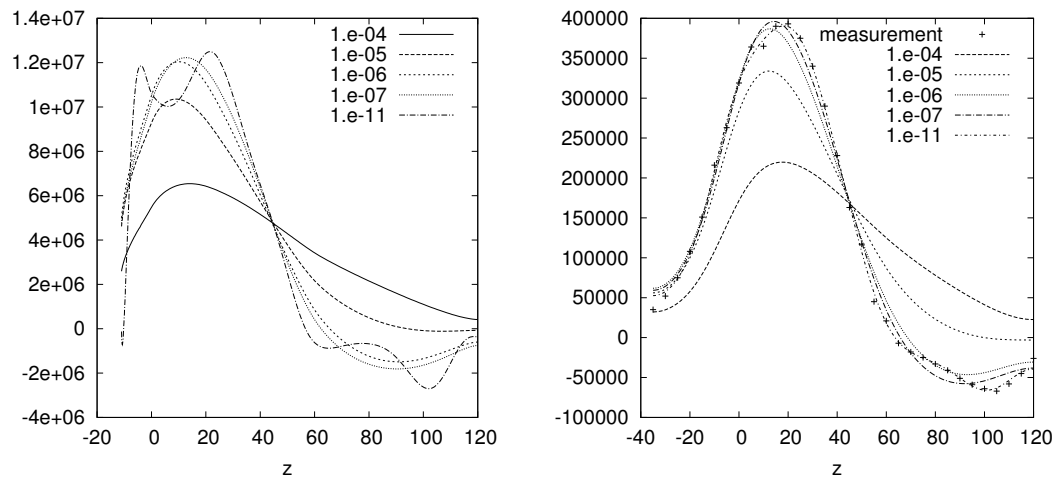
Figure B.4: $\partial_n u_h|_{\Gamma_C}$ (left), $\partial_n u_h|_{\Gamma_O}$ and the given measurements for different regularisation parameters.

Bibliography

[1] *DEAL, Differential Equations Analysis Library.* http://www.gaia.math.uni-siegen.de/suttmeier/deal/deal.html, 1992.

[2] *Lineare Funktionalanalysis.* Springer, 2006.

[3] Robert A. Adams. *Sobolev Spaces.* Academic Press, 1975.

[4] Douglas N. Arnold, Franco Brezzi, Bernardo Cookburn, and L. Donatelle Maini. Unified analysis of discontinouos galerkin methods for elliptic problems. *SIAM J. Numer. Anal*, 39(5):1749–1779, 2002.

[5] J. Baumeister. *Stable Solution of inverse problems.* Vieweg, 1987.

[6] R. Becker, P. Hansbo, and R. Stenberg. A finite element method for domain decomposition with non-matching grids. *M2AN*, 2003.

[7] Yu. Ya. Belov. *Inverse Problems for partial differential equations.* VSP, 2002.

[8] Dietrich Braess. *Finite Elemente.* Springer, 1997.

[9] James H. Bramble. *Multigrid methods.* Longman scientific and technical, Pitman Research Notes in Mathematics series 294, 1993.

[10] S. C. Brenner and L.R. Scott. *The mathematical theory of finite element methods.* Springer, 2002.

[11] Ivan Cherlenyak. *Numerische Lösungen inverser Probleme bei elliptischen Differentialgleichungen.* PhD thesis, Universität Siegen, 2009.

[12] D. Colton, R. Ewing, and W. Rundell, editors. *Inverse problems in partial differential equations.* Siam, 1989.

[13] Gilbarg D. and Trudinger N. *Elliptic partial differential equations of second order.* Springer, 1977.

[14] M. Dobrowolski. *Angewandte Funktionalanalysis.* Springer, 2006.

[15] Gene H. Golub and Charles F. van Loan. *Matrix Computations.* John Hopkins University Press, 1996.

[16] C. W. Groetsch. *Generalized inverses of linear operators.* Dekker, 1977.

[17] W. Hackbusch. *Theorie und Numerik elliptischer Differentialgleichungen.* Teubner, 1986.

[18] W. Hackbusch. *Iterative Lösung großer schwachbesetzter Gleichungssysteme.* Teubner, 1993.

[19] P. Hansbo. Nitsche´s method for interface problems in computational mechanics. pages 183–206, 2005.

[20] P. Hansbo and M. G. Larson. Discontinuous Galerkin methods for incompressible and nearly incompressible elasticity by Nitsche's method. *Computer methods in applied mechanics and engineering*, pages 1895–1908, 2002.

[21] Victor Isakov. *Inverse source problems.* American Mathematical Society, 1990.

[22] Claes Johnson. *Numerical solution of partial differential equations by the finite element method.* Cambridge Univ. Press, 1992.

[23] D. Kinderlehrer and G. Stampacchia. *An Introduction to variational inequalities and their application.* Academic Press, 1980.

[24] J.L. Lions. *Optimal Control of Systems Governed by Partial Differential Equations.* Springer-Verlag, 1971.

[25] A.K. Louis. *Inverse und schlecht gestellte Probleme.* Teubner, 1989.

[26] Frank Mauseth. *Charge accumulation in rod-plane air gap with covered rod.* PhD thesis, Norwegian University of Science and Technology, Faculty of Information Technology, Mathematics and Electrical Engineering, 2007.

[27] S. F. McCormick. *Multigrid Methods.* Siam, 1987.

[28] Th. Meis and U. Marcowitz. *Numerische Behandlung partieller Differentialgleichungen.* Springer, 1978.

[29] J. Nitsche. Über ein Variationsprinzip zur Lösung von Dirichlet-Problemen bei Verwendung von Teilräumen, die keinen Randbedingungen unterworfen sind. *Abh. Math. Sem., Univ. Hamburg*, 36:9–15, 1970/71.

[30] A. Rieder. *Keine Problem mit Inversen Problemen.* Vieweg, 2003.

[31] Saad. *Iterative methods for sparse linear systems.* PWS, 1996.

[32] O. Steinbach. *Numerische Näherungsverfahren für elliptische Randwertprobleme.* Teubner, 2003.

[33] Stoer. *Numerische Mathematik 1.* Springer, 2004.

[34] J. Stoer and R. Bulirsch. *Introduction to Numerical Analysis.* Springer, 2002.

[35] F. Stummel and K. Hainer. *Praktische Mathematik.* Teubner Studienbücher, 1971.

[36] F.-T. Suttmeier. On concepts of pde-software: The cellwise oriented approach in deal. *International Mathematical Forum*, 2(1):1–20, 2007.

[37] A. Tarantola. *Inverse Problem Theory.* Elsevier, 1987.

[38] Vidar Thomee. *Galerkin Finite Element Methods for Parabolic Problems.* Springer-Verlag, 1984.

[39] F. Tröltzsch. *Optimale Steuerung partieller Differentialgleichungen.* Vieweg, 2005.

[40] D. Werner. *Funktionalanalysis.* Springer, 2005.

[41] P. Wesseling. *An introduction to multigrid methods.* Wiley, 1992.

[42] J. Wloka. *Partielle Differentialgleichungen.* Teubner, 1982.

[43] K. Yosida. *Functional analysis.* Springer, 1980.